5-2018

Innovation in Commercial Supersonic Aircraft with Candidate Engine for Next Generation Supersonic Aircraft

Christopher D. Roper
Kennesaw State University

Jordan Fraser
Kennesaw State University

Alain J. Santos
Kennesaw State University

Innovation in Commercial Supersonic Aircraft with Candidate Engine for Next Generation Supersonic Aircraft

Authors:

Christopher D. Roper | Jordan Fraser | Alain J. Santos

Kennesaw State University

Southern Polytechnic College of Engineering and Engineering Technology

Department of Systems and Industrial Engineering

Faculty Advisor: Adeel Khalid, Ph.D.

May 2018

Abstract

The objective of this design study and competition - Next Generation Supersonic Candidate Engine and Aircraft Design, is a response to a proposal and is motivated by NASA's National Research Announcement in 2006. The requirements of this design study are provided by AIAA (American Institute of Aeronautics and Astronautics). The aircraft designed is a private business class. The aircraft engine performs at a maximum speed of Mach 1.8 and supersonic cruise speed of Mach 1.6 at 55,000 feet and a range of 4000 nmi. A generated mission profile through considerations in flight regime will drive the design involved in the development of aircraft characteristics. Interior cabin configurations are expected to support seating for up to 100 passengers. Using parametric cycle analysis, computational fluid dynamics, and system modeling/experimentation, a refined aircraft and engine design will be produced. Detailed analyses to meet the baseline requirements involve interpretation of trends of current generation aircraft engines are considered for the finalized design. The performance of the aircraft engine will involve calculations on wave drag, supersonic turbulent flow, and integrated methods of design of the nacelle enveloped within the aircraft fuselage. Through these various iterative methods, considerations in supersonic aircraft propulsion and aircraft design are presented. Projected technical specifications are to be implemented for the next generation of supersonic aircraft expected to be debuted in 2025. A robust composition of advanced material composites, methods of manufacturing, and forecasted advancements in technology are utilized to develop a proposal for the next generation of supersonic aircraft.

Table of Contents

Chapter 1: Introduction 13

1.1 - System Overview & Major Developments 13

1.2 - Design Requirements & Specifications 14

1.3 - Trade Study Items 15

1.4 - Concepts 17

1.5 - Verification Plan 20

1.7 - Simulation: Computational Fluid Dynamic Analysis & Finite Element Analysis 21

1.8 - Test: Wind Tunnel Testing 21

1.9 - Minimum Success Criteria 21

Chapter 2: Literature Review 25

2.1 - Aircraft Designs 25

2.2 - Engine Design 28

2.3 - Numerical Methods 29

2.4 - Computational Methods 30

2.5 - Engine Material 30

2.6 - Inlet Design 32

2.7 - Engine Selection 33

2.8 - Nozzle Design 34

Chapter 3: Design Approach 36

3.1 - Problem Solving Approach 36

3.2 - Gantt Chart 37
3.3 - Flowchart 38
3.4 - Resources 39
Chapter 4: Engineering Analysis 41
4.1 - Parametric Cycle Analysis (PCA) 41
4.2 - Supersonic Wave Drag Calculations 46
4.3 - Inlet Design Calculations 50
4.4 - Initial Weight Calculations 52
4.5 - Computational Fluid Dynamics 54
4.6 - Computational Methods - PARA 54
4.7 - Computational Methods - TURBN 57
Chapter 5: Results and Discussion 60
5.1 - Historical Data 60
5.2 - Trade Study Engine Design 60
5.3 - Discussion of Historical Data 61
Chapter 6: Prototype 62
6.1- Component Design 62
6.2 - Aircraft Model 65
6.3 - Engine Model 70
6.4 - Interior Design Configuration 71
Chapter 7: Conclusion 79

Chapter 8: Future Work 81

Acknowledgements 83

References 84

Appendices 87

Appendix A: Computational Fluid Dynamic Analysis 87

Appendix B: Inlet Design Analysis Trade Studies 88

Appendix C: Nozzle Design Analysis 91

Appendix D: Carpet Plots 93

Appendix E: Aircraft Design Computer Aid Models 97

Appendix F: Engine Initial Concepts 101

Appendix G: Final Engine Design Powerplant 103

Appendix H: Historical Data Plots 104

Appendix I: Parametric Cycle Analysis 120

Appendix J: TOPSIS Analysis and Design Matrix 123

Appendix K: Initial Weight Calculations 125

Appendix L: TURBN Turbine Analysis Program 126

Appendix M: Reflections 129

Appendix O: Contributions 131

List of Tables

Table 1: General Aircraft Characteristics (Welge, et al, 2010) 13

Table 2: Baseline Engine: Basic Data, Overall Geometry and Performance 15

Table 3: Respective cycle times for subsonic and supersonic engines 23

Table 4: Thrust and TSFC requirements for an installed engine 23

Table 5: Thrust and TSFC requirements for an uninstalled engine 24

Table 6: The design matrix used to identify a preliminary selection 27

Table 8: Parametric Cycle Analysis Excel Sheet 120

Table 9: Table of constant values for parametric cycle analysis 121

Table 10: Detailed calculations involving propulsive and thermal efficiency 121

List of Figures

Figure 1: General Engine Schematic (AIAA) 14

Figure 2: Supersonic geometry aircraft designs iteration 1 17

Figure 3: Supersonic inlet designs, aerospike and door panel configurations 18

Figure 4: Supersonic inlet designs, body diffuser and diamond shaped spike configurations. 18

Figure 5: Supersonic Vehicle Design Concepts 19

Figure 6: Supersonic Vehicle Design Concepts 19

Figure 7: Boeing Icon-II 25

Figure 8: Boeing 765-072B aircraft design 26

Figure 9: Boeing 765-076E design 26

Figure 10: Lockheed N+2 concept 27

Figure 11: Wide Chord Fan Blade 28

Figure 12: Screenshot from [26] showing GE's concept TAPS II combustor 29

Figure 13: Supersonic Plug Spike Nozzle **Figure 14**: Supersonic Plug Nozzle 34

Figure 15: Nozzle with chevrons 35

Figure 16: Implemented Gantt Chart 38

Figure 17: Design Flow Chart 39

Figure 18: Numerical and analytical wave drag estimation for high speed supersonic compressible flow 49

Figure 19: Supersonic spike CFD analysis for inlet design 50

Figure 20: Supersonic panel channel CFD analysis for inlet design 51

Figure 21: Supersonic extended and optimized panel channel CFD analysis for inlet design (a) Pressure (b) Mach Number (c) Velocity 52

Figure 22: The mission profile of the aircraft 52

Figure 23: Computer Aid Model demonstrating cruise climb prior to supersonic cruise mission. 54

Figure 24: Input parameters into the program 55

Figure 25: Output values from the program based on iterated LPC Pressure Ratio 56

Figure 26: Output values from the program based on iterated LPC Pressure Ratio 57

Figure 27: TURBN Stage 1 calculations 58

Figure 28: Turbine Blade Profile 59

Figure 29: Table of Turbine Constraints (Angular Vel. vs. Mean Radius) 59

Figure 30: Engine Fan Blade **Figure 31**: Engine Fan Hub 63

Figure 32: NASA Calculations for Nozzle Behavior 63

Figure 33: Models of: nozzle (a), plug design (b), fully opened nozzle exit (c), fully closed nozzle exit (d) 64

Figure 34: Isometric and profile view of supersonic prototype aircraft 65

Figure 35: Computer Aid Model body lofting process of supersonic aircraft vehicle 66

Figure 36: Design 1 concept with double delta straight wing geometry (isometric and right side respectively profiles) 66

Figure 37: Design 2 concept with double delta straight wing geometry (isometric and right side respectively profiles) 67

Figure 38: Design 3 concept with arced delta straight wing geometry (isometric, front, right side respectively profiles) 68

Figure 39: Design 3 concept with computational fluid dynamic model measuring (a) Mach number, (b) pressure, and (c) temperature respectively 69

Figure 40: Design concept with engine location configuration for Orientation 1 (one engine above, with one below). 70

Figure 41: Design concept with engine location configuration for Orientation 2 (two engines below fuselage) 70

Figure 42: Design concept for supersonic engine power plant (a) side profile (b) front profile 71

Figure 43: Standard configuration layout 72

Figure 44: Side view of standard seating 72

Figure 45: Overhead view of standard configuration (Left), ... 73

Figure 46: Isometric View (Right) 73

Figure 47: Detailed view of seating [28] 74

Figure 48: Detailed view of seating [28] 74

Figure 49: Luxury/Premium Economy Seating 75

Figure 50: Side view of seating 75

Figure 51: Overhead view of configuration 76

Figure 52: Isometric View (Bottom Right) 76

Figure 53: Detailed views of modern and updated luxury class seating 77

Figure 54: (a) ride side profile of simulated pressure and mach speeds (b) Shear stress and pressure formation (c) Acoustic power level reading at cruise conditions..... 87

Figure 55: Trade Study and Baseline Inlet Design Choice Selection..... 88

Figure 56: Design 1 side cut plot profile view for: (a) Pressure (b) Velocity (c) Acoustic Power Level 89

Figure 57: Design 2 side cut plot profile view for: (a) Pressure (b) Velocity (c) Temperature 90

Figure 58: Design 1 side cut plot profile view: (a) Pressure, (b) Mach Number, (c) Temperature, and (d) Velocity. 91

Figure 59: Design 2 side cut plot profile view: (a) Pressure, (b) Mach Number, (c) Temperature, and (d) Velocity. 92

Figure 60: Design 1 concept with straight delta wing geometry (isometric, front, right side respectively profiles)..... 97

Figure 61: Design 2 concept with double delta straight wing geometry (isometric, front, right side respectively profiles) 98

Figure 62: Design 3 concept with arced delta straight wing geometry (isometric, front, right side respectively profiles) 99

Figure 63: Frontal nose aircraft design baseline: (isometric, right side, front respectively profiles) 100

Figure 64: Frontal nose aircraft design extended nose optimization: (isometric, right side, front respectively profiles) 100

Figure 65: Engine Concept.....101

Figure 66: Concept Nozzle Geometries 102

Figure 67: Engine isometric and side profile of internal viewing of supersonic geometry 103

Figure 68: Specific Fuel Consumption vs overall efficiency for commercial/civil aircraft 104

Figure 69: Bypass Ratio vs Overall Efficiency for commercial/civil aircraft 104

Figure 70: Overall Pressure Ratio vs Overall Efficiency for commercial/civil aircraft 105

Figure 71: Specific fuel consumption vs thrust for commercial/civil aircraft 105

Figure 72: Graph of overall efficiency versus bypass ratio for military aircraft. 106

Figure 73: Specific fuel consumption vs Overall efficiency for military vehicles..... 106

Figure 74: Overall pressure ratio vs overall efficiency for military/civil aircraft 107

Figure 75: Specific fuel consumption vs thrust for military/civil aircraft 107

Figure 76: Overall Pressure Ratio vs Thrust for Military Aircraft 108

Figure 77: Bypass Ratio vs Thrust for Military Aircraft. 108

Figure 78: Weight vs Thrust for Military Aircraft 109

Figure 79: Inlet Temperature vs Thrust for Military Aircraft..... 109

Figure 80: TSFC vs Thrust for Military Aircraft 110

Figure 81: Bypass Ratio vs TSFC and Fan Pressure Ratio for Military Aircraft 110

Figure 82: Inlet Temperature vs Overall Pressure Ratio and TSFC for Military Aircraft ... 111

Figure 83: Inlet Temperature vs Bypass Ratio and TSFC for Military Aircraft 111

Figure 84: Inlet Temperature vs Overall Pressure Ratio and Engine Weight for Military Aircraft 112

Figure 85: Inlet Temperature vs Bypass Ratio and Engine Weight for Military Aircraft ... 112

Figure 86: Overall Pressure Ratio vs Thrust for Commercial Aircraft ... 113

Figure 87: Bypass Ratio vs Thrust for Commercial Aircraft ... 113

Figure 88: Weight vs Thrust for Commercial Aircraft ... 114

Figure 89: TSFC vs Thrust for Commercial Aircraft ... 114

Figure 90: Fan Pressure Ratio vs Bypass Ratio for Commercial Aircraft ... 115

Figure 91: Fan Pressure Ratio vs BPR vs SFC for Supersonic Military Aircrafts ... 115

Figure 92: Fan Pressure Ratio vs OPR vs SFC for Supersonic Military Aircrafts ... 116

Figure 93: Fan Pressure Ratio vs BPR vs Engine Weight for Supersonic Military Aircrafts ... 116

Figure 94: Fan Pressure Ratio vs OPR vs Engine Weight for Supersonic Military Aircrafts ... 117

Figure 95: Fan Pressure Ratio vs BPR vs Engine Weight for Commercial Aircrafts ... 117

Figure 96: Fan Pressure Ratio vs OPR vs SFC for Commercial Aircrafts ... 118

Figure 97: Fan Pressure Ratio vs BPR vs Engine Weight for Commercial Aircrafts ... 118

Figure 98: Fan Pressure Ratio vs OPR vs Engine Weight for Commercial Aircrafts ... 119

Figure 99: Parametric Cycle Analysis Program for Candidate Engine (Trial 1) ... 122

Figure 100: Design matrix for preliminary selection ... 123

Figure 101: Prioritization Matrix for TOPSIS ... 123

Figure 102: Qualitative Scale and Final Ranking for TOPSIS ... 123

Figure 103: Finalized TOPSIS Data Matrix ... 123

Figure 104: Normalized, criteria, weighted data, ideal solution, distance from the positive, and negative matrices for TOPSIS.....124

Figure 105: Sizing Calculation.....125

Figure 106: Inputs for the Beguet Range equation.....125

Figure 107: Breguet Range Equation calculation.....126

Figure 108: TURBN Stage 2 Analysis.....126

Figure 109: TURBN Stage 3 Analysis.....127

Figure 110: TURBN Stage 4 Analysis.....127

Figure 111: TURBN Stage 5 Analysis.....128

Figure 112: TURBN Stage 6 Analysis.....128

Chapter 1: Introduction

1.1 - System Overview & Major Developments

The progression of time ignites the invention of many exciting and daring technologies as the world becomes more demanding. Doctors must travel across states to retrieve organs, businessmen have to venture across countries to negotiate corporate dealings, and everyone has to get somewhere faster. This dire need for promptness has become the catalyst for aerospace leaders to begin designing next generation supersonic transport vehicles. To power such forceful and fast vehicles, new engine designs are being explored and created. NASA is one of the major facilitators of this engineering movement. What they need is an aircraft that goes beyond current supersonic business aircraft in performance but is smaller than past NASA airliners of the same class. The engine that will be used as a reference point is the one demonstrated in NASA/CR-2010-216842. The aircraft will have the use baseline characteristics shown in Table 1.

Table 1: General Aircraft Characteristics (Welge, et al, 2010)

General Charasteristics	
Max. Take-off Weight	317,499 lb
Payload Weight	21,000 lb
Operating Empty Weight	146,420 lb
Wing Loading (Take-off)	77.5 psf
Power Plant	2 x Mixed-flow Turbofans; 61,000 lbf each @ SLS
Performance	
Maximum Speed	Mach 1.8 at 55,000 feet
Cruise Speed	Mach 1.6 at 50,000 - 55,000 feet
Range	4000 nmi
Cruise L/D	9.2

New materials will be explored for the different components in the engine based on predicted discoveries that could be made from now until 2025. These materials can help with many factors that will be studied in great detail and incorporated into the engine design and performance tests.

By the completion of the project, the prototype will show improvements in TSFC (thrust specific fuel consumption) of at least 5% with significant weight savings, meet the cruise emissions goals, and address specified noise constraints (exit jet velocity). A preliminary schematic of our engine design is shown in Figure 1 with the major parts being labeled.

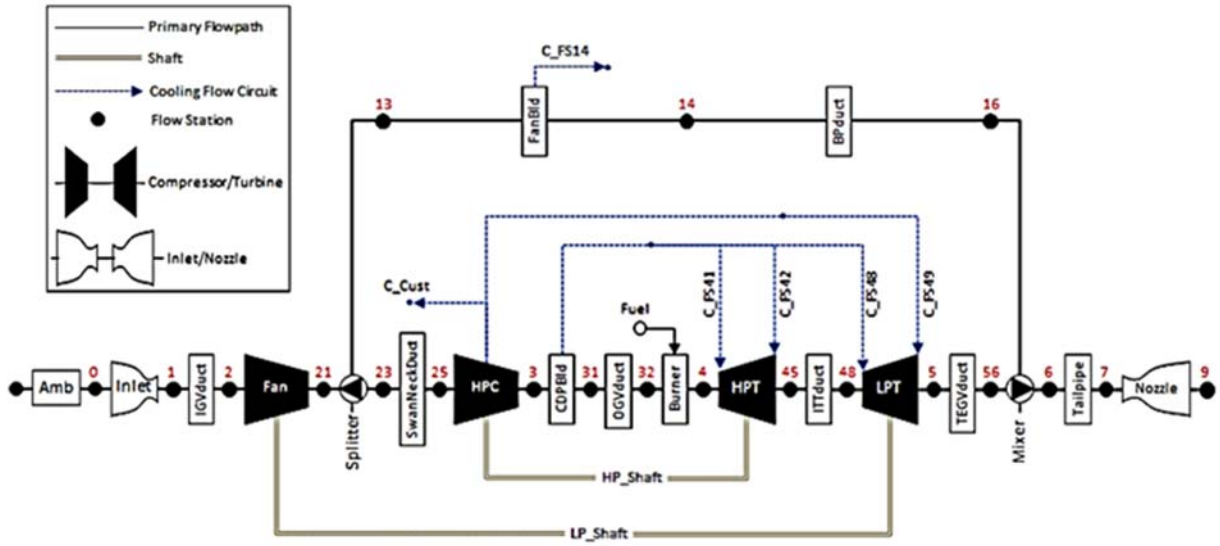

Figure 1: General Engine Schematic (AIAA)

1.2 - Design Requirements & Specifications

The engine designed by Team Supersonic will power a transport vehicle that can carry 100 passengers at Mach 1.6 over 4000 nmi. The engine will be a dual spool mixed-flow turbofan. The baseline fan diameter is 87.5 inches, and the engine weight excluding the inlet

will be 13,000 pounds. The new engine design will be, based on trade studies, optimized for minimum engine mass and fuel consumption by determining the best mixture of fan pressure ratio, overall pressure ratio, bypass ratio, and turbine entry temperature. It will be also optimized to maximize the flight range. Using the factors from the trade studies, possible compromises can be made between engine weight and fuel consumption on the aircraft's performance. Below initial design specifications can be found in Table 2. The initial installed thrust characteristics are shown below in Table 4, and the uninstalled ones are in Table 5.

Table 2: Baseline Engine: Basic Data, Overall Geometry and Performance

Design Features of Baseline Engine	
Engine Type	Mixed-flow Turbbofan
Fan Pressure Ratio	2.25
Overall Pressure Ratio at Max. Power	35.0
Bypass ratio at Max. Power	1.71
Max. Net Thrust at Sea Level	69,600 lbf
Specific Fuel Consumption at Max Power	0.51 lbm/hr/lbf
Fan Diameter	89 inches
Number of Fan Stages	2
Number of Compressor Stages	11
Number of HP Turbine Stages	2
Number of LP Turbine Stages	4

For the inlet, one must be designed to optimize internal performance and minimize inlet propulsion system drags. The nozzle must also meet certain design specifications to allow efficient supersonic cruise and meet current noise restrictions. This will be done by designing a convergent-divergent noise-attenuating nozzle. The nozzle will be made to optimize the gross thrust coefficient and to minimize nozzle propulsion system drags. Many different methods will be explored for noise reduction.

1.3 - Trade Study Items

A thorough investigation will be made on varying conditions to the geometry and the parametric cycle analysis. The geometries selected will determine the supersonic engine

parameters. Using a design matrix, a compilation of concept design ideas will be assessed, and key features and highlights will be taken into consideration for the applied approach in the preliminary design. The parametric cycle analysis trade studies will investigate the trends associated with the respective variables to determine a thorough description of the overall performance of our engine design. Below are a list of trade studies that will be done.

- Geometry
    - Inlet Geometry
    - Wing Geometry
    - Fuselage
    - Engine Placement
- Parametric Cycle Analysis
    - FPR vs. BPR vs. Mission Fuel Burn
    - OPR vs. T4.1 max vs. Mission Fuel Burn
    - FPR vs. OPR vs. Mission Fuel Burn
    - BPR vs. T4.1 vs. Mission Fuel Burn
    - FPR vs. BPR vs. cruise TSFC
    - OPR vs. T4.1 max vs. cruise TSFC
    - FPR vs. OPR vs. cruise TSFC
    - BPR vs. T4.1 vs. cruise TSFC
    - FPR vs. BPR vs. engine weight
    - OPR vs. T4.1 max vs. engine weight

- FPR vs. OPR vs. engine weight
- BPR vs. T4.1 vs. engine weight

This list of trade studies will guide the engine design. An analysis will be done comparing values such as overall pressure ratio, turbine inlet temperature, overall pressure ratio to mission fuel burn, cruise TSFC and Engine weight. Given that the requirements for the engine design are to create an engine that increases the TSFC margin by five percent while maintaining a lower weight, analysis of these trade study items will assist in design parameters for the engine.

1.4 - Concepts

Concept sketches are created to generate a visual on the aircraft and the inlet for the nacelle for the engine. Three view sketches for the aircraft as well as inlet designs are covered. These sketches are a basis for the framework in which analysis will be done. Below are the attached concept sketches that will aid in creating the finalized CAD for the aircraft.

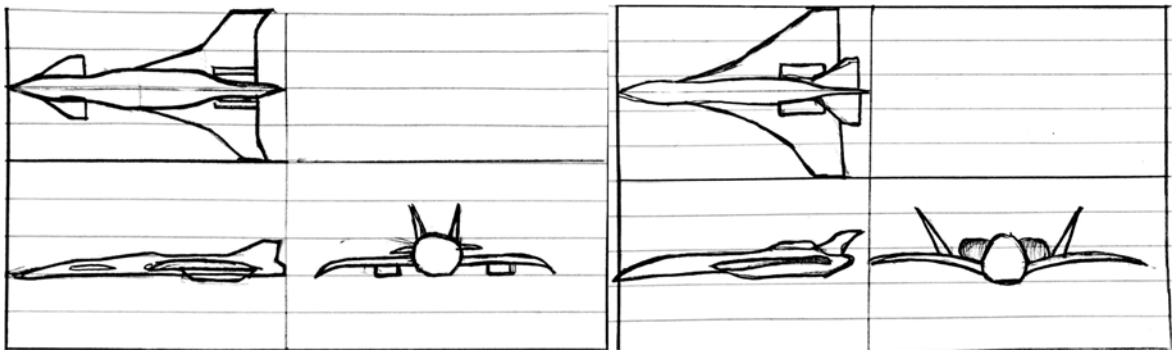

Figure 2: Supersonic geometry aircraft designs iteration 1

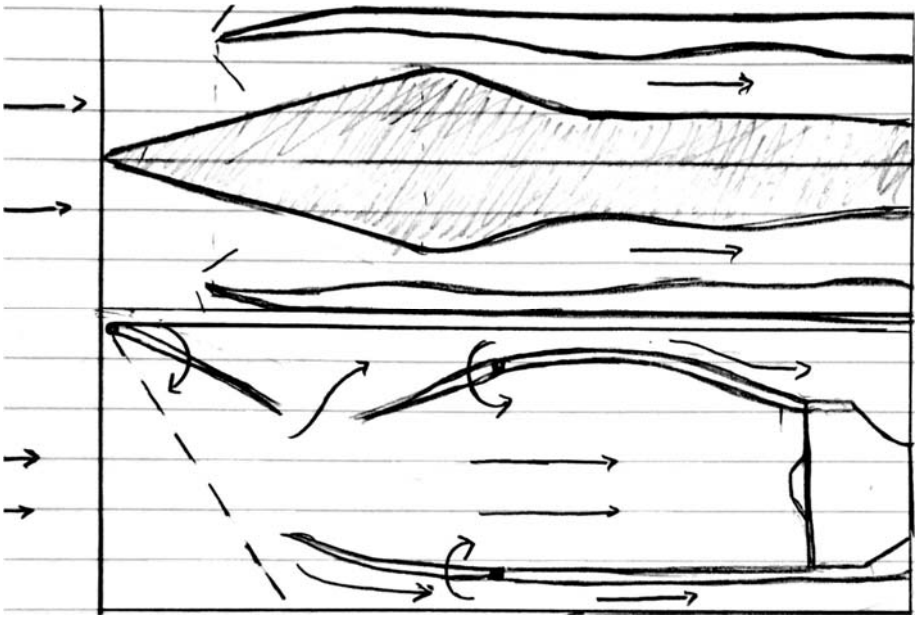

Figure 3: Supersonic inlet designs, aerospike and door panel configurations

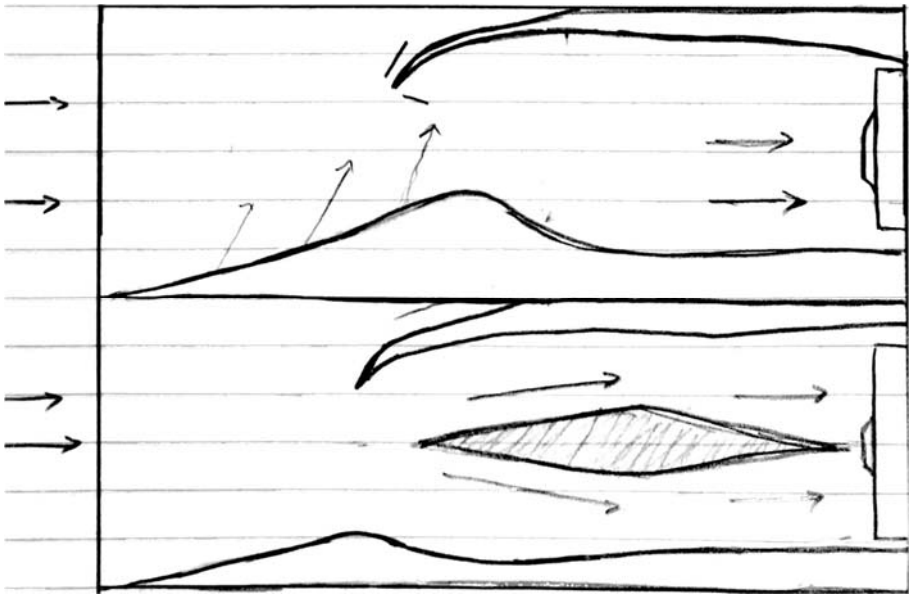

Figure 4: Supersonic inlet designs, body diffuser and diamond shaped spike configurations.

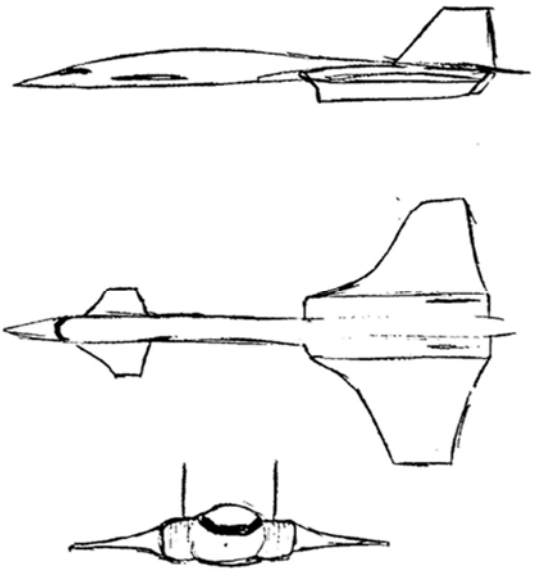

Figure 5: Supersonic Vehicle Design Concepts

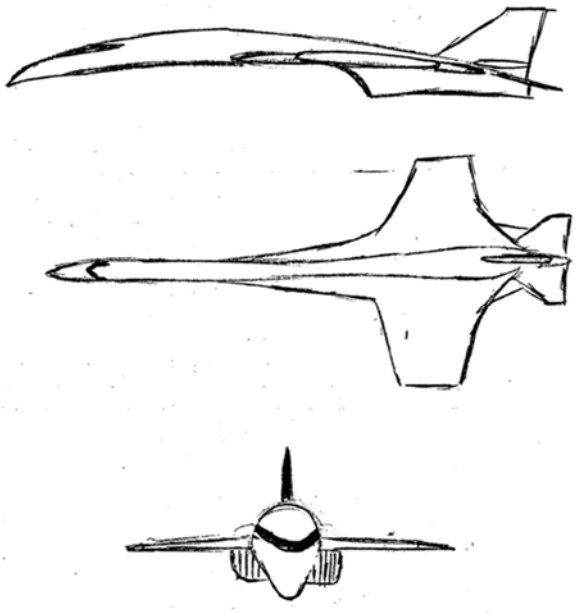

Figure 6: Supersonic Vehicle Design Concepts

1.5 - Verification Plan

Analysis

Numerical analysis is conducted for the overall project. Using parametric cycle analysis, empirical equations, and initial sizing calculations, an analysis of the aircraft was made. Further applications and studies for this project are later discussed in the following chapters.

Simulation

By using simulations, a refined design can be accomplished. The main source of simulations for this project are completed using SolidWorks. Computational Fluid Dynamics (CFD) allows for the simulation of air under various conditions. The main condition this project focuses on is supersonic cruise. CFD Simulations for the engine components and aircraft design are seen in the following chapters.

Testing

Testing for this project will be set in place as a plan of action for future work. The main scope of this project was to create models and conduct numerical and computational analyses. Further testing can be generated using a wind tunnel using 3D printed models and utilizing the wind tunnel at Kennesaw State University. Given the scaling factors with the wind tunnel, testing and experimentation will be placed under future work.

1.6 - Analysis: Parametric Cycle Analysis and Numerical Analysis

Design baseline engine parameters are given in section 4 of AIAA supersonic engine design challenge. To conduct parametric cycle analysis, optimization techniques can be performed with various parameters such as: engine mass and fuel burn, based on trade studies to determine the best combination of:

1. Fan pressure ratio
2. Bypass ratio

3. Overall pressure ratio

4. Turbine entry temperature

In order to help quantify and tabulate the numerical analysis values, AIAA approved packages such as: AxSTREAM by SoftInWay Inc, Numerical Propulsion System Simulation (NPSS), GasTurb 12. These software packages will serve as a guide in order to shape the computational fluid dynamic analysis and finite element analysis with respect to fan pressure ratio, bypass ratio, overall pressure ratio, and turbine entry temperature.

1.7 - Simulation: Computational Fluid Dynamic Analysis & Finite Element Analysis

The team will explore advanced and sophisticated computational simulations in order to verify the design compliance matrix. CFD and FEA simulations will work coincidently with the parametric cycle analysis. The numerical and analytical calculations will shape and structure the environmental conditions for both CFD and FEA. The next proceeding steps will allow an iterative design and sequential process.

1.8 - Test: Wind Tunnel Testing

The team will undergo 3D physical printing processes for rapid prototyping. The ideology allows for wind tunnel testing for aerodynamic design exploration. Possible components to undergo dynamic testing are: fan blades, high pressure turbines, low pressure turbines, aircraft wing, airfoils, the completed assembly aircraft and engine etc.

1.9 - Minimum Success Criteria

Minimum success criteria for this project is to design components for a mixed-flow turbofan engine that meet the baseline requirements set forth by AIAA and create a preliminary aircraft design to supplement the engine design. The minimum criteria for

deliverables on this project include the report, presentation, and video associated with aeronautics senior design. Some of the design specifications and goals are outlined by the objectives in the request report by AIAA. Based on the design decisions and calculations throughout the duration of this project, efforts will be made to focus on meeting baseline specifications outlined. The design must be able to take-off from static sea-level. The design must be able to meet cruise requirements and overcome the effects of wave drag.

The design must be also be able to be prototyped to generate a scaled 3D model or parts to display. Using SolidWorks, a working CAD model must also be utilized to successfully conduct CFD and FEA analysis. Computation and studies of a working design are closely dependent on how much is accomplished in developing a working CAD model. Through wind tunnel testing, a more thorough understanding of the aerodynamic design can be assessed to determine outcomes and to optimize a final design for review. Below are a list of specified conditions and requirements along with tabulated values for various conditions for the engine.

Prototype: Develop a scaled model in SolidWorks to be utilized for future working regarding wind tunnel testing

CAD Model: Generate a working CAD model to utilize CFD and FEA analysis on engine components and aircraft

Baseline Engine Fan Diameter: 87.5 inches (7.29 ft)

Conditions for Take-Off: Static Sea-Level Conditions

Conditions for Cruise: 55,000 ft, Mach 1.6

As per AIAA, a set of tables and values are provided for a starting point and will aid in starting analysis on the required engine design. Each table will provide set parameters are various conditions during flight. Within each of these flight regimes, characteristics of the engine are changed. For this project, the focus will be to optimize the design based on the flight characteristics during cruise. Below are the various tables used in the design.

Table 3: Respective cycle times for subsonic and supersonic engines

Landing Takeoff (LTO) Cycle Definitions

Mode	Subsonic Engines		Supersonic Engines	
	Power (%)	Time in Mode (min)	Power (%)	Time in Mode (min)
Takeoff	100	0.7	100	1.2
Climbout	85	2.2	65	2.0
Descent	N/A	N/A	15	1.2
Approach	30	4.0	34	2.3
Taxi/Idle	7	26.0	5.8	26.0

Table 4: Thrust and TSFC requirements for an installed engine

Installed Engine Thrust and TSFC Requirements

Conditions	Altitude (ft)	Mach	dTamb (F)	FN (lbf)	TSFC (lbm/hr/lbf)
SLS	0	0	0	64 625	0.520
Hot Day Take-Off	0	0.25	27	56 570	0.652
Transonic Pinch	40 550	1.129	0	14 278	0.950
Supersonic Cruise	52 500	1.6	0	14 685	1.091

Table 5: Thrust and TSFC requirements for an uninstalled engine

Uninstalled Engine Thrust and TSFC Requirements

Conditions	Altitude (ft)	Mach	dTamb (F)	FN (lbf)	TSFC (lbm/hr/lbf)
SLS	0	0	0	70 551	0.494
Hot Day Take-Off	0	0.25	27	61 190	0.620
Transonic Pinch	40 550	1.129	0	17 197	0.804
Supersonic Cruise	52 500	1.6	0	16 471	0.993

Chapter 2: Literature Review

2.1 - Aircraft Designs

Various concept designs currently exist in the aerospace industry in regards to supersonic flight. A number of aircraft were selected based on the appropriate geometry necessary for supersonic conditions. The effects of supersonic wave drag play a significant role in selecting the geometries to overcome it. Main features that were observed are the fineness ratio, wing geometry, engine placement, nacelle design, and seating configurations. Designs from Boeing, NASA, and Lockheed were selected for the prototype design. Below are the aircraft designs which were considered.

Figure 7: Boeing Icon-II

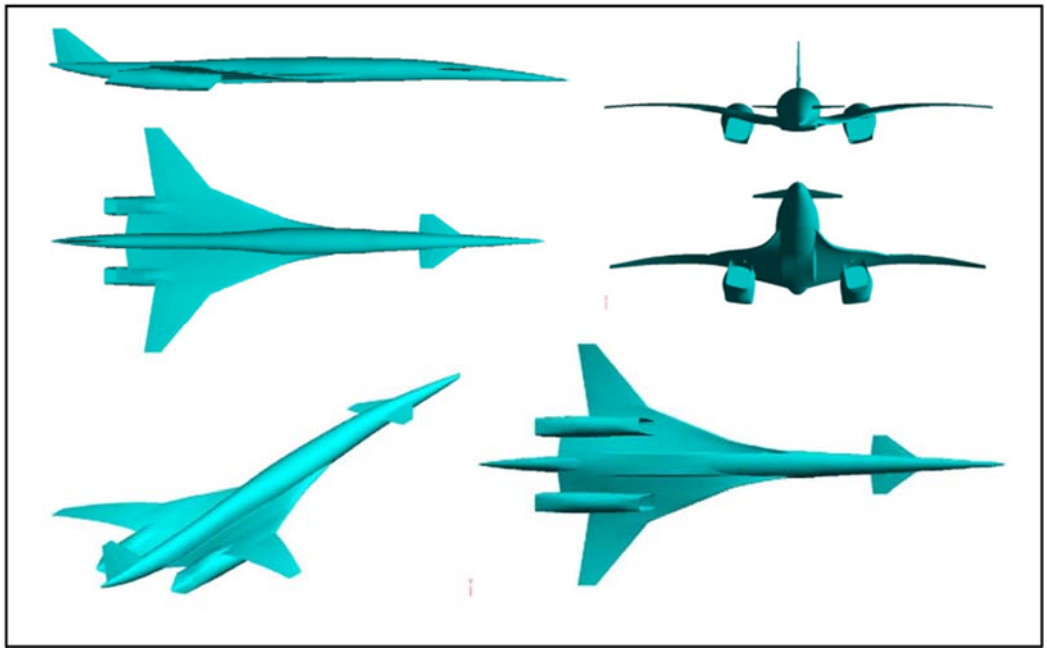

Figure 8: Boeing 765-072B aircraft design

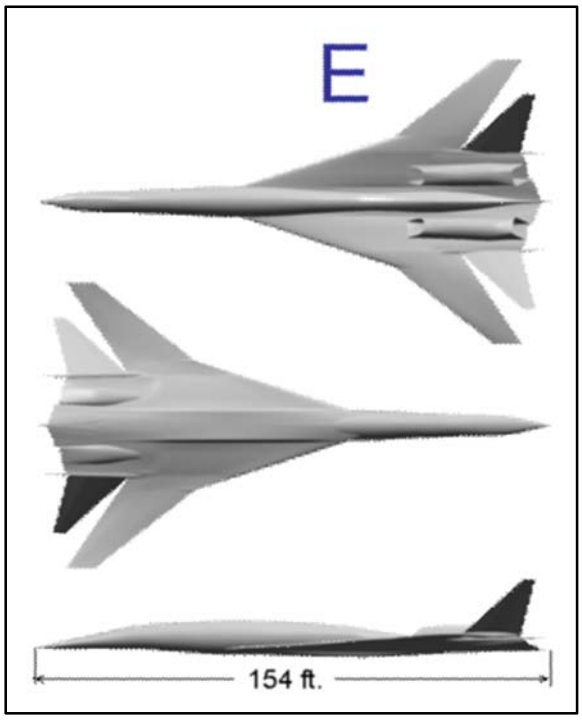

Figure 9: Boeing 765-076E design

Figure 10: Lockheed N+2 concept

These designs provide insight on the selection of geometries at supersonic speeds. Based on a set of design criteria, tools such as TOPSIS analysis and design matrices were used to select the aircraft which proved the most effective in meeting the requirements. The design matrix allowed a preliminary observation on each aircraft design. The TOPSIS analysis shows a more objectified and detailed selection seen in the appendix. The design matrix shown below, will display the thought process on a preliminary selection.

Table 6: The design matrix used to identify a preliminary selection

Design Matrix									
		Concept							
		Icon-II		765-072B		765-076E		Lockheed N+2 Concept	
Selection Criteria	Weight	Rating	Weighted Score	Rating	Weighted Score	Rating	Weighted Score	Rating	Weighted Score
Weight	18%	5	0.9	4	0.72	4	0.72	3	0.54
Material Cost	0%	0	0	0	0	0	0	0	0
Manufacturability	17%	4	0.68	5	0.85	4	0.68	5	0.85
Avoidance of Shock Cone	20%	6	1.2	5	1	6	1.2	5	1
Maintenancability	10%	3	0.3	6	0.6	3	0.3	5	0.5
Aesthetics	5%	7	0.35	4	0.2	4	0.2	5	0.25
Stability	20%	6	1.2	6	1.2	7	1.4	6	1.2
Wing Geometry	10%	6	0.6	4	0.4	5	0.5	5	0.5
	100%								
	Total Weighted Score	5.23		4.97		5		4.34	
	Rank	3		1		5		4	
	Continue?	NO		YES		NO		NO	

2.2 - Engine Design

The engine design has to be suited for efficient and fast travel. For these reasons certain engines may qualify as a baseline even though their original mission can be extraordinarily different from the one of this project. Starting with the fan, major considerations are the blade airfoil, material selection, geometry, and connection methods (dovetail). “Thin blades are ideal from an aerodynamic perspective, whereas thicker blades are important structurally with respect to impact and vibratory stress tolerance” [23]. Because of this and new technologies that hollow out the fan blades to decrease torsional rigidity by up to 16% [23], thick blades prove ideal for high speed engines. Fan blades can spin at speeds greater than 2000 rotations per minute at take-off speed. This comes with both stresses and centrifugal forces that could cause damage over time and decrease the aircraft’s time between overhaul. Having hollowed out blades also helps decrease overall engine weight and fuel consumption. Increasing thrust to achieve supersonic speeds can still be done just by increasing the fan diameter or accelerating the flow into the engine.

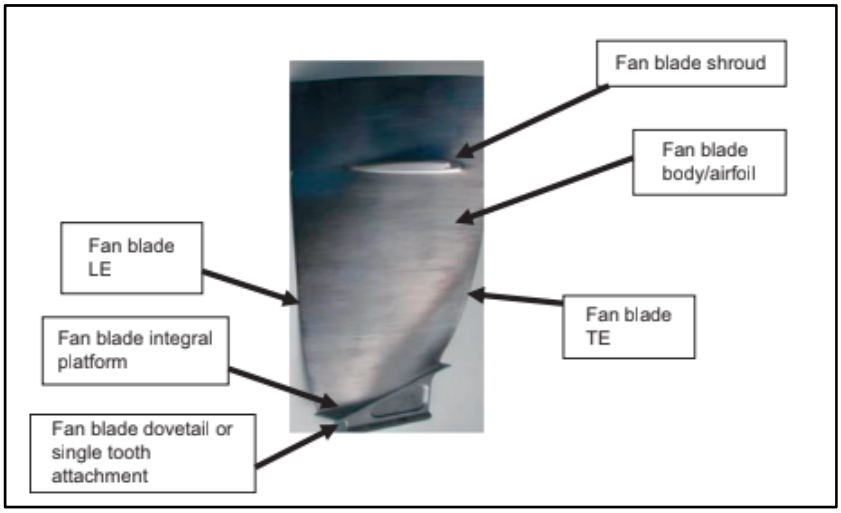

Figure 11: Wide Chord Fan Blade

For the combustion chamber, it seemed necessary to go with a rich-burn, quick-mix, lean-burn (RQL) combustor concept. “It was introduced in 1980 as a strategy to reduce oxides of nitrogen emission from gas turbine engines” [25]. It is the dominant combustor

technology in engine design today with leaders such as Pratt & Whitney creating their own models known as TALON (Technology for Advanced Low NOx). “Due to safety considerations and overall performance (e.g. stability) throughout the duty cycle, the RQL is preferred over lean premixed options in aeroengine applications” [25]. The latest RQL combustor found was the TAPS II combustor being developed by General Electric for the Continuous Lower Energy, Emissions and Noise (CLEEN) Program. Because “TAPS II has significant reduction for all 4 regulated pollutants and the TAPS II technology NOx emissions are at 39.3% of CAEP/6 (or 60.7% margin to CAEP/6), which meets the CLEEN NOx goal of 60% margin to CAEP/6,” the TAPS II combustion system was chosen to be in the team’s candidate engine to help reduce emissions [26].

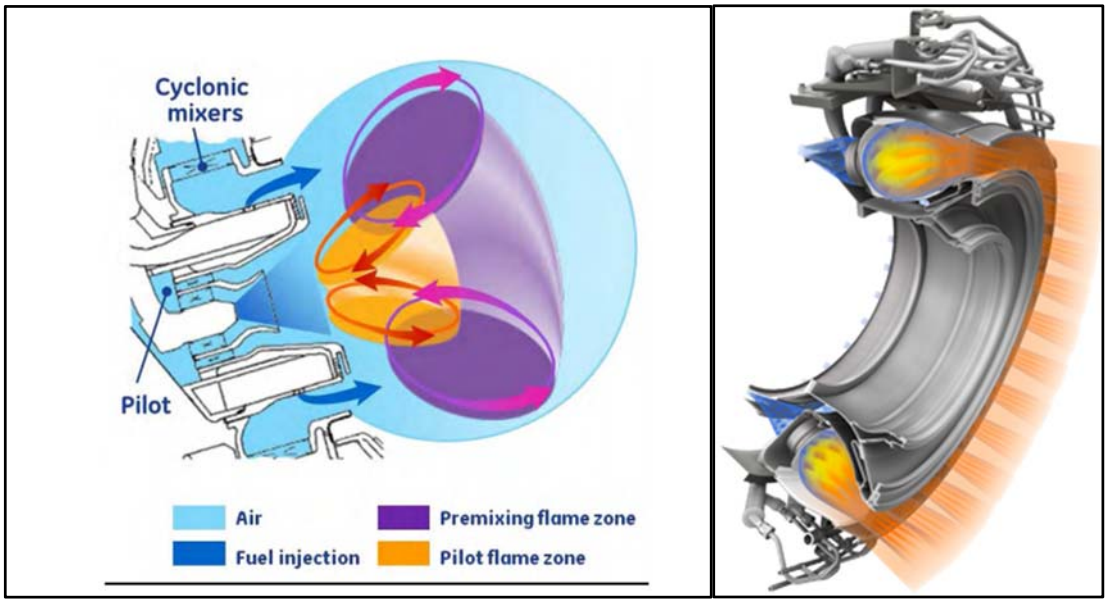

Figure 12: Screenshot from [26] showing GE’s concept TAPS II combustor

2.3 - Numerical Methods

Numerical Propulsion System Simulation (NPSS) is a multi-physics and engineering design numerical software program that enables an environment of various aircraft engines. This powerful software allows the user to generate engine cycle models with various components of engines, such as: inlet, compressor, combustion chamber, turbines, ducts,

nozzle, etc. For several problems, the engineer has the ability to define specific dependent and independent variables. NPSS allows execution with solver constraints tied directly to the problem solution. By doing so, this reduces the number of interacting software, thus reducing error [3].

2.4 - Computational Methods

Advanced computational fluid dynamic codes are implemented in various industry and research institutions in order to explore the effects of sonic boom energy dispersion. In the N+2 study, are some guidelines to explore and test two supersonic concept models: both -072B and -076E [1]. From this extensive study, the -076E model has a lower boom signature but does not meet the standards displayed by FAA. Lessons from NASA's design low boom trade studies will serve as a baseline in order to further future supersonic research.

2.5 - Engine Material

Historically, engines have been made of metal. They incorporate aluminum, steel, and titanium for different purposes such as availability, strength, heat resistance, and cost. Selecting the material of different parts depends on the stresses, loads, and purpose of the different sections. Usually, "materials are characterized by their damage tolerance, ductility, high cycle fatigue (HCF) strength, and yield strength" [22]. Because the front of the engine, including the fan and compressor are the some of the most important parts, they had to be built to resist impact damage, be light, and be able to decrease aircraft downtime. These requirements made titanium a prime candidate, and it has been used widely in industry for decades.

As time and technology progressed, new design requirements became important such as engine weight, strength, fuel consumption, and strength. Currently, leaders in industry such as CFM International (GE/Snecma joint venture) and Pratt and Whitney have begun

research and the use of composite material. Examples would include the Boeing B787 Dreamliner and Airbus A350 XWB, in which almost half of the aircrafts' structure by weight is composed of reinforced plastics [23]. "Similarly, the containment case, there to contain the results of any blade separation and prevent high-speed debris from impacting the airframe or aircraft systems, can now be composite rather than metal or a metal-composite hybrid (typically aluminum over-wrapped with aramid). Weight saved in the fan/containment case pairing has a knock-on effect, enabling components such as shafts and bearings, the pylons which attach the engine to the wing and the associated wing structure to be made lighter also. In aggregate, half a ton or more can be saved per engine, a prize well worth having given the high price of aviation fuel today" [23]. Metal-composite hybrid materials such as aluminum over-wrapped with aramid have proven effective. These uses of composites result in an astounding loss in engine weight of more than a thousand pounds.

Composites are also more durable than their metal counterparts, possessing greater tolerance to fatigue and the ability to be molded into approximately three dimensional shapes ideal for aerodynamics. Composites also resist creep that arise from centrifugal forces generated by the fan's high speed revolution, "meaning that the clearance engineered initially between the blade tips and the surrounding duct has to be greater than it should be for optimum engine performance" [23]. Composites also help make engines more fuel efficient as seen from CFM's LEAP engine that boasts a 15% higher fuel efficiency.

Research into new and exciting materials has been very beneficial to the aerospace industry. However, many manufacturers still fall back on titanium during material selection. Titanium is very versatile, readily available, easy to fabricate, very ductile, and has a low life cycle cost, great performance historically, excellent high cycle fatigue (HCF), tensile, and yield strength, low density, and a naturally regenerative corrosion resistant protective film. The higher material cost is offset by savings from longer life and reduction in equipment maintenance and aircraft downtime. More significantly, titanium has the highest strength-to-weight ratio out of all other structural materials. However, thousands of operating hours lead to damage such as high strain LCF, FOD (predominantly), wear, and fretting.

While titanium may be a very reliable and proven material choice, many are still looking to composites and other material. Composites have high strength-to-density ratios, stiffness-to-density ratios three times higher than aluminum, steel, and titanium, and have yielded engine weight savings of more than half a ton. “The high strength and stiffness of composite materials combined with the ability to tailor the material to specific aerodynamic loads have led to their increased use in fan blades” [22]. Most composite blades are reinforced with a titanium leading edge (LE) and metal cladding. This gives them lightness, improved strength, and damage resistance. The lower mass yields lower centrifugal loads and stresses which can lead to longer life. Thus there is less damage and reduced noise when the engine turns off and the fan blades are still revolving at lower speeds.

Unfortunately, composites also have low aerodynamic efficiency which is still being researched. This research led to the testing of metal matrix composites (MMC) which have high strength, stiffness, and versatility but also really high costs. Another new material that has been researched is hybrid-metallic material (HMM). “Unlike composite materials, hybrid-metallic materials are easier to transfer among designs, meaning they are well-suited to the fabrication of fan blades of any size or dimension” [22]. These structures exploit certain properties of varying materials to improve structural integrity in specific areas. They are currently being developed by Pratt and Whitney to provide both weight and structural benefits. Unlike composites, HMMs are more versatile and can be adapted to different designs for fan blades of any size or dimension. They are more resistant to bird impact strikes and have a reduced cost. “Research efforts to promote the greater applicability of hybrid-metallic materials to fan blade structures are recommended. Nonetheless, significant efforts have been made to ensure the durability and long service life of these materials” [22].

2.6 - Inlet Design

NASA Glenn Research Center conducted a “Supersonics Project” under the Inlet and Nozzle Branch in conjunction with the Supersonic Cruise Efficiency Propulsions group. The team designed a powerful computational tool to perform aerodynamic design and

computational analysis specifically for supersonic inlets [7]. This code serves as a baseline to determine supersonic inlet geometry and performance characteristics. This code could serve as a powerful approach to allow researchers and engineers solve aerodynamic and propulsion challenges. The code, SUPIN (SUPersonic INlet) Design Code, is capable of designing and analysis of external - compression, for supersonic inlets of (Mach 1.6-2.0) along with its measurements of flow rates, total pressure recovery, and inlet drag [7]

2.7 - Engine Selection

Most engines on the market that are used for supersonic flight tend to serve military purposes. Aircraft such as the F-22, Concorde, and the F-11 are few of the many that can fly at Mach 1 and faster. They utilize turbojet engines equipped with afterburners for short bursts of supersonic thrust during combat. Most supersonic craft require such engines that are small in diameter, relatively, and can reach such speeds quickly. As powerful as these engines are, they are equally inefficient compared to engines used for civil and recreational aircraft.

To compensate for efficiency, aircrafts tend to use turbofan engines. However, most turbofans can't reach sonic or supersonic speeds unaided. Regardless, the focus for the type of engine that will be selected for the mission will be towards medium to large bypass turbofans. These engines are efficient and powerful in their own right. They use the air coming into the fan bypass to help propel the aircraft.

Throughout the years, turbofans have seen many improvements from the materials built into the components to the shapes of the fan, compressor, and turbine blades. All of the changes are attempts at creating the most durable and efficient engines. To help the aircraft reach supersonic speeds will require a specially designed inlet and nozzle.

2.8 - Nozzle Design

Preliminary research has guided the nozzle design choice in favor of a convergent-divergent design. This will help turn subsonic flow after the turbine stage into supersonic flow at the nozzle exit. With supersonic aircraft, the customer will experience levels of noise that far surpass those of most commercial aircraft that travel at sub- to transonic speeds. "Jet noise…seeks advanced solutions, especially in the case of high-speed aircraft" [20]. Because the trend shows a shift toward supersonic travel in the upcoming decades, technological advancements are required to make such travel methods feasible and desirable. Many things contribute to the noise signature given off from supersonic engines; however, "jet noise is dominated by Mach wave emission, which arises when turbulent eddies in the jet travel with supersonic velocity relative to the surrounding medium" [20]. 85% of the far-field jet noise that humans are sensitive to comes from Mach waves. Other phenomena can contribute to the high noise levels. "High level acoustic emission also occurs in jets with strong shocks, i.e. in under- or over-expanded jets… [which] can be substantially removed by operating at pressure-matched conditions" [20].

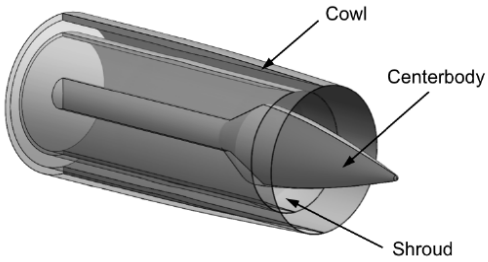

Figure 13: Supersonic Plug Spike Nozzle

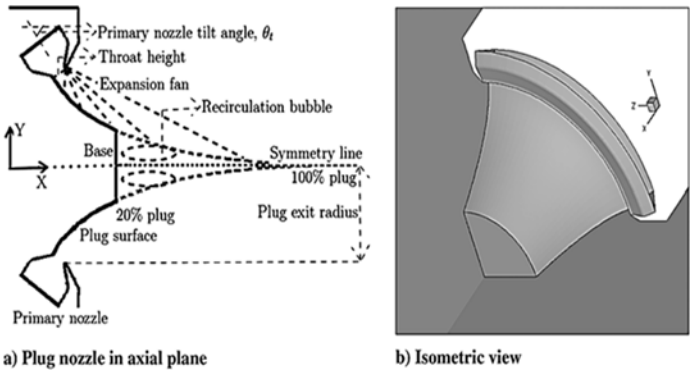

Figure 14: Supersonic Plug Nozzle

Fortunately, many researchers have begun to look into ways to correct this issue. Methods to reduce noise emission such as those that "enhance the mixing of the jet and the

surrounding air" [20] come with "appreciable thrust and weight penalties. Other solutions, like the Inverted Velocity Profile (IVP) supersonic plug nozzles, or a Thermal Acoustic Shield have shown some encouraging results but have not found wide implementation" [20]. Other methods incorporate changing the properties of the jet stream by surrounding it with a secondary stream of the right characteristics will inhibit Mach wave formation. Above and below are images of supersonic plug nozzles along with one of chevron nozzle panels that disrupt the Mach waves at the end to reduce the noise levels.

Figure 15: Nozzle with chevrons

Chapter 3: Design Approach

3.1 - Problem Solving Approach

To represent how the team will approach the many design challenges will require the use of different modeling software. The use of CFD (computational fluid dynamics) software such as SolidWorks' flow package, will help model the flow of the air entering the "cold" parts of our engine (i.e. inlet, fan, compressor etc.) as well as the flow along the fuselage. These models will generate key results through calculations using given parameters to represent a prediction for how a full scale component will behave realistically. The figures will yield results that will be used within further calculations and charts to show if the challenges were met within the desired 5% margins. They will also help aid in the design of the engine components after the combustor (i.e. turbine and nozzle).

Another software to possibly be used for the completion of the project will be Numerical Propulsion System Simulation (NPSS). NPSS is a simulation program that is "block oriented" and can be used for engineering design and to simulate aerospace systems. This program works by taking the different elements specified by the engineer and the respective technical data that details their individual performance and solves the system. The program takes the input text files filled with code typed in C++ language and launches them via the system command window. For this project, NPSS will be used as a computational model of the engine's parametric cycle analysis.

To model and analyze the behavior of the turbomachinery inside the engine and find certain data parameters such as the temperature and pressure at various stages, the team can potentially use the program AxSTREAM. AxSTREAM is a software package that is used for a representative design of the compressor and turbine, and also to solve thermodynamic calculations of industry turbomachinery for both on and off-design operation. Given certain initial parameters for the inlet and the outlet, the program can then perform 1D, 1D/2D, and 3D calculations that encompass CFD analyses to create a model for the different components. This software will help validate certain design choices made regarding the engine and its

components, and it will also serve to reveal parameters that would have been otherwise unknown to the group.

Throughout majority of the project, Microsoft Excel was used for the numerical calculations. Having to perform parametric cycle analysis, besides Matlab, Excel would be an easier program to use. Using Excel also helped to correlate data from different sheets and workbooks to create plots for the necessary trade studies. Excel also helped highlight different values and data points from the collection of historical data gathered on the hundreds of engines used in industry. Transposing the data to Matlab is still a viable option and may be done for future numerical simulations and calculations.

3.2 - Gantt Chart

The flow of work in this project is crucial given the strict deadline. Thus, to ensure tasks are completed on time and progress was made, a Gantt chart is created. The Gantt chart proved useful for setting main tasks and goals to complete. The Gantt chart also provides a visual on the progress made on the project throughout the entire semester it was worked on. Within each respective task, a weekly progress report was made. Specific tasks were delegated to ensure progress within each goal. The Gantt chart which was used is provided below.

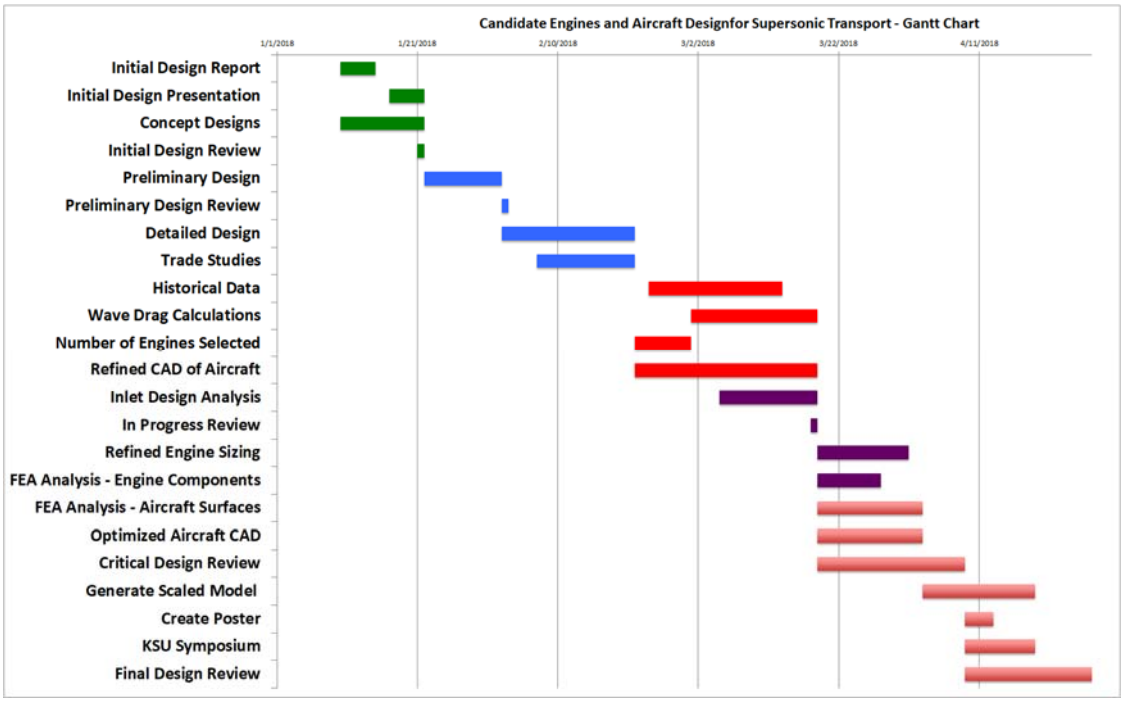

Figure 16: Implemented Gantt Chart

3.3 - Flowchart

In order to complete this project, a systematic flow chart was generated to characterize the design process. Utilizing similar design flows of aircraft design, the same could be used for the engine and various components of this project. The flow chart shown below describes the iterative process used that allowed multiple versions, optimizations and designs for the overall project. By utilizing trade studies, sizing configurations and design trades, a finalized design was concluded for this project. Although, future refinements can always be made to this project, deliverables are important thus this flow chart accounts for that.

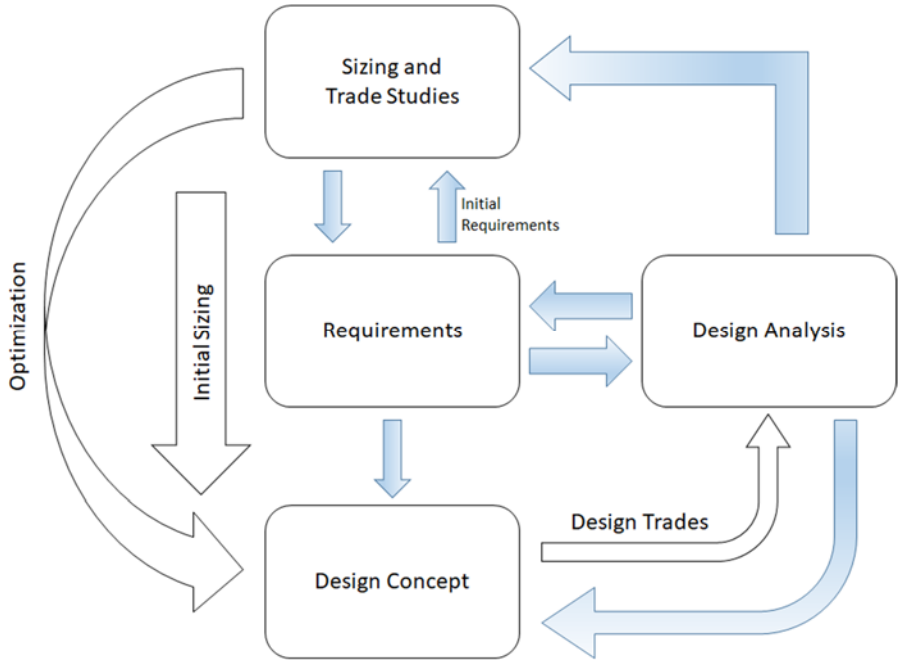

Figure 17: Design Flow Chart

3.4 - Resources

Kennesaw State University offers a vast number of resources to ensure a complete project. The facilities on the Marietta campus of Kennesaw State University offers multiple avenues to explore and create models and observe characteristics of flight. A list of them is provided below. In addition to resources on campus, a list of possible sponsors is provided when completing future work and possible partnerships with the university to obtain access to certain laboratory materials or supplies. Lastly, a list of hardware and software available in completion of this project is generated where access is readily available.

Facilities:

Fluid Dynamics Laboratory

Controls and Vibrations Laboratory

3D Printing Laboratory

Flight Simulator Laboratory

Architecture Woodshop

Possible Sponsors:

1. Kennesaw State University
2. Georgia Tech Research Institute
3. Lockheed Martin
4. Spaceworks
5. Northrop Grumman
6. CATIA
7. ANSYS

Available Software:

1. Solidworks
2. ANSYS
3. MATLAB
4. SIMULINK
5. Microsoft Office
6. Latex
7. AxSTREAM by SoftInWay Inc.
8. Numerical Propulsion System Simulation (NPSS)
9. GasTurb 12

Hardware:

1. 3D Printer(s)
2. COX parts (Commercial off the shelf)- McMaster Carr etc.
3. Wind Tunnel

Chapter 4: Engineering Analysis

4.1 - Parametric Cycle Analysis (PCA)

To determine if the baseline engine was a suitable engine, the team performed parametric cycle analysis. Research was conducted to find the input values that were required for the calculations. For the values that were not given through research, assumptions were made from the trend studies of similar engines. After the inputs were found, an Excel sheet was designed that incorporated the PCA equations (1) - (45) from *Elements of Propulsions* [11]. After the program finished, the propulsive and thermal efficiencies were calculated and found to be 98.53% and 51.46%, respectively. These efficiencies would yield an overall efficiency of 50.7%. This was deemed acceptable because it was close to the efficiencies of typical high bypass turbofan engines. Below are the inputs, outputs, and equations used for the PCA program excluding any afterburner parameters given their absence from all engines tested.

Inputs:

$$M_0,\ T_0(\mathrm{K},\ ^\circ\mathrm{R}),\ \gamma_c,\ c_{pc}\left(\frac{\mathrm{kJ}}{\mathrm{kg}\cdot\mathrm{K}},\ \frac{\mathrm{Btu}}{\mathrm{lbm}\cdot{}^\circ\mathrm{R}}\right),\ \gamma_t,\ c_{pt}\left(\frac{\mathrm{kJ}}{\mathrm{kg}\cdot\mathrm{K}},\ \frac{\mathrm{Btu}}{\mathrm{lbm}\cdot{}^\circ\mathrm{R}}\right),$$

$$h_{PR}\left(\frac{\mathrm{kJ}}{\mathrm{kg}},\ \frac{\mathrm{Btu}}{\mathrm{lbm}}\right),\ \gamma_{\mathrm{AB}},\ c_{p\mathrm{AB}}\left(\frac{\mathrm{kJ}}{\mathrm{kg}\cdot\mathrm{K}},\ \frac{\mathrm{Btu}}{\mathrm{lbm}\cdot{}^\circ\mathrm{R}}\right),\ \pi_{d\,\max},\ \pi_b,\ \pi_{\mathrm{AB}},\ \pi_{M\,\max},$$

$$\pi_n,\ e_c,\ e_f,\ e_t,\ \eta_b,\ \eta_{\mathrm{AB}},\ \eta_m,\ P_0/P_9,\ T_{t4}(\mathrm{K},\ ^\circ\mathrm{R}),\ T_{t7}(\mathrm{K},\ ^\circ\mathrm{R}),\ \pi_c,\ \pi_f,\ M_6$$

Outputs:

$$\frac{F}{\dot{m}_0}\left(\frac{\mathrm{N}}{\mathrm{kg/s}},\ \frac{\mathrm{lbf}}{\mathrm{lbm/s}}\right),f,f_{\mathrm{AB}},f_O,\ S\left(\frac{\mathrm{g/s}}{\mathrm{kN}},\ \frac{\mathrm{lbm/h}}{\mathrm{lbf}}\right),\ \alpha,\ \eta_{Th},\ \eta_P,\ \eta_O,\ \eta_c,\ \eta_t,\ \text{etc.}$$

Equations:

$$R_c = \frac{\gamma_c - 1}{\gamma_c} c_{pc} \tag{1}$$

$$R_t = \frac{\gamma_t - 1}{\gamma_t} c_{pt} \tag{2}$$

$$R_{\mathrm{AB}} = \frac{\gamma_{\mathrm{AB}} - 1}{\gamma_{\mathrm{AB}}} c_{p\mathrm{AB}} \tag{3}$$

$$a_0 = \sqrt{\gamma_c R_c g_c T_0} \tag{4}$$

$$V_0 = a_0 M_0 \tag{5}$$

$$\tau_r = 1 + \frac{\gamma_c - 1}{2} M_0^2 \tag{6}$$

$$\pi_r = \tau_r^{\gamma_c/(\gamma_c - 1)} \tag{7}$$

$$\eta_r = 1 \quad \text{for } M_0 \le 1 \tag{8}$$

$$\eta_r = 1 - 0.075(M_0 - 1)^{1.35} \quad \text{for } M_0 > 1 \tag{9}$$

$$\pi_d = \pi_{d\,\max}\eta_r \tag{10}$$

$$\tau_\lambda = \frac{c_{pt} T_{t4}}{c_{pc} T_0} \tag{11}$$

$$\tau_{\lambda AB} = \frac{c_{pAB} T_{t7}}{c_{pc} T_0} \tag{12}$$

$$\tau_c = \pi_c^{(\gamma_c - 1)/(\gamma_c e_c)} \tag{13}$$

$$\eta_c = \frac{\pi_c^{(\gamma_c - 1)/\gamma_c} - 1}{\tau_c - 1} \tag{14}$$

$$f = \frac{h_{t4} - h_{t3}}{\eta_b h_{PR} - h_{t4}} \tag{15}$$

$$\tau_f = \pi_f^{(\gamma_c - 1)/(\gamma_c e_f)} \tag{16}$$

$$\eta_f = \frac{\pi_f^{(\gamma_c - 1)/\gamma_c} - 1}{\tau_f - 1} \tag{17}$$

$$\alpha = \frac{\eta_m (1 + f)(\tau_\lambda / \tau_r)\{1 - [\pi_f / (\pi_c \pi_b)]^{(\gamma_t - 1)e_t/\gamma_t}\} - (\tau_c - 1)}{\tau_f - 1} \tag{18}$$

$$\tau_t = 1 - \frac{1}{\eta_m (1 + f)} \frac{\tau_r}{\tau_\lambda} [\tau_c - 1 + \alpha(\tau_f - 1)] \tag{19}$$

$$\pi_t = \tau_t^{\gamma_t / [(\gamma_t - 1)e_t]} \tag{20}$$

$$\eta_t = \frac{1 - \tau_t}{1 - \tau_t^{1/e_t}} \tag{21}$$

$$\frac{P_{t16}}{P_{t6}} = \frac{\pi_f}{\pi_c \pi_b \pi_t} \tag{22}$$

$$M_{16} = \sqrt{\frac{2}{\gamma_c - 1}\left\{\left[\frac{P_{t16}}{P_{t6}}\left(1 + \frac{\gamma_t - 1}{2}M_6^2\right)^{\gamma_t/(\gamma_t - 1)}\right]^{(\gamma_c - 1)/\gamma_c} - 1\right\}} \quad (23)$$

$$\alpha' = \frac{\alpha}{1 + f} \quad (24)$$

$$c_{p6A} = \frac{c_{pt} + \alpha' c_{pc}}{1 + \alpha'} \quad (25)$$

$$R_{6A} = \frac{R_t + \alpha' R_c}{1 + \alpha'} \quad (26)$$

$$\gamma_{6A} = \frac{c_{p6A}}{c_{p6A} - R_{6A}} \quad (27)$$

$$\frac{T_{t16}}{T_{t6}} = \frac{T_0 \tau_r \tau_f}{T_{t4} \tau_t} \quad (28)$$

$$\tau_M = \frac{c_{pt}}{c_{p6A}} \frac{1 + \alpha'(c_{pc}/c_{pt})(T_{t16}/T_{t6})}{1 + \alpha'} \quad (29)$$

$$\phi(M_6, \gamma_6) = \frac{M_6^2\{1 + [(\gamma_t - 1)/2]M_6^2\}}{(1 + \gamma_t M_6^2)^2} \quad (30)$$

$$\phi(M_{16}, \gamma_{16}) = \frac{M_{16}^2\{1 + [(\gamma_c - 1)/2]M_{16}^2\}}{(1 + \gamma_c M_{16}^2)^2} \quad (31)$$

$$\Phi = \left[\frac{1 + \alpha'}{\frac{1}{\sqrt{\phi(M_6, \gamma_6)}} + \alpha'\sqrt{\frac{R_c \gamma_t}{R_t \gamma_c}\frac{T_{t16}/T_{t6}}{\phi(M_{16}, \gamma_{16})}}}\right]^2 \frac{R_{6A}\gamma_t}{R_t \gamma_{6A}} \tau_M \quad (32)$$

$$M_{6A} = \sqrt{\frac{2\Phi}{1 - 2\gamma_{6A}\Phi + \sqrt{1 - 2(\gamma_{6A} + 1)\Phi}}} \quad (33)$$

$$\frac{A_{16}}{A_6} = \frac{\alpha' \sqrt{T_{t16}/T_{t6}}}{\frac{M_{16}}{M_6}\sqrt{\frac{\gamma_c R_t}{\gamma_t R_c}\frac{1+[(\gamma_c-1)/2]M_{16}^2}{1+[(\gamma_t-1)/2]M_6^2}}} \tag{34}$$

$$\pi_{M\,\text{ideal}} = \frac{(1+\alpha')\sqrt{\tau_M}}{1+A_{16}/A_6}\frac{\text{MFP}(M_6, \gamma_t, R_t)}{\text{MFP}(M_{6A}, \gamma_{6A}, R_{6A})} \tag{35}$$

$$\pi_M = \pi_{M\,\max}\pi_{M\,\text{ideal}} \tag{36}$$

$$\frac{P_{t9}}{P_9} = \frac{P_0}{P_9}\pi_r\pi_d\pi_c\pi_b\pi_t\pi_M\pi_{\text{AB}}\pi_n \tag{37}$$

$$M_9 = \sqrt{\frac{2}{\gamma_9 - 1}\left[\left(\frac{P_{t9}}{P_9}\right)^{(\gamma_9-1)/\gamma_9} - 1\right]} \tag{38}$$

$$\frac{V_9}{a_0} = M_9\sqrt{\frac{\gamma_9 R_9 T_9}{\gamma_c R_c T_0}} \tag{39}$$

$$f_O = \frac{f}{1+\alpha} + f_{\text{AB}} \tag{40}$$

$$\frac{F}{\dot{m}_0} = \frac{a_0}{g_c}\left[(1+f_O)\frac{V_9}{a_0} - M_0 + (1+f_O)\frac{R_9}{R_c}\frac{T_9/T_0}{V_9/a_0}\frac{1-P_0/P_9}{\gamma_c}\right] \tag{41}$$

$$S = \frac{f_O}{F/\dot{m}_0} \tag{42}$$

$$\eta_P = \frac{2g_c V_0(F/\dot{m}_0)}{a_0^2[(1+f_O)(V_9/a_0)^2 - M_0^2]} \tag{43}$$

$$\eta_{Th} = \frac{a_0^2[(1+f_O)(V_9/a_0)^2 - M_0^2]}{2g_c f_o h_{PR}} \tag{44}$$

$$\eta_O = \eta_P\eta_{Th} \tag{45}$$

After the initial PCA program was completed, the team decided to do one for the candidate engine. By using the results from the wave drag calculations along with input values from industry (e.g. GE GenX fan ratio and bypass ratio) depending on what engine parts were used for the team's design. Because the new design was performing under different conditions, the program yielded different results. The propulsive and thermal efficiencies were 61.8% and 30.9% respectively to yield an overall efficiency of 19.1%. The latter program involved engine performance under the AIAA conditions set in the design characteristics, while the first was under typical mission conditions for current turbofans. In Appendix X are figures of the Excel program created for the PCA.

4.2 - Supersonic Wave Drag Calculations

Modeling wave drag is conducted both numerically (analytically) and computationally for initializing baseline supersonic wave drag calculations. In order to determine a baseline inviscid wave drag, various projected areas of the aircraft mainframe body such as; fuselage, wings, and control surfaces are constructed in mathematically relationships. Estimated from Euler differential equation, each component is simplified to achieve bounds on obtaining minimum drag [21]. Equation (1), Slender Body Wave Drag, describes the fuselage main body frame in integrating along for slender bodies with considerably high fineness ratios.

Slender Body Wave Drag

$$D_{wave} = -\frac{\rho_\infty U_\infty^2}{4\pi}\int_0^l\int_0^l S''(x_1)S''(x_2)\ln|x_1 - x_2|dx_1dx_2 \qquad (46)$$

The minimum wave drag estimation is crude and simplistic formula that provides projected area of drag due to supersonic thin airfoil theory. Due to air density compressibility effects at supersonic speeds, the approximation of drag among an airfoil is explored. Equation (46), V represents the sonic velocity of airflow, l represents the length of the airfoil, ρ is the density of air, and U displays the dynamic pressure.

Minimum Wave Drag

$$D_{wave} = \frac{64V^2}{\pi l^4}\rho_\infty U_\infty^2 \tag{47}$$

Volume-Dependent Wave Drag uses the estimated wave drag of a wing. Specifically referenced in J.H.B Smith text, he derives the expression for the volume dependent wave drag for an ellipse shape shown in Equation (47). In the equation *t* is maximum thickness, *b* is the semi-major axis, and *a* is the semi-minor axis.

Volume-Dependent Wave Drag

$$C_{D_{ow}} = \frac{t^2}{b^2}\left[\frac{\beta^2 + 2\,b^2/a^2}{(\beta^2 + b^2/a^2)^{3/2}}\right] \tag{48}$$

Using Euler principle, R.T. Jones' expression describes the mathematical relationship for lift-dependent wave drag [2]. It considered the ellipse of the same area, S, and length, l as seen in Equation (49)

Lift Dependent Wave Drag

$$C_{D_{wl}} = \frac{\pi l^2}{16\,S} C_L^2\left[\sqrt{1 + (M^2-1)\left(\frac{4\,S}{\pi l^2}\right)^2} - 1\right] \tag{49}$$

Using the governing equations estimating wave drag referencing equations 1 through 4, a numerical baseline estimation of wave drag can be calculated. The design challenged aircraft will explore a trade study of total drag and the number of engines needed to overcome the resistance force. Displayed in Figure 18 are sample calculations of estimated supersonic wave drag at Mach conditions of 1.3, 1.6, and 1.8.

3 High Speed Cases		Max Condition	Cruise Condition	Low Condition
	Mach	1.8	1.6	1.3
Inputs	Units			
Physics Parameters				
Lift (Weight)	lbf	317499	317499	317499
Velocity (ft/s)	ft/s	2009.59	1786.3	1451.37
Altitude	ft	55,000	55,000	55,000
density	lbm/ft^3	0.00922	0.00922	0.00922
Viscosity	lbm/ft-s	0.00000955	0.00000955	0.00000955
Reynold's Number	(unitless)	202794039.7	180261144.4	146462306
Projected [with respect to area]				
Wing Area (ft^2)	ft^2	3351.5	3351.5	3351.5
Tail Area (ft^2)	ft^2	537.45	537.45	537.45
Aspect Ratio (unitless)	(unitless)	2.211051851	2.211051851	2.211051851
Taper Ratio (unitless)	(unitless)	0.082	0.082	0.082
Span (in)	in	1033	1033	1033
Root Chord (in)	in	1254.3	1254.3	1254.3
Tip Chord (in)	in	102.9	102.9	102.9
M.A.C. (in)	in	485.6	485.6	485.6
Sweep C/4	deg	64.41	64.41	64.41
Avg Exposed Chord	in	426.1	426.1	426.1
Chord S.O.B.	in	1159.8	1159.8	1159.8
Dihedral	deg	0	0	0
Length (of aircraft)	in	1848	1848	1848
Length Ratio (length^2/area)	(unitless)	0.5513948978	0.5513948978	0.5513948978
t	in	0.031	0.031	0.031
t/c	(unitless)	0.00002672874634	0.00002672874634	0.000026728746
Wetted Surface Area	ft^2	4372.11	4372.11	4372.11
Fineness Ratio (l/d)	(unitless)	21	21	21
Interference Factor		1	1	1
Reference [with respect to area]				
Area	ft^2	3197.779	3197.779	3197.779
Sweep C/4	deg	64.41	64.41	64.41
Sweep Leading Edge	deg	72/52/48	72/52/49	72/52/50

Figure 18: Numerical and analytical wave drag estimation for high speed supersonic compressible flow

Sweep Trailing Edge	deg	-21.62/-84.99/34.00	-21.62/-84.99/34.01	-21.62/-84.99/34.02
Slat Area	ft^2	126.71	126.71	126.71
Plain Flap Area	ft^2	156.12	156.12	156.12
Aileron Area	ft^2	82.44	82.44	82.44
Control Surface Area	ft^2	117.89	117.89	117.89
Coefficients				
Lift	(unitless)	0.002544235424	0.00644011194	0.009755419034
Zero-Lift Drag	(unitless)	0.002206293656	0.002258883998	0.00235466528
Induced Drag (Body)	(unitless)	0.00000093189244	0.000005970875731	0.000013700709
Skin Friction	(unitless)	0.001613692135	0.001652156925	0.001722211743
Wave-Lift (Wing)	(unitless)	0.002814462931	0.002224050378	0.00126074727
Wave Volume (Wing)	(unitless)	2.02E-09	2.44E-09	3.78E-09
Induced (Wing)	(unitless)	0.001446864341	0.001446864341	0.001446864341
e_effective (Wing)	(unitless)	0.3395337295	0.3941427279	0.5343692336
Wave Volume (Fuselage)	(unitless)			
Total Cd	**(unitless)**	**0.003820917684**	**0.003917011798**	**0.004090577733**
Total Cd_wave	**(unitless)**	**4.26E-03**	**3.67E-03**	**2.71E-03**
Total Drag	***lbf***	***33,116.00***	***24,588.26***	***14,542.71***
Total Thrust Required Per Engine		1.8	1.6	1.3
2	***lbf***	***16558.00169***	***12294.12847***	***7271.357137***
3	***lbf***	*11038.66779*	*8196.085644*	*4847.571425*
4	***lbf***	*8279.000845*	*6147.064233*	*3635.678569*

Figure 18: Numerical and analytical wave drag estimation for high speed supersonic compressible flow (continued)

4.3 - Inlet Design Calculations

CFD on supersonic inlet pressure recovery

Computational Fluid Dynamic Analysis is conducted to validate and test two inlet design configurations. These configurations are analyzed to explore the pressure recovery to maximize efficiency for the fan and engine. As seen in Figure 19, the spike design CFD analysis shows a greater pressure recovery than the door panels in Figure 20.

Subsonic Mil Spec Pressure Recovery Calculation

$$\text{Mil. Spec: } M > 1 : pt2 / pt0 = ni * (1 - .075 * [M - 1] ^{1.35}) \qquad (50)$$

$$M > 1 : pt2 / pt0 = ni * (1 - .075 * [M - 1] ^{1.35})$$

$$= 3.994095965$$

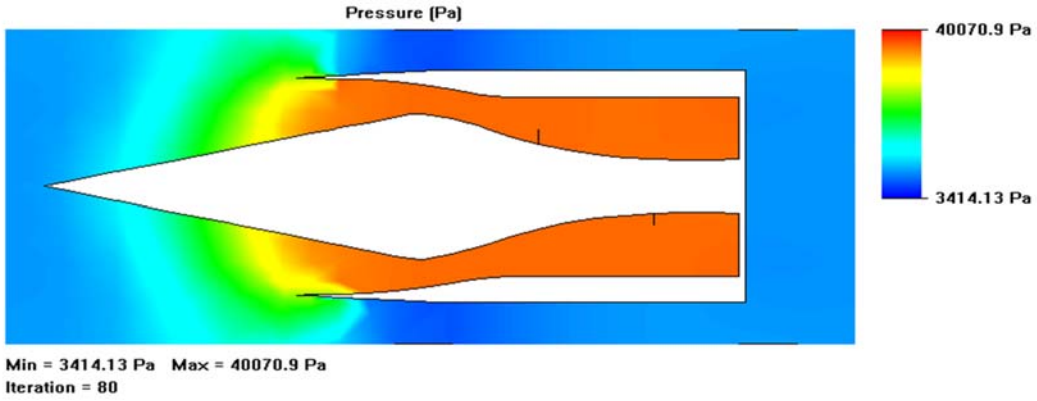

Figure 19: Supersonic spike CFD analysis for inlet design

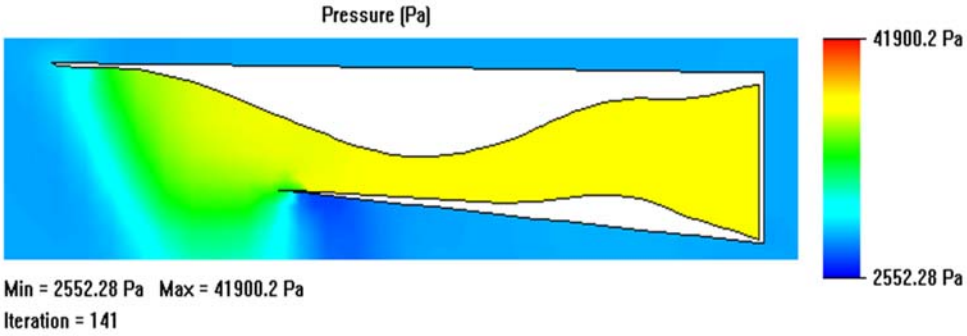

Figure 20: Supersonic panel channel CFD analysis for inlet design

Mil. Spec: Pressure Recovery

$$M > 1 : pt2 / pt0 = ni * (1 - .075 * [M - 1] ^{1.35}) \qquad (51)$$

$$= 3.292803708$$

During the optimization phase, a design trade study can be viewed in Appendix B Inlet Design Analysis Trade Studies. The final selection displays the CFD resultant analysis in Figure 21a, b, and c.

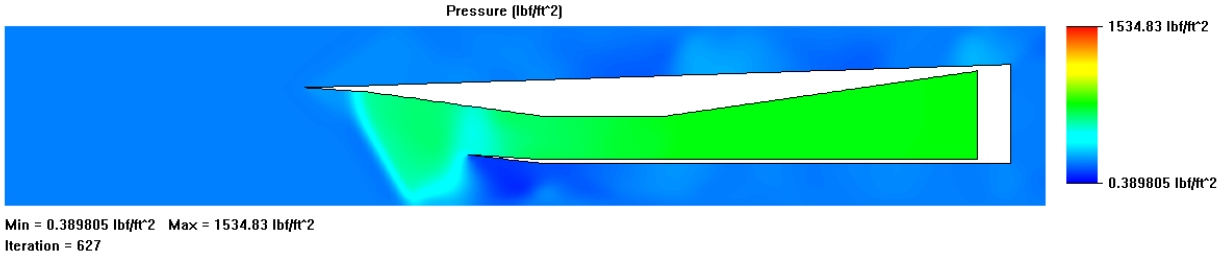

(a)

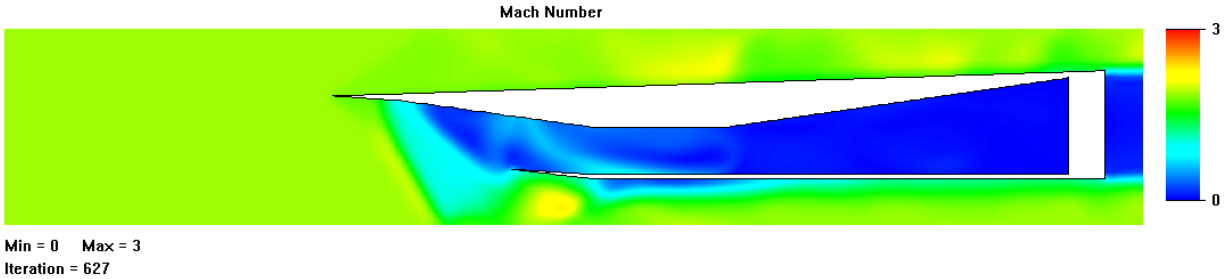

(b)

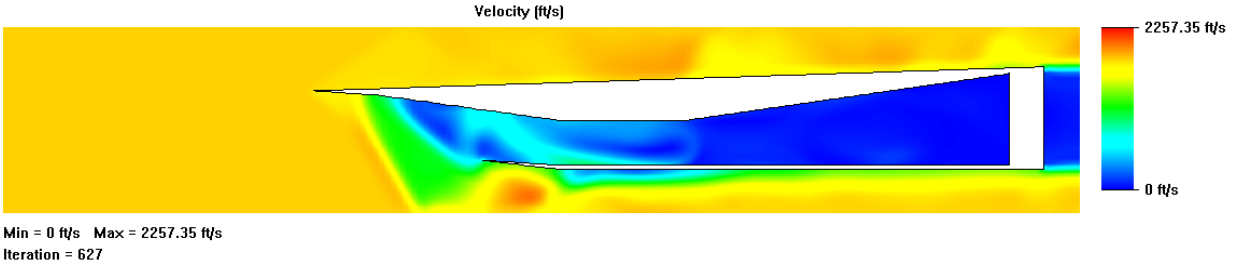

(c)

Figure 21: Supersonic extended and optimized panel channel CFD analysis for inlet design (a) Pressure (b) Mach Number (c) Velocity

4.4 - Initial Weight Calculations

Initial sizing calculations are done to determine the empty weight as well as the take-off weight of the aircraft design. These calculations for this particular design are based on empirical equations and historical data found in similar aircraft with similar properties.

Mission Profile of the Aircraft

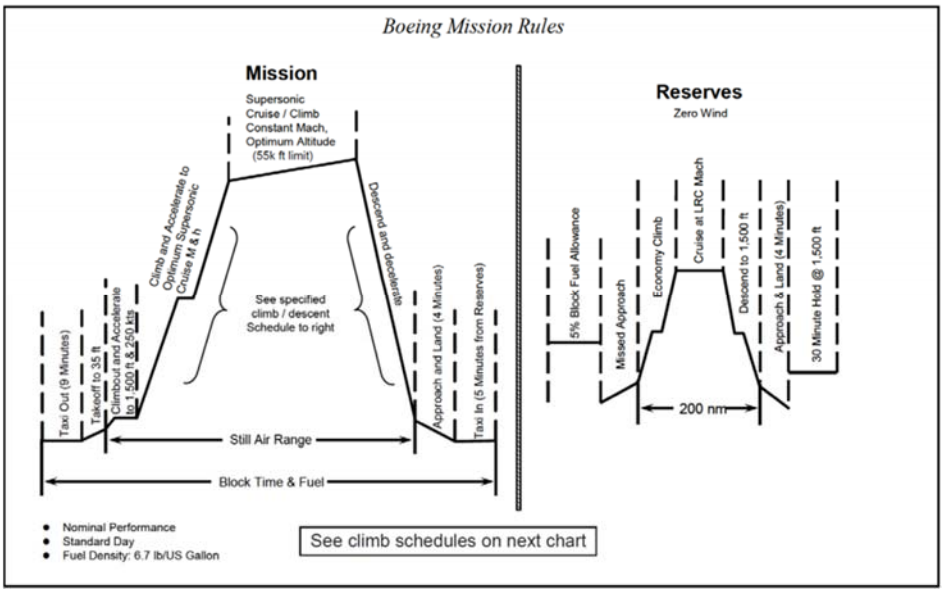

Figure 22: The mission profile of the aircraft

Estimate of Take-Off Gross Weight

Calculating take-off weight uses the following equation using the weight of the passengers and the weight of the payload. From the Aircraft Design textbook [10], mission segment weight fractions were found using Table 3.2.

The following equation is used to calculated an approximated gross take-off weight.

$$W_0 = \frac{W_{crew} + W_{payload}}{1 - \frac{W_{fuel}}{W_0} - \frac{W_{empty}}{W_0}} \quad (52)$$

The fuel weight fraction is calculated using the following equation in regards to the mission segment.

$$\frac{W_f}{W_0} = 1.06 \times \left(1 - \frac{W_4}{W_0}\right) \quad (53)$$

The empty weight fraction is calculated using the equation below. Since the design will be in supersonic conditions, the most approximate value that is most similar would be a military jet fighter. Thus, values for a military jet fighter were used in the empty weight fraction calculation.

$$\frac{W_e}{W_0} = 2.264 \times W_0^{-0.13} \quad (54)$$

Using the Breguet range equation, this was used to calculated the weight fraction for climb.

$$\frac{W_3}{W_2} = e^{-\frac{RC}{V_\infty\left(\frac{L}{D}\right)}} \quad (55)$$

By using these equations, an approximated weight was calculated using an iterative process. The calculated empty weight of the aircraft was found to be approximately 138,482.04 pounds and the take-off weight was found to be 317,432.72 pounds. A detailed calculation can found in the Appendix I.

Figure 23: Computer Aid Model demonstrating cruise climb prior to supersonic cruise mission.

4.5 - Computational Fluid Dynamics

SolidWorks is used to perform the CFD analyses for varying parts of the aircraft and engine. It was selected as the team's sole source of CFD analyses due to ease of use and common familiarity. Depending on the parts examined, certain key parameters were solved for. For example, when studying the flow through the nozzle, the velocity, Mach number, pressure, and temperature were the key aspects. These tests would enlighten the team about how hard the nozzle would expel the flow, if the jet could reach Mach 1.6 - 1.8 at 55 kft, and how much noise the engine would produce via the exit velocity. Seen in Appendix A, B, and C are various CFD analyses performed on some of the components of the aircraft.

4.6 - Computational Methods - PARA

PARA is a supplemental piece of software provided by AIAA through the Elements of Propulsion text by Jack D. Mattingly. PARA is a useful software package for this project because it is capable of conducting simultaneous equations involved in parametric cycle analysis. With this ability, various trade studies were conducted on the baseline engine. For this program, input data is required to solve for the iteration variables desired. In this program, a set of input data was provided by AIAA. PARA allows for a through comparison

of varied input values which not only tabulates the data but also graphs it. The input values as well as the output deliverables are seen below.

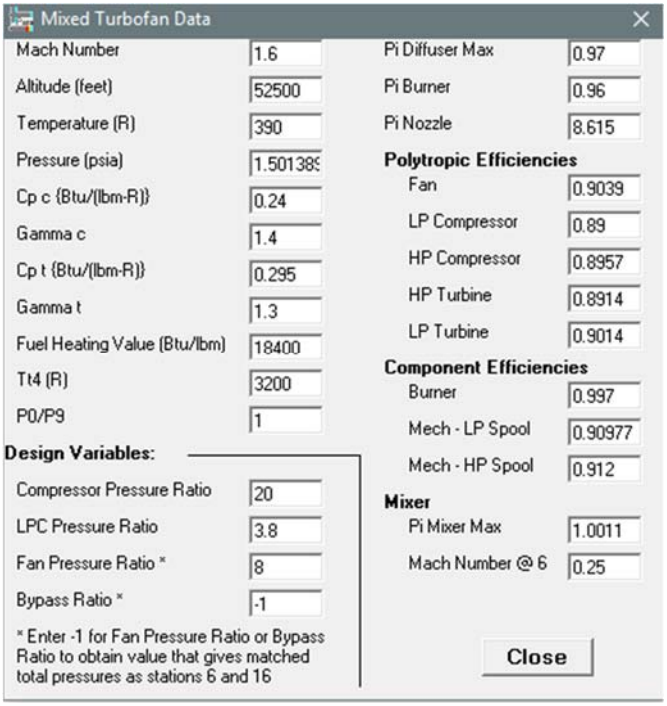

Figure 24: Input parameters into the program

The parameters placed inside the PARA program are placed shown in Figure 24. The design values are shown on the bottom left corner of the input window. These values are designated for trade studies and are used to determine the combination of parameters that will meet the needs of the desired design.

```
Parametric Calcs (PARA V5.0)              Date: 4/29/2018 1:27:07 PM
File: D:\Google Drive\School\Spring 2018\ISYE 4803 - Aero Senior Design\Innovat
                Real Turbofan Engine with Mixed Exhaust
**********************      Input Data      **********************
      Mach No    =  1.600                Alpha         =-001.000
      Alt (ft)   =  52500                Pi f / Pi cL  =8.000/3.800
      T0 (R)     = 390.00                Pi d (max)    =  0.970
      P0 (psia)  =  1.501                Pi b          =  0.960
      Density    = .0003229              Pi n          =  8.615
       (Slug/ft^3)                      Efficiency
      Cp c       = 0.2400 Btu/lbm-R      Burner        =  0.997
      Cp t       = 0.2950 Btu/lbm-R      Mech Hi Pr    =  0.912
      Gamma c    = 1.4000                Mech Lo Pr    =  0.910
      Gamma t    = 1.3000                Fan/LP Comp   =0.904/0.890 (ef/ecL)
      Tt4 max    = 3200.0 R              HP Comp       =  0.896 (ecH)
      h - fuel   =  18400 Btu/lbm        HP Turbine    =  0.891 (etH)
      P0/P9      = 1.0000                LP Turbine    =  0.901 (etL)
      *** Mixer ***                      Pi Mixer max  =  1.001
************************     RESULTS     ************************
      Tau r      =  1.512                a0 (ft/sec)   =  968.2
      Pi r       =  4.250                V0 (ft/sec)   = 1549.1
      Tau L      = 10.085
  Pi c F/mdot     S     M6    M16 TauTL Alpha Pt9/P9  V9/V0  T Eff  P Eff
 *** LP Compressor Pressure Ratio reset to   8.00
  8.00  Low Pressure Turbine Pressure Ratio > 1. This case is meaningless.
  8.50  Low Pressure Turbine Pressure Ratio > 1. This case is meaningless.
  9.00 138.74 0.8963 .250 .010 .9961 0.000273.457  3.752 79.581 42.490
  9.50 137.64 0.8949 .250 .000 .9906 0.000273.457  3.731 79.355 42.677
 10.00 136.60 0.8934 .250 .000 .9856 0.000273.457  3.711 79.160 42.855
 10.50 135.61 0.8918 .250 .000 .9809 0.000273.457  3.693 78.993 43.024
 11.00 134.68 0.8900 .250 .000 .9766 0.000273.457  3.675 78.852 43.186
 11.50 133.79 0.8882 .250 .000 .9726 0.000273.457  3.658 78.734 43.341
 12.00 132.94 0.8862 .250 .000 .9689 0.000273.457  3.642 78.637 43.489
 12.50 132.13 0.8842 .250 .000 .9655 0.000273.457  3.627 78.559 43.632
 13.00 131.36 0.8821 .250 .000 .9622 0.000273.457  3.612 78.497 43.770
 13.50 130.61 0.8800 .250 .000 .9592 0.000273.457  3.598 78.452 43.902
 14.00 129.90 0.8778 .250 .000 .9564 0.000273.457  3.584 78.421 44.030
 14.50 129.21 0.8755 .250 .000 .9537 0.000273.457  3.571 78.404 44.154
```

Figure 25: Output values from the program based on iterated LPC Pressure Ratio

Figure 25 is an example of the output results that come from the PARA program. The results show the iterations on the LPC pressure ratio. For each iteration, values for the thermal efficiency, propulsive efficiency, fuel to air ratio, and many other engine values are calculated. The PARA program is powerful in conducting multiple trade studies on multiple parameters. An example of one trade study is shown with Figure 26.

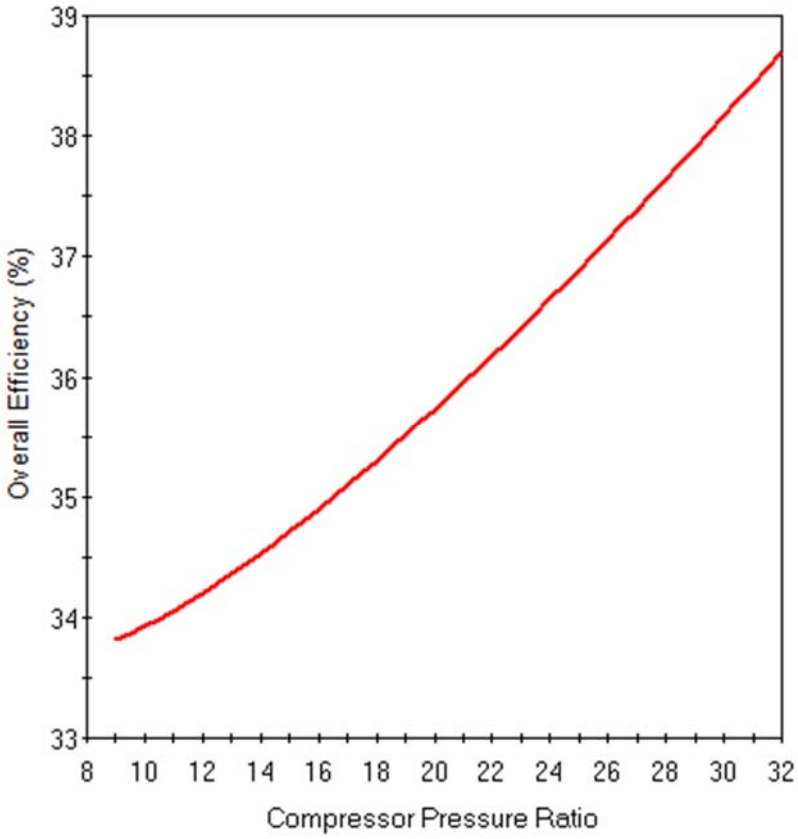

Figure 26: Output values from the program based on iterated LPC Pressure Ratio

In Figure 26, the output values from the LPC compressor iterations allowed for plots of varying results. For Figure 26, the overall efficiency of the engine can be observed with regards to the LPC pressure ratio. A more detailed analysis of plots are seen in Appendix D. In Appendix D, carpet plots were generated to plot multiple sets of data in one graph. The carpet plots will aid in refining the overall engine design.

4.7 - Computational Methods - TURBN

TURBN is another supplemental software provided through the Elements of Propulsion text by Mattingly. It is valuable because with it, one can solve simultaneous equations concerning turbine performance. However, the software has some constraints with certain parameters such as limitations for the mean radius and the temperature. But with it, simulations were able to be done on a similar engine. To initiate the program, input

variables must be submitted for the software to solve for the specified variables. The input data is provided by AIAA with assumptions also being made for certain values based on the software's suggestion and the text. Below are sample calculations done from the program for the first stage of the turbine along with a chart generated showing the trends of different variables in relation to others and the velocity triangle for the rotor and stator blades.

```
TURBN V5.50 - Data File: Default Data
Stage #01    Date - 4/28/2018    Time - 5:55:17 PM
 Corr Flow =   2.70 lbm/s  M1  = 0.4000  Tt1 = 3200.0 R   Pt1 = 300.00 psia
 Mass Flow =  22.20 lbm/s  M2  = 1.0500  AL2 = 41.79      AL1 = 30.00
 u3/u2 = 1.0000 phis= 0.020 et  = 0.900  Um  =  1182 ft/s rm  = 10.00 in
 Stator: Z = 1.0000   c/h = 1.0000   Rotor: Z = 1.0000   c/h = 1.0000
 Gamma = 1.3000 Gas Const = 53.40ft-lbf/lbm-R  w =  1418 rad/s  AL3 =  0.00
 Omega = 0.2421        Cp = 0.2974 Btu/lbm-R

RESULT: Tt3/Tt1 = 0.9141  Pt3/Pt1 = 0.6488  DTt = 275.00 R  AN^2=2.011E+09
  Reaction  Hub = 0.2537  Mean    = 0.2667  Tip = 0.2793    Eff = 90.44%
  Flow   Area 1 =  14.95  Area 2  =  10.97  Area 3 =  12.41  in^2
  Coeff.  Load = 1.4667  Flow = 1.6409  Vel Rat = 0.5839  RPM  = 13,539
  Nozzle - # of Vanes  = 189   c/s = 0.620
  Rotor  - # of Blades = 449   c/s = 1.330  M3Rt = 0.9318

   Station    1h    1m    1t    2h    2m    2t   2Rm   3Rm    3h    3m    3t
Prop:     ------------------------------------------------------------------
 Tt     R |  3200  3200  3200  3200  3200  3200  3019  3019  2925  2925  2925
 T      R |  3125  3125  3125  2742  2746  2749  2746  2673  2673  2673  2673
 Pt  psia | 300.0 300.0 300.0 297.1 297.1 297.1 230.8 223.2 194.6 194.6 194.6
 P   psia | 270.5 270.7 270.9 152.2 153.1 153.9 153.1 131.6 131.6 131.6 131.6
 M        | 0.401 0.400 0.399 1.055 1.050 1.045 0.814 0.929 0.794 0.794 0.794
 Vel ft/s |  1060  1057  1054  2611  2600  2590  2016  2270  1939  1939  1939
 u   ft/s |   915   915   915  1939  1939  1939  1939  1939  1939  1939  1939
 v   ft/s |   535   528   522  1748  1733  1718   551  1182     0     0     0
 alpha deg| 30.30 30.00 29.71 42.04 41.79 41.54                0.00  0.00  0.00
 beta  deg|                                        15.88 31.36
 radius in|  9.88 10.00 10.12  9.91 10.00 10.09 10.00 10.00  9.90 10.00 10.10
```

Figure 27: TURBN Stage 1 calculations

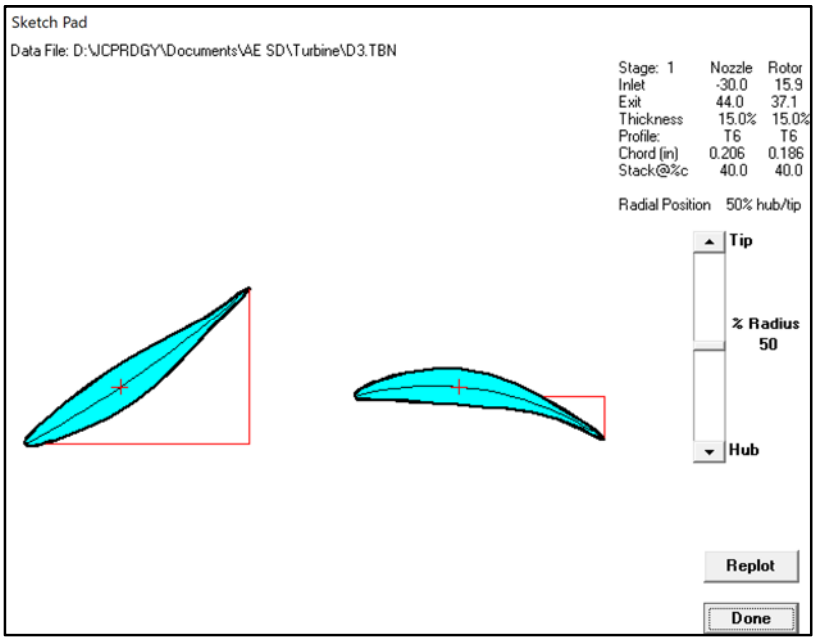

Figure 28: Turbine Blade Profile

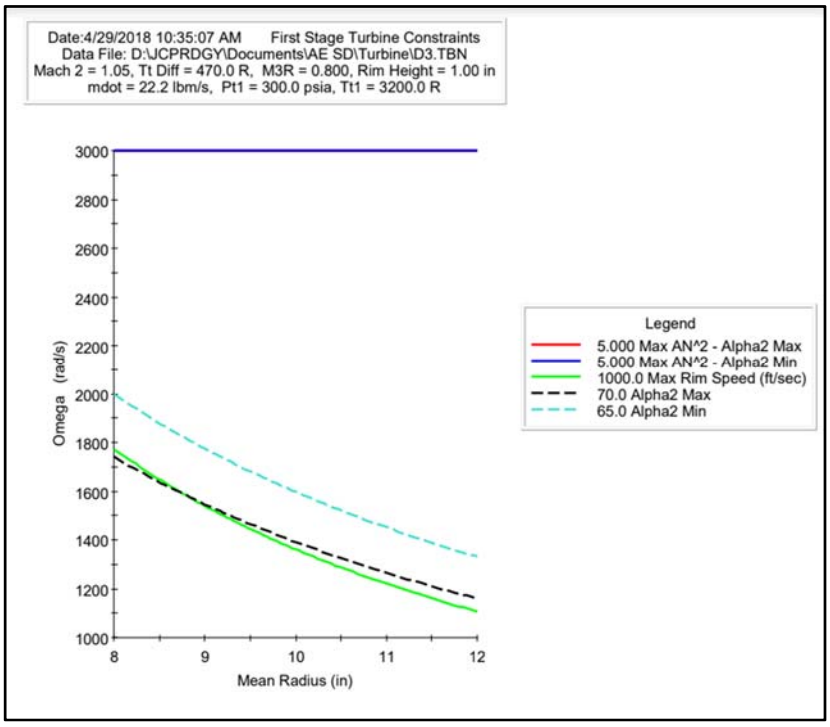

Figure 29: Table of Turbine Constraints (Angular Vel. vs. Mean Radius)

Chapter 5: Results and Discussion

5.1 - Historical Data

The ensure feasibility in the design decisions for candidate engines for supersonic transport, considerations needed to be made in relation to existing engines. Research was done on existing engines to determine their respective technical specifications. Through various sources, a compiled tabulated list of values of technical specifications for existing engines was created. Specifications tabulated include: Thrust, Specific Fuel Consumption, Overall Pressure Ratio Fuel Pressure Ratio, Bypass Ratio, Thrust at Cruise, Specific Fuel Consumption at Cruise, Cruise Speed, Cruise Altitude, and other parameters were tabulated. A more detailed view of these values can be seen in the appendix.

Given that the information for each engine is provided, plots were generated to determine historical trends based on engine type. Multiple plots were generated using values found specific to each engine. Parameters for each of these engines were compared and plotted to obtain trends that would allow design decisions for candidate engines. To observe the differences between each engine, these plots can be found in the Appendix H. Using the tabulated data, reasonable values can be determined for each engine. Based on the requirements provided by AIAA and NASA, sound decisions can be made for each parameter. The process for selecting design parameters will point to the generated plots from the historical data to align design selections within a reasonable range.

5.2 - Trade Study Engine Design

To generate trade studies from the tabulated historical data, a comparison was made between two varying specifications. Using these respective parameters, trends can be observed. For the thrust plots, the points were extracted from the historical data and plotted against other values to determine the trends for both military and commercial aircraft. For

efficiency plots, baseline values were selected and kept consistent. To observe changing effects, a single parameter was changed to observe the efficiencies. Thermal and propulsive efficiencies were determined for each engine. Given the varying geometries of each engine, values that were kept constant were:

Cruise constant parameters:

- Altitude
- Airspeed
- Temperature
- Nozzle and core exit velocities
- Speed of sound
- Fuel to air ratio

These listed parameters are then used in the corresponding efficiency calculations located in the Appendix I. The data from our graphs are with respect to varying bypass ratio, thus, there is a constant increase in relation to overall efficiency seen in the appendix.

5.3 - Discussion of Historical Data

Trade studies were conducted for both military and commercial aircraft and their respective engines. By comparing thrust to several other parameters such as OPR, TSFC, and BPR, different trends can be found. As seen in Appendix I, thrust is directly related to the OPR, displaying a linearly increasing trendline. This makes sense since the difference in pressure is a contributing factor to how fast an aircraft can travel.

A variety of trends can be observed from the generated plots. These trends are useful when determining the parameters for selecting values for the final design of the engine. Based on the trends observed from the plots generated, a value within the plotted range can be selected. For a specific design parameter, an associated plot and value comes as a result. Given the data through multiple aircraft engines, it provides perspective on the overall state

of jet engine technology. Not only can a decision on parameters for the engine can be made, but if a certain parameter is targeted, an associated set of data will come as a result. Thus, through backlogging of all previously plotted engines, a deeper investigation can be done. For that selected parameter, an engine is associated and analysis can be made on engine geometries, number of compressor stages, and other parameters crucial to engine design can be extracted. The depth of the historical plots will aid in further research and investigation for optimization of the final engine design.

As a result of generating historical plots for the given engines, a baseline parametric cycle analysis program was also generated. During the duration of progress made for this project, the parameters used to calculate and generate efficiency plots also streamlined the process for designing an engine. Through the compiled data, further analysis can be made for various design changes later. Due to the iterative nature of parametric cycle analysis, by generating the extensive and involved program for calculating overall efficiency, the processes needed for further investigation and optimization of the designed engine. As the challenge of designing an engine becomes more involved, through the designed program, values can be changed on the fly for refined decision making and comparison of parameters chosen experimentally to compare results such as efficiency, TSFC, and turbine inlet temperature.

Chapter 6: Prototype

6.1- Component Design

For the fan design, one modeling the fan for the GE Genx-1B engines is used. The fan has a bypass ratio of 9 and a fan pressure ratio of 2.25. The diameter of the fan is 70.3 inches. It is made from composite material and for the sake of the design should be hollowed out to reduce weight. The leading edge will be made from titanium for reasons discussed in the literature review section. Below are pictures of the fan blade and the fan hub assembly.

Figure 30: Engine Fan Blade

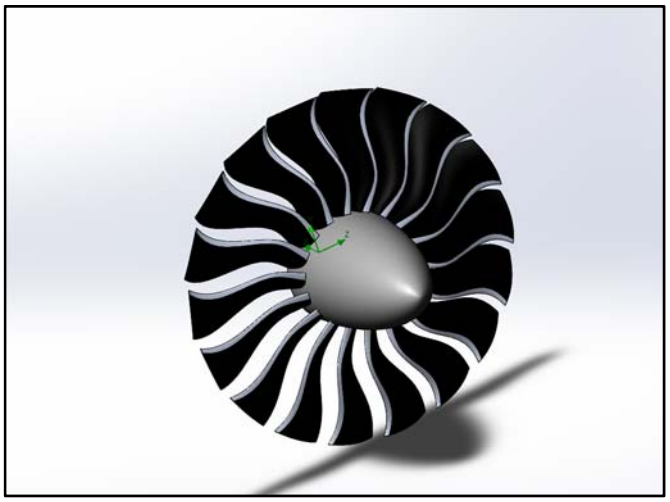

Figure 31: Engine Fan Hub

The next part of the engine that was developed using methods other than numerical analysis was the nozzle. Using the below equations and the design requirements, the team was able to determine what exit to throat area ratio was needed for Mach 1.6 flight.

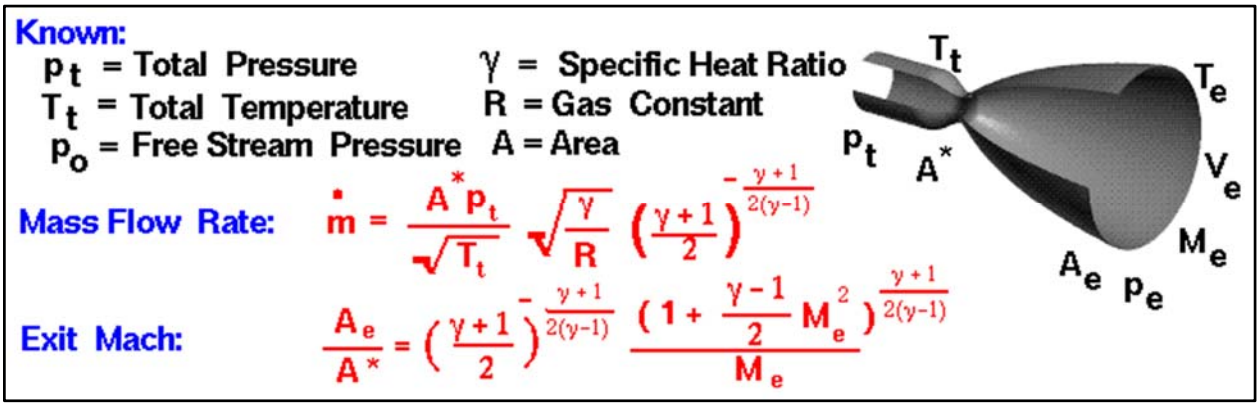

Figure 32: NASA Calculations for Nozzle Behavior

Calculations suggest an area ratio of 2.16 and a nozzle pressure ratio around 9.25. These calculations along with results from simulations for the thermodynamics involved in the turbomachinery will help complete a nozzle suitable for the mission. After Calculations were finished different designs for the nozzle were tested to confirm the calculations using SolidWorks and CFD analyses. See Appendix C for the CFD analysis results. The CFD showed that both the convergent-divergent nozzle and the plug nozzle design were able to achieve

Mach 1.6. Because the plug design was more reliable (consistent flow behavior) than the convergent-divergent nozzle also depicted in Appendix C, it was chosen for the final design. The aircraft must also reach speeds of Mach 1.8. To compensate for this, the team chose to go with a varying-area nozzle design to increase and decrease the exit area accordingly to achieve whatever speed the aircraft will require throughout the mission. Below are CAD models of the final design of the Varying Plug Nozzle.

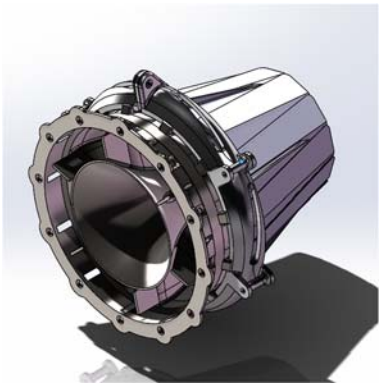

(a)

(b)

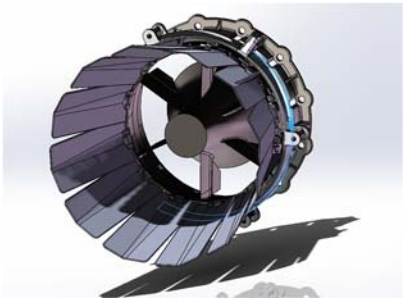

(c)

(d)

Figure 33: Models of: nozzle (a), plug design (b), fully opened nozzle exit (c), fully closed nozzle exit (d)

The model was created using some parts and methods found online in order to demonstrate how the nozzle panels can change area. The panels will ideally be tested to see if adding chevrons can help decrease the velocity of the exhaust jet. Preliminary tests showed exit velocities up to 4,000 ft/s in certain areas as seen in the CFD analysis in Appendix C. However, this was not consistent with the maximum Mach number calculated which insists that an error occurred during the analysis. Other ideas considered were to add a thermal

acoustic shield and chevrons at the end of the panels to see how that would change the velocity results.

6.2 - Aircraft Model

The design of the fuselage well undergoes various design configuration. In supersonic flow, every aspect of the vehicle must be utilized to maximize thrust, as well as reducing drag and specific fuel consumption. Airfoil have strong historical database and archives to access airfoil characteristics. Fuselage have a small selection of general shapes that base of the cylindrical geometry. In the next vehicle design challenge, a mathematical oval-conical shape will be modeled to integrate the high factors of aerodynamics and maintain feasibility spacing for passengers. The design selection combines various combinations of sized fuselage sections. This desired design will to maximize passengers in specific business economy sections.

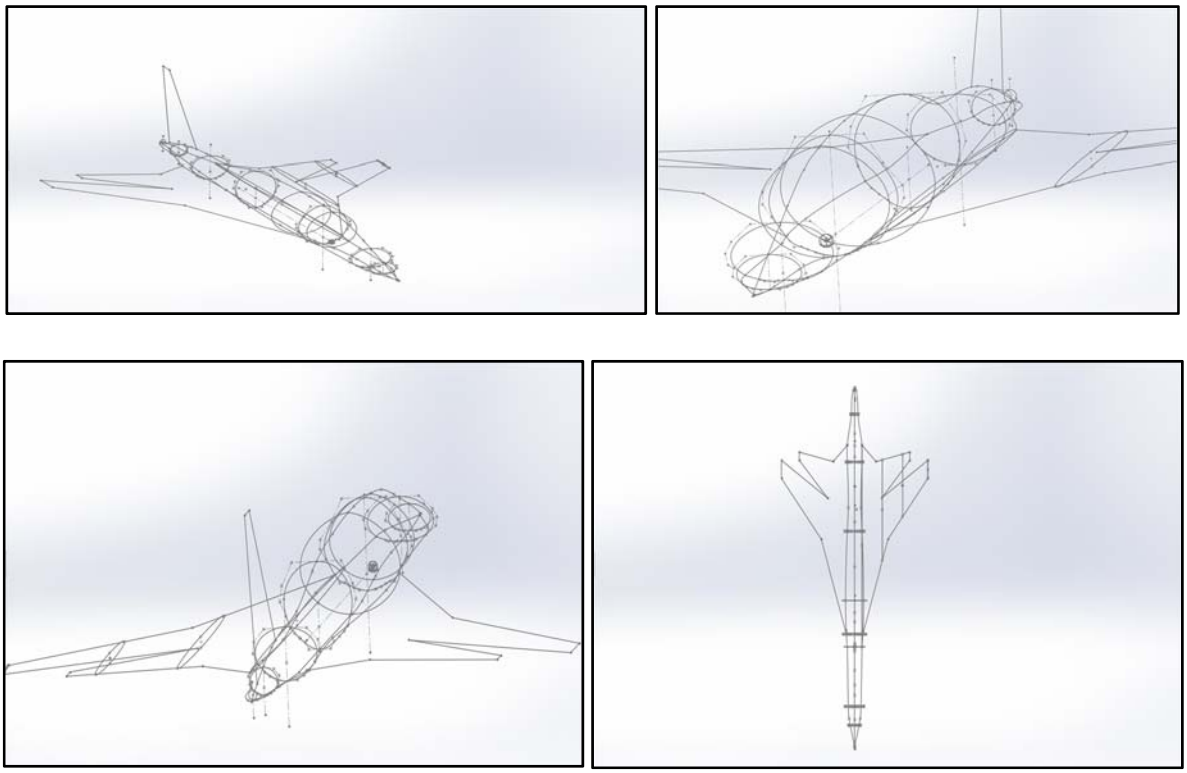

Figure 34: Isometric and profile view of supersonic prototype aircraft

Due to supersonic shock waves, the fuselage will house all its passengers and crew near the front of the vehicle. This allows the environmental control systems to be stored in the rear of fuselage. This promotes safer connections for the energy supply to the mixed flow turbofan engines. Also, as the aircraft applies an enormous amount of thrust to the engines, loud vibrations are more prone to resonate through the fuselage. Having the placement of engines further back reduces the amount of vibrations the passengers will experience. Shown in Figure 35, the profile loft views of the developmental supersonic prototype model.

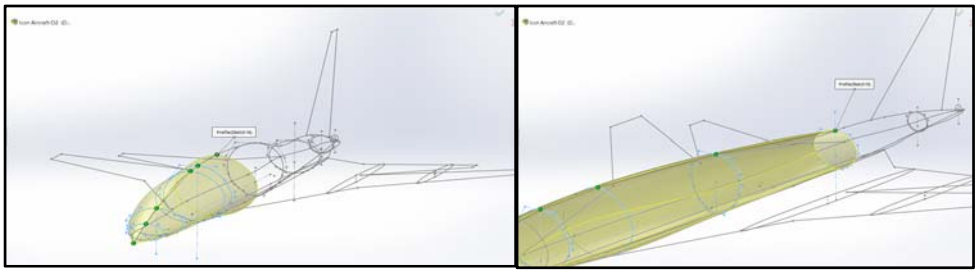

Figure 35: Computer Aid Model body lofting process of supersonic aircraft vehicle

For the designed targeted goal, a series of configurations of aircraft models are explored. The first design focused on a simplistic, yet effective delta triangle wing shown in Figure 36. Design 1 has a large vertical stabilizer in order to counteract aggressive unwanted moments.

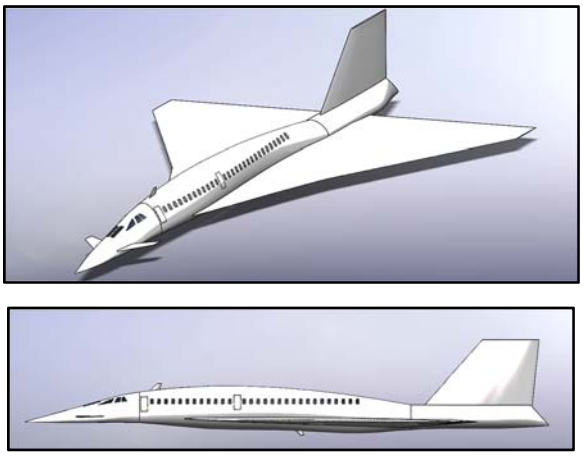

Figure 36: Design 1 concept with double delta straight wing geometry (isometric and right side respectively profiles)

With further analysis and numerical calculation, an optimization phase is approached in order to meet weight requirements. The weight from Design 1 exceeded the maximum

requirements. Thus, Design 2 aims to reduce weight by trimming area from the wing geometry. As seen in Figure 36, the wing geometry is now inspired and integrating a double delta wing configuration.

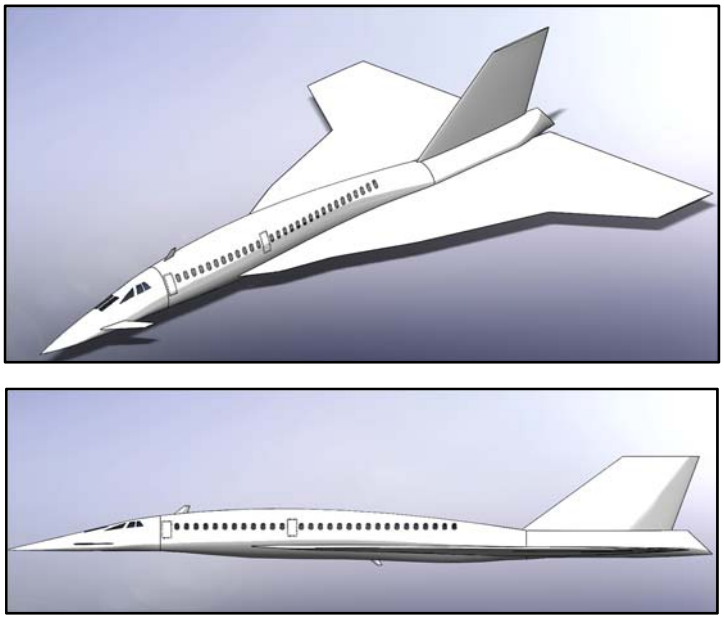

Figure 37: Design 2 concept with double delta straight wing geometry (isometric and right side respectively profiles)

The third iteration is an integrated design using cues from Design 1 and 2 by reducing both weight and drag. An extensive computational fluid dynamic analysis is conducted to understand the compressible effects of the vehicle. Appendix A displays computational fluid results for Design 3.

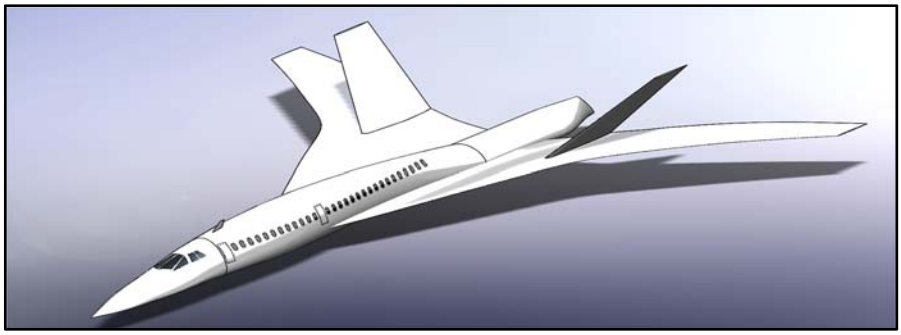

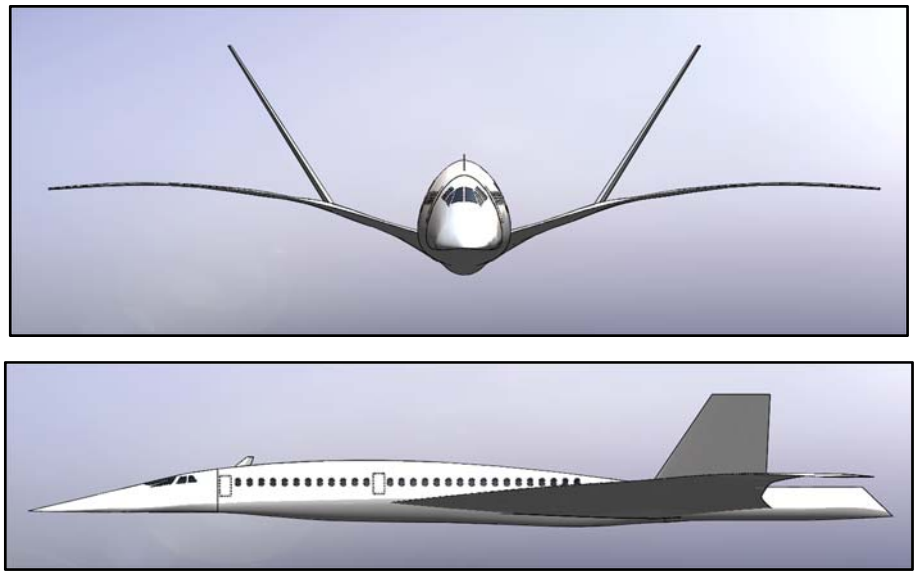

Figure 38: Design 3 concept with arced delta straight wing geometry (isometric, front, right side respectively profiles)

During the physics flow simulations, the objective is to understand the flow field as it interacts with the mail body. The lessons from Design 3, it improves and reduces the drag coefficient as well as maintains stability in flight shown from the computational model. Figures 39 shows the resultant Mach number, pressure and temperature comparison.

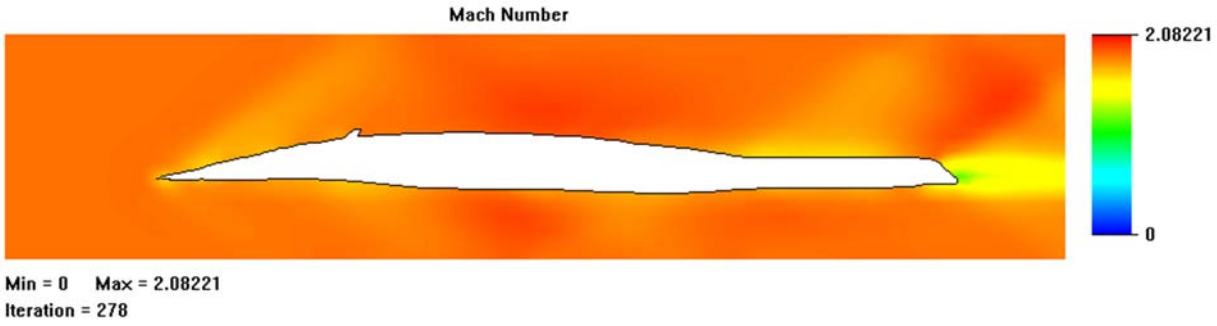

(a)

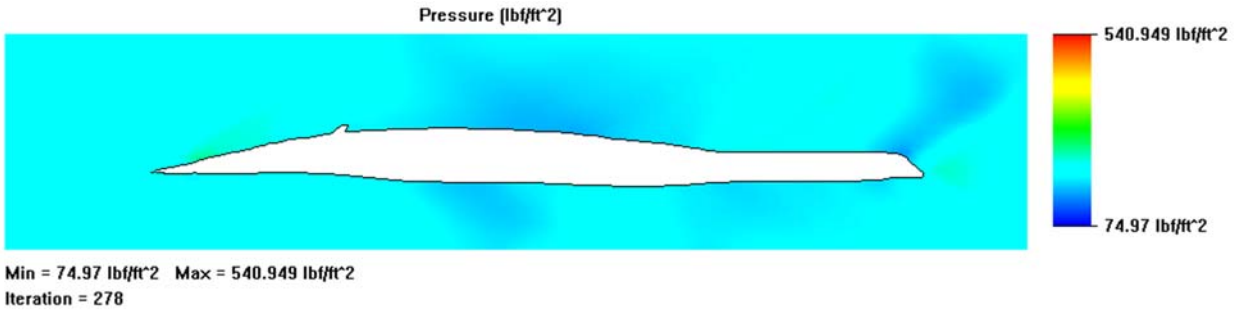

(b)

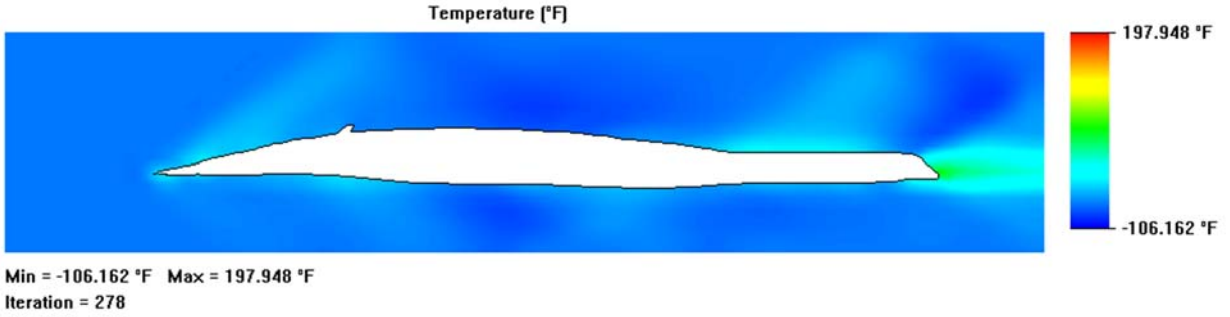

(c)

Figure 39: Design 3 concept with computational fluid dynamic model measuring (a) Mach number, (b) pressure, and (c) temperature respectively

After extensive simulation both numerically and computationally, the design of the vehicle becomes more matured overtime. From engine inlet and engine analysis, the geometry of the design requires the inlet length and width to be increases approximately by 15% for optimal efficiency. For the resizing of the inlet, configuration of engine placement is considered in two locations. The first orientation depicted in Figure 40, shows ducts located both above and below the vehicle. In comparison, Figure 41 demonstrates both ducts and engines underneath the fuselage. This eases maintenance capabilities and allows clean streamline airflow. In retrospect, the aircraft's center of gravity shifts backward requiring more structural support and longer landing gears.

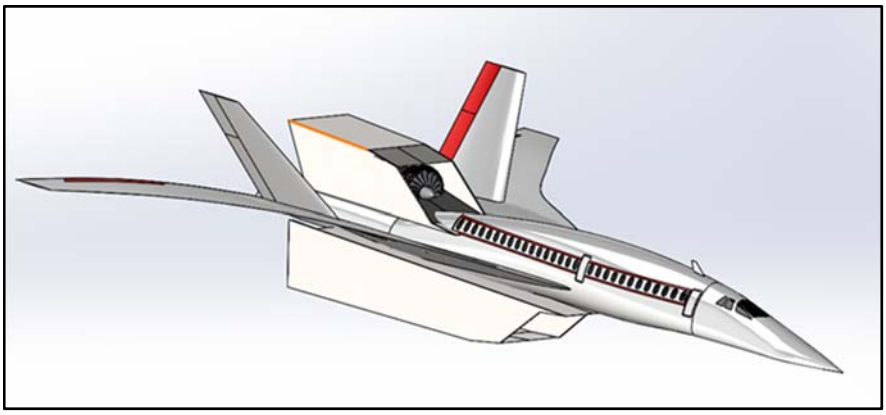

Figure 40: Design concept with engine location configuration for Orientation 1 (one engine above, with one below).

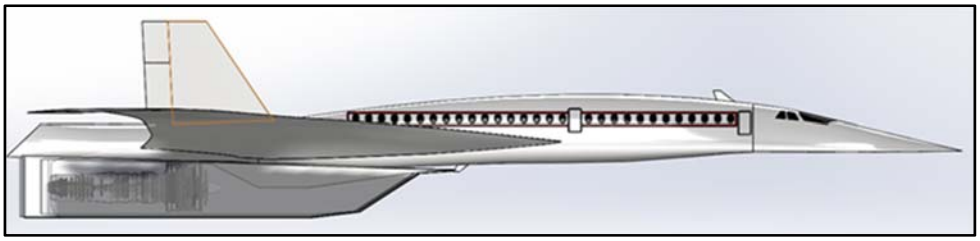

Figure 41: Design concept with engine location configuration for Orientation 2 (two engines below fuselage)

6.3 - Engine Model

A comprehensive assembly of each main driving component of the supersonic power plant is modeled to the required size shown in Figure 42 a and b. The propulsion system is a high bypass turbofan engine with baseline components influenced from both military and commercial vehicles. The engine is composed of composite swept fan blades with a diameter of 70.3 inches. The compressor has 11 stages with 10 stages of stator blades. The burner, or also known as combustion chamber is modeled from the TAPS II Combustor Clean Project (CLEEN).

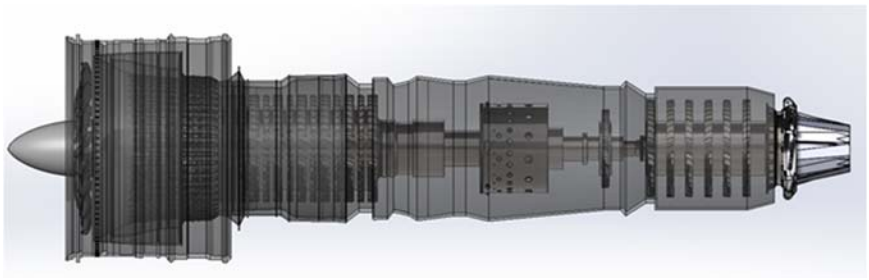

(a)

(b)

Figure 42: Design concept for supersonic engine power plant (a) side profile (b) front profile

6.4 - Interior Design Configuration

A design study was conducted to identify possible seating configurations for the interior of the aircraft. Considering this aircraft is designated as a business class aircraft, accommodations must be made to ensure a sense of luxury in the cabin. Two approaches were made in terms of identifying the seating desired. One approach was to implement standard seating found in economy plus seating found in the current state of commercial aircraft. The other approach was to utilize a more modern and private class seating configuration. In addition, the various seating configurations can be utilized with each seating arrangement. Using the two styles yield a slightly varying seating arrangement inside the cabin. The different configurations are shown in this section.

Standard Configuration

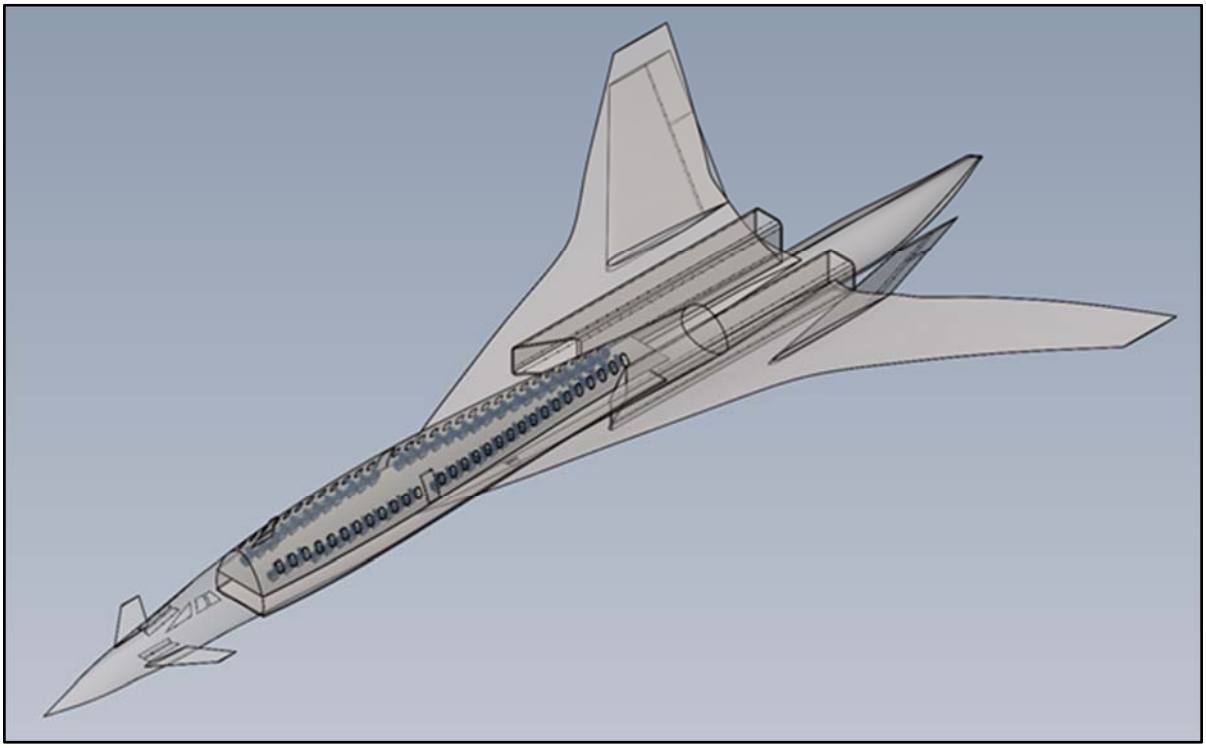

Figure 43: Standard configuration layout

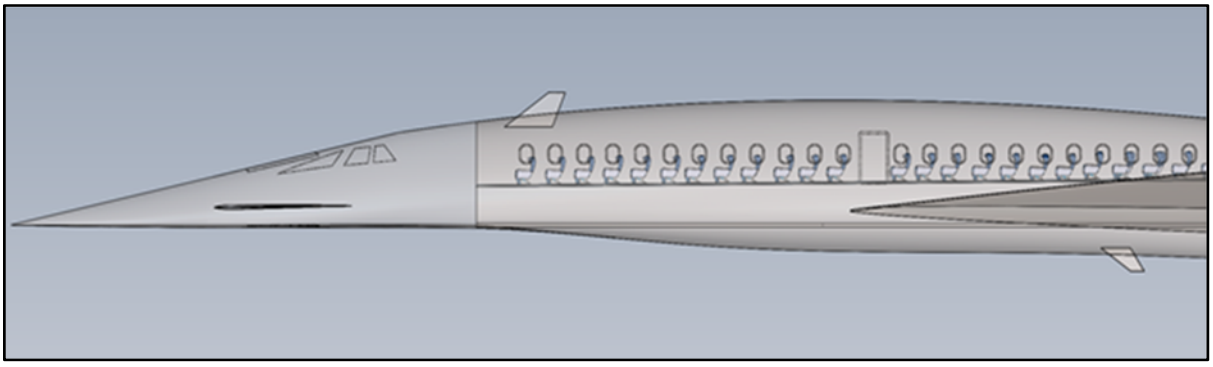

Figure 44: Side view of standard seating

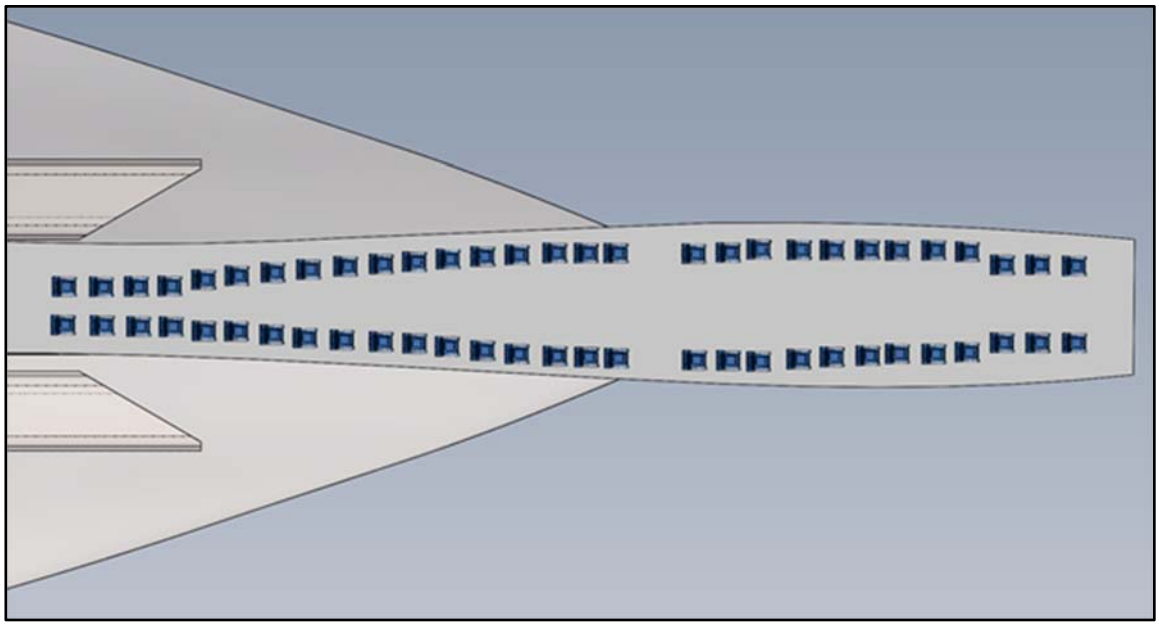

Figure 45: Overhead view of standard configuration (Left),

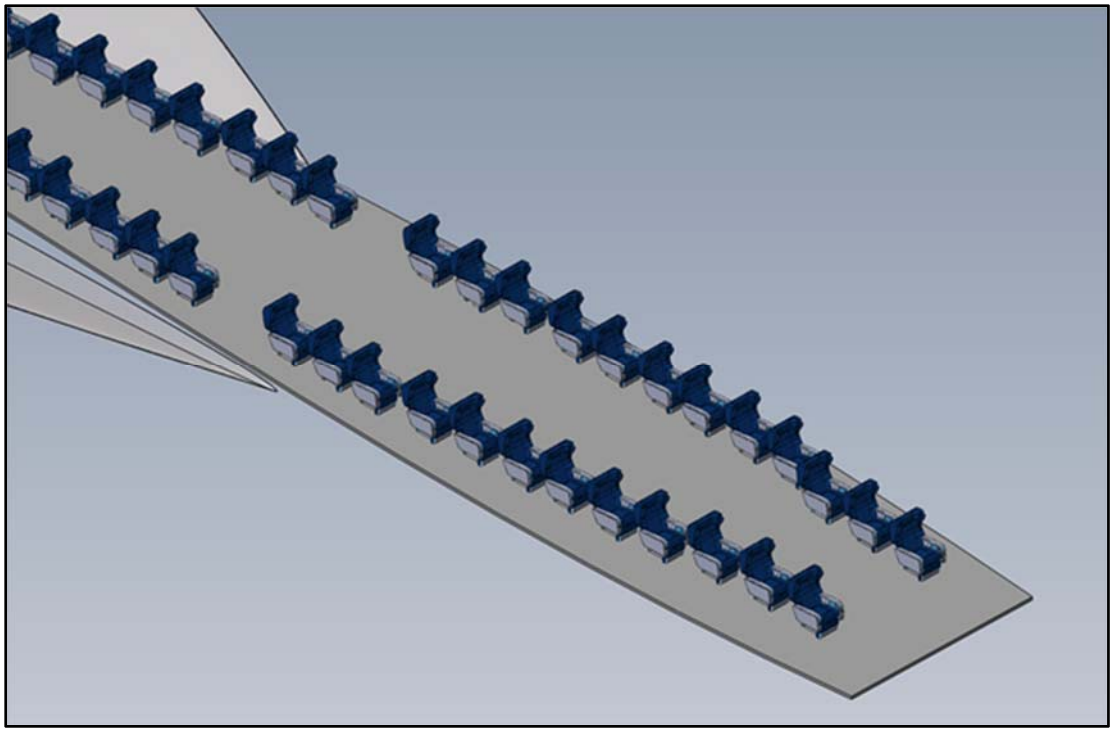

Figure 46: Isometric View (Right)

Figure 47: Detailed view of seating [28]

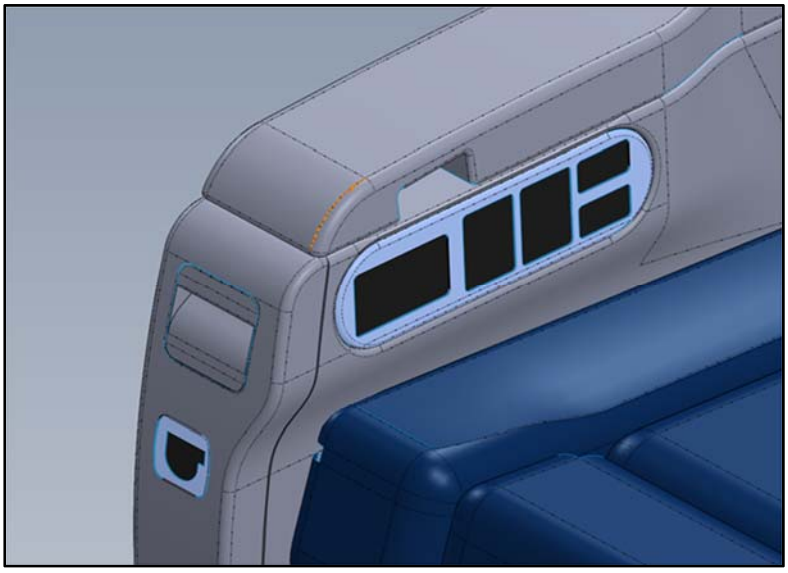

Figure 48: Detailed view of seating [28]

Luxury Class Configuration

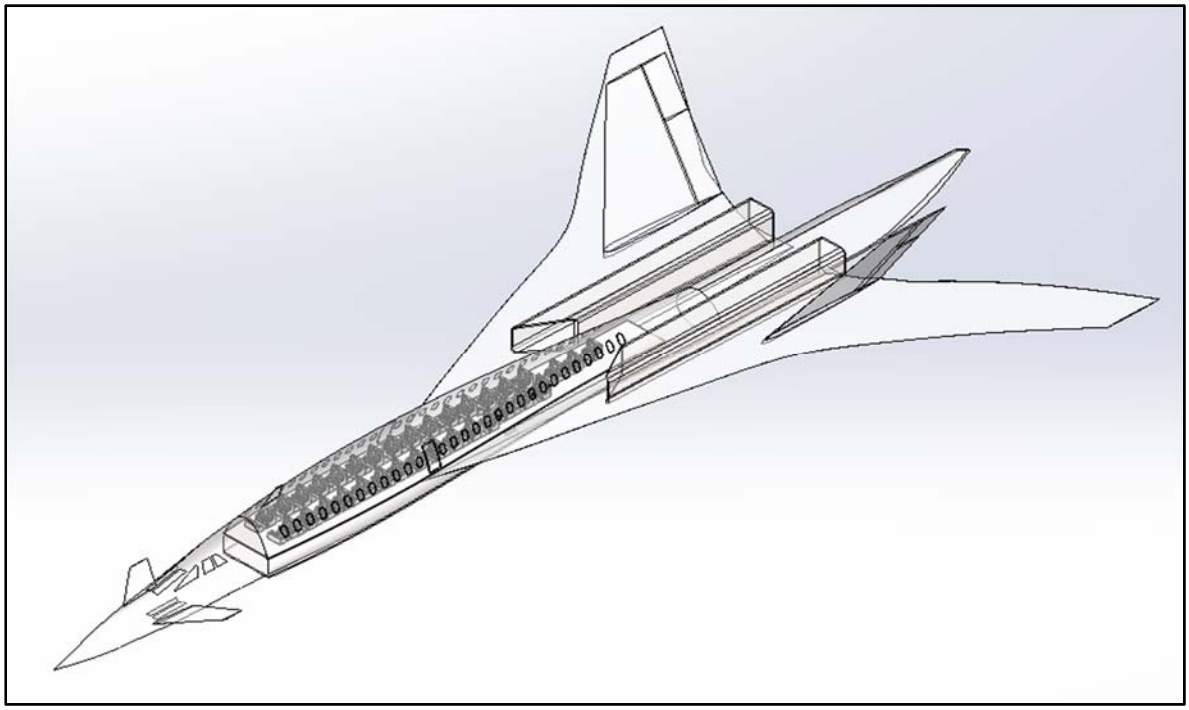

Figure 49: Luxury/Premium Economy Seating

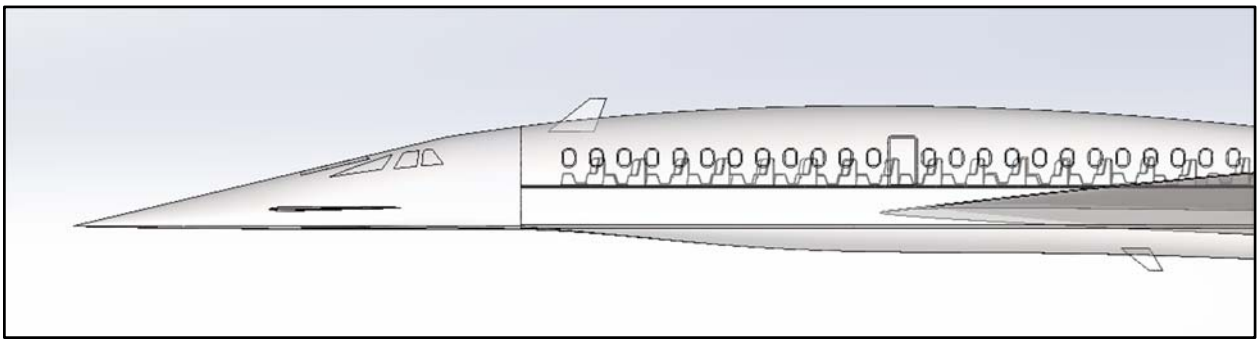

Figure 50: Side view of seating

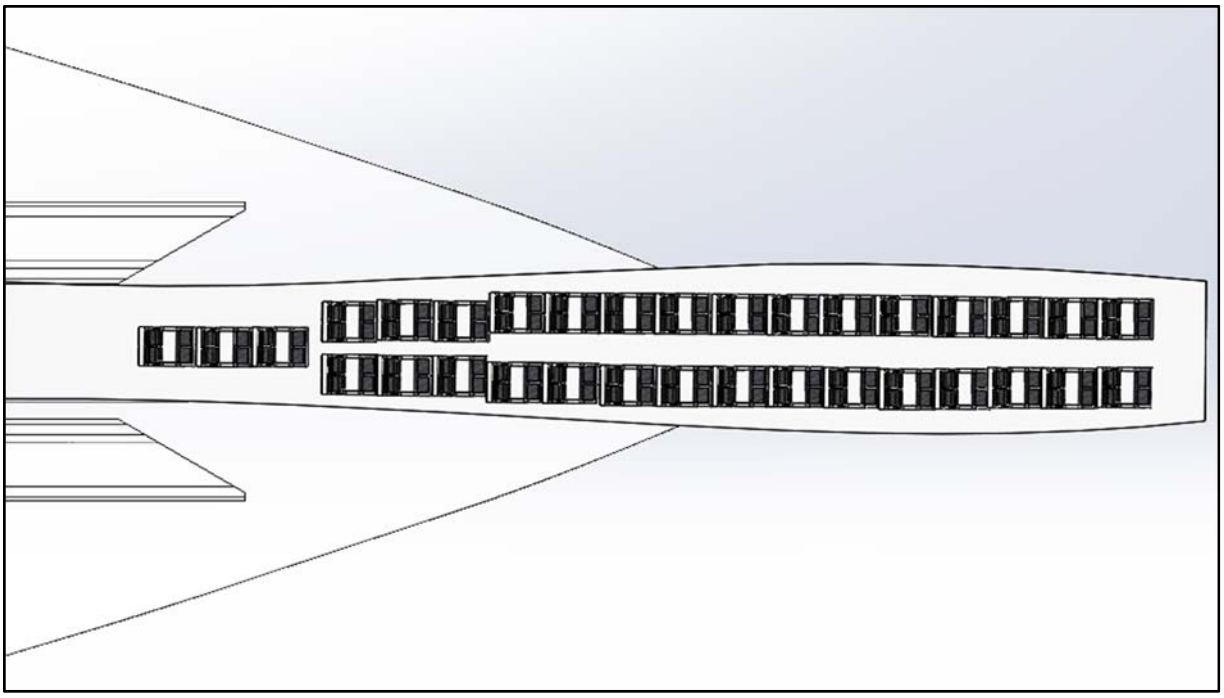

Figure 51: Overhead view of configuration

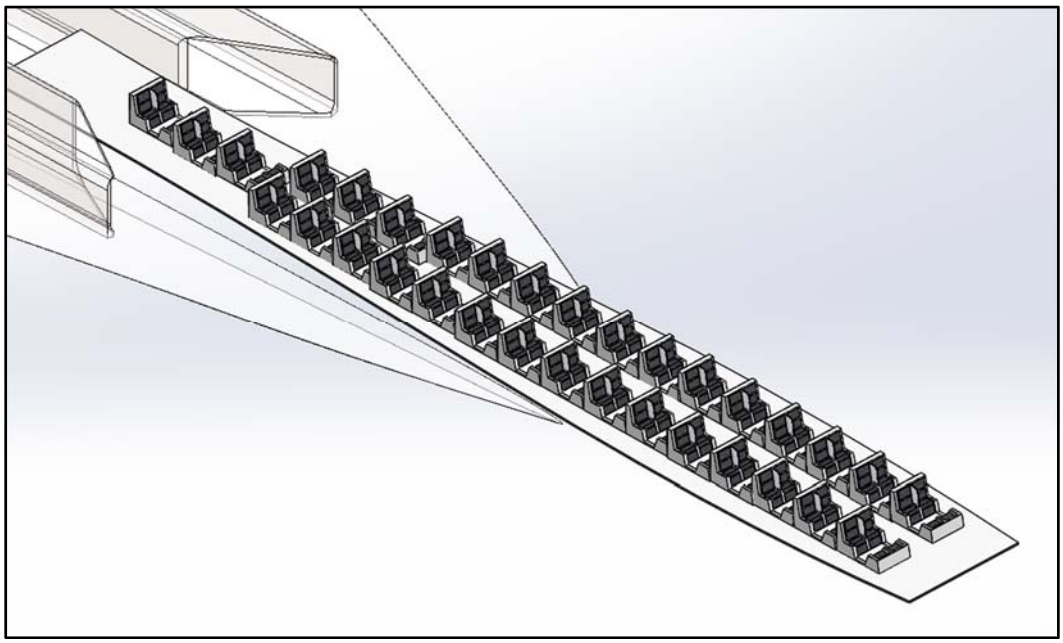

Figure 52: Isometric View (Bottom Right)

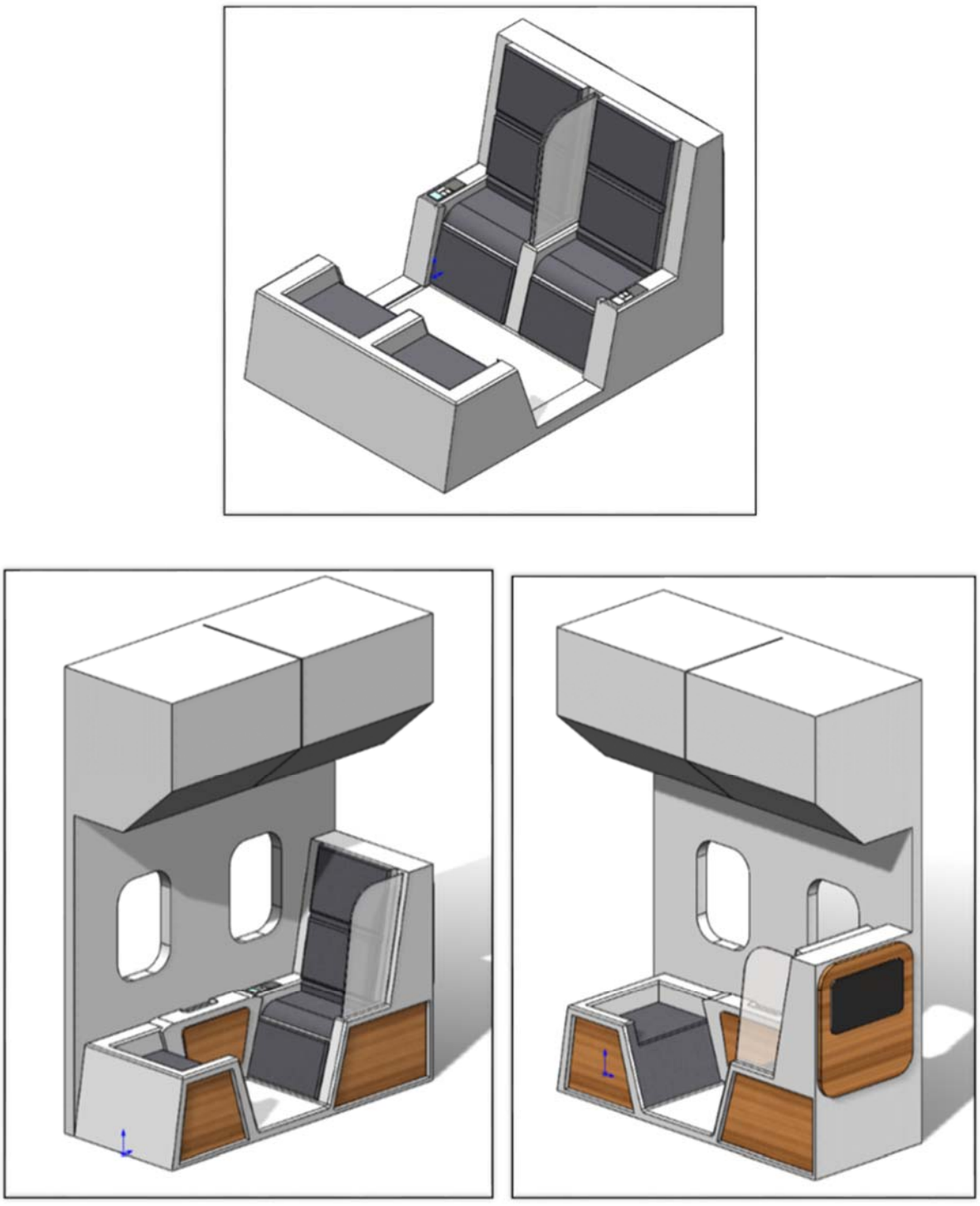

Figure 53: Detailed views of modern and updated luxury class seating

The standard seating configuration of this aircraft will seat over 100 passengers comfortably. The only downside to this configuration is that it only offers very basic seating with minimal features for a business class seat. One aspect with the more basic seating configuration is that, depending on the target, if more passengers are desired then the commercial standard configuration can be utilized. Although, a negative side effects of this configuration is that it does not offer luxury or first class amenities for passengers. If additional seats were added to the existing configuration it would seat 132 passengers comfortably.

Luxury/Premium Economy seating allows for the maximum amount of passengers onboard the D3 aircraft. Using a two by two seating configuration, multiple passengers can be accommodated on the aircraft. A business class suite seating option is also available for implementation in the aircraft. Each premium economy seat features controls on the arm rest. The premium economy configuration seats 132 passengers using the two by two seating arrangement. The seats can also act as a bed platform by extending the seat out. Further studies can be made on the interior seating configuration, although these models will assist in describing the overall design of this aircraft.

Chapter 7: Conclusion

The initial design of the aircraft and engine have been created. Using numerical and computational methods, the designs have gone through verification of feasibility and validity in design choices. From the trade study items for the engine, performance calculations and simulations were created to determine a prototype phase for the engine design. Through simulations, various conditions were selected to observe the characteristics of the aircraft through SolidWorks.

After literature review, aircraft designs were also selected based on a design matrix and an objective TOPSIS analysis. Engine design parameters and geometries were studied and implemented in the iterative design. Advanced calculations for numerical methods were found through various publications and text books. To ensure valid calculations, supersonic equations and studies were reviewed. A thorough study of inlet designs was also reviewed and simulated using SolidWorks. Then, through existing engines and nozzle designs, further reviews allowed further investigations on other alternatives along with similar selections to implement in the working design.

Through the engineering analysis, Parametric Cycle Analysis was conducted on the baseline engine and a trade study was completed using computational methods using the PARA and TURBN programs provided by AIAA. Supersonic wave drag calculations were found after extensive research on previous publications and papers in the same field. For the aircraft and engine, supersonic wave drag guided many of the component selections for this project. Inlet design calculations were also found and created to determine a suitable inlet to slow down the freestream air entering the core and bypass of the engine. By conducting this, it will reduce the stresses on engine components and ensure a smooth transition of air for the overall engine. CFD was conducted on the various designs for varying supersonic conditions. Of these simulations, the inlet, aircraft, and engine components underwent a CFD simulation to observe effects on pressure, Mach number, temperature, and velocity.

The prototypes for this project include component design, engine models, and interior design configurations for the finalized aircraft. The component design involves generated detailed models of the fan, inlet, compressor, turbine and nozzle. For the aircraft, various configurations using varying aircraft properties and geometries are generated. In addition, detailed CFD was conducted on the overall aircraft design. The interior configuration of the aircraft was created using two varying styles, one approach involves using a similar format and seat of standard commercial airliners and the second approach involves using a more modern design. Each configuration seats at least 100 passengers although the first approach seats 100 passengers exactly with the trade-off of lacking any luxury features. By generating seating configurations, it allows a visual on the fuselage design as well as considerations for space of passengers inside.

This project involves various trade studies and designs. A finalized model of the aircraft with various engine placement configurations are made to accommodate the engine size as well as to observe the effects of clean and disturbed air on the aircraft. To take this project further, 3D prints of the components, aircraft, and engine can be made to observe manufacturing processes the complexity of manufacturing. Also, 3D prints can also be used in a wind tunnel to observe the effects of drag on the aircraft. Weight reduction in various components can be made as well as acoustic levels of this design can also be generated to further refine the design. New technologies are always advancing and the implementation of these in the finalized design should be taken into consideration.

Chapter 8: Future Work

Given more time to develop the design, further exploration of different fan blade airfoils and technologies can be done. Given how far researchers have come now and where they are projected to go, the possibilities are endless. More exploration of ceramic and metal matrix material along with conducting more tests to see which materials would best fit each component could be done. Another area to expand upon would be the hub assembly. A common concern found during initial research was finding better ways to connect the varying components to achieve maximum weight savings and efficiency.

Trying to develop new or enhance current studies on the TAPS II lean burn combustor could also be initiated. The technology seems very promising and will propel the low-emissions challenge forward to bounds yet foreseen. Being fairly new technology not much public knowledge was found on it in a way to see how it would perform with various engines and engine configuration.

Concerning the turbine and compressor, unfortunately, time was spent studying the effects due to limited time and resources. However, that did not stop the team from wanting to carefully develop an analysis plan to determine what would be the best geometry and configuration to create an efficient flow through the core of the engine. With our low efficiency of about 19%, there seems to be reason to believe that more could be done to improve the propulsive efficiency through these two components.

With the nozzle, there are numerous approaches to noise reduction. Further research can be made to determine the noise effects on humans by exit velocity could be developed and studied upon. Each method would require different geometries and could result in weight gains, so improving upon current noise reducing methods could be very beneficial to the industry.

Concerning emissions, the engine can be designed to lower nitrogen oxide (NOx) emissions. Emission levels will be in terms of the total mass of the emission created during a certain landing-takeoff (LTO) operational cycle per kilo newton of rated takeoff thrust at

sea level (std). For next generation supersonic aircraft, NOx emissions contribute to the deterioration of the stratospheric ozone because they cruise at higher altitudes. A NOx emissions index of 5 g/kg fuel during cruise is the design requirement for our supersonic engine for further development to fulfil the AIAA requirements.

After all of the studies and analyses would be done, the team would like to explore 3-D printing and supersonic wind tunnel testing of the aircraft fuselage, inlet, nozzle, and any appropriate component that could be done to gather real-life test results. This along with a system analysis of the entire engine could be performed to show how the engine would function realistically. After the tests are done, all of the material data and weights could be gathered to give a real-time rendering of what an aircraft such as the one created would require to be used in industry. This would include pricings, maintenance requirements, suggested missions, etc.

Acknowledgements

- **Kennesaw State University**
  - Department of Industrial and System Engineering
  - Adeel Khalid, Ph.D.
  - Christina Turner
- **American Institute of Aeronautics and Astronautics**
- **National Aeronautics and Space Administration**

References

[1] Welge, Harry R, et al. *N+2 Supersonic Concept Development and Systems Integration* . NASA, 5 Aug. 2010.

[2] Coen, Peter. *ARMD Strategic Thrust 2: Innovation in Commercial Supersonic Aircraft*. NASA, 24 May 2016.

[3] *What Is Numerical Propulsion System Simulation (NPSS®)?* Southwest Research Institute, Mechanical Engineering Division Fluids & Machinery Engineering Department, 3 June 2016.

[4] GOLINVAL, J C. "Mechanical Design of Turbojet Engines ." Mechanical Design of Turbomachinery Mechanical Design of Turbojet Engines . Mechanical Design of Turbomachinery Mechanical Design of Turbojet Engines .

[5] Mason, F. *Supersonic Aerodynamics*. 2016, *Supersonic Aerodynamics*, www.dept.aoe.vt.edu/~mason/Mason_f/ConfigAeroSupersonicNotes.pdf.

[6] Cantwell, B J. *Aircraft and Rocket Propulsion*. pp. 1–21, *Aircraft and Rocket Propulsion*.

[7] Slater, John W. "External-Compression Supersonic Inlet Design Code." 2011 Technical Conference. 2011 Technical Conference, 11 Mar. 2011, Ohio, Cleveland.

[8] "Inlet Performance." *NASA*, NASA, 5 May 2015, www.grc.nasa.gov/www/k-12/airplane/inleth.html.

[9] "Gas Turbine Theory", H.I.H Saravanamuttoo, G.F.C Rogers &.H. Cohen, Prentice Hall, 5th Edition 2001.

[10] "Aircraft Engine Design", J.D. Mattingly, W.H. Heiser, & D.H. Daley, AIAA Education Series, 1987.

[11] "Elements of Propulsion – Gas Turbines and Rockets", J.D. Mattingly, AIAA Education Series, 2006.

[12] “Jet Propulsion”, N. Cumpsty, Cambridge University Press, 2000. 5. “Gas Turbine Performance”, P. Walsh & P. Fletcher, Blackwell/ASME Press, 2nd Edition, 2004.

[13] “Fundamentals of Jet Propulsion with Applications”, Ronald D. Flack, Cambridge University Press, 2005.

[14] “The Jet Engine”, Rolls-Royce plc. 2005.

[16] “Mechanics and Thermodynamics of Propulsion”, Hill, Philip G. and Peterson Carl R., Addison-Wesley Publishing Company, Reading, Massachusetts, 1965.

[17] Kareliusson, Joakim, and Melker Nordqvist. *Conceptual Design of a Supersonic Jet Engine*. Sept. 2014.

[18] Heath, Christopher & Gray, Justin & Park, Michael & J. Nielsen, Eric & Carlson, Jan-Renee. (2015). *Aerodynamic Shape Optimization of a Dual-Stream Supersonic Plug Nozzle.* 10.2514/6.2015-1047.

[19] Chutkey, Kiran & Vasudevan, B & Balakrishnan, N. (2014). *Analysis of Annular Plug Nozzle Flowfield.* “Journal of Spacecraft and Rocket.” 51. 10.2514/1.A32617.

[20] Debiasi, Marco, and Dimitri Papamoschou. *Cycle Analysis for Quieter Supersonic Turbofan Engines.* “37th Joint Propulsion Conference and Exhibit”. 2001, doi:10.2514/6.2001-3749.

[21] “Applied Aerodynamics: A Digital Textbook.” *Supersonic Drag Estimation*, docs.desktop.aero/appliedaero/compress3d/ssdragest.html.

[22] Amoo, Leye M. *On the Design and Structural Analysis of Jet Engine Fan Blade Structures.* “Progress in Aerospace Sciences.” Vol. 60. 01 July 2013, pp. 1-11. EBSCOhost, doi:10.1016/j.paerosci.2012.08.002.

[23] Marsh, George. *Feature: Aero Engines Lose Weight Thanks to Composites.* “Reinforced Plastics.” Vol. 56. 01 Nov. 2012, pp. 32-35. EBSCOhost, doi:10.1016/S0034-3617(12)70146-7.

[24] “GE Adaptive Cycle Engine.” GE Aviation, www.geaviation.com/military/engines/ge-adaptive-cycle-engine.

[25] Samuelsen, Scott. *Rich Burn, Quick-Mix, Lean Burn (RQL) Combustor*. University of California.

[26] Stickles, Rick, and Jack Barrett. *TAPS II Technology Final Report - Technology Assessment Open Report*. "FAA Continuous Lower Energy, Emissions and Noise (CLEEN) Technologies Development." June, 2013.

[27] Peterson, Christopher O, et al. *Performance of a Model Rich Burn-Quick Mix-Lean Burn Combustor at Elevated Temperature and Pressure*. NASA, 2002, pp. 1–81.

[28] "Cabin Seats" GRAB CAD, https://grabcad.com/library/cabin-seats-1

Appendices

Appendix A: Computational Fluid Dynamic Analysis

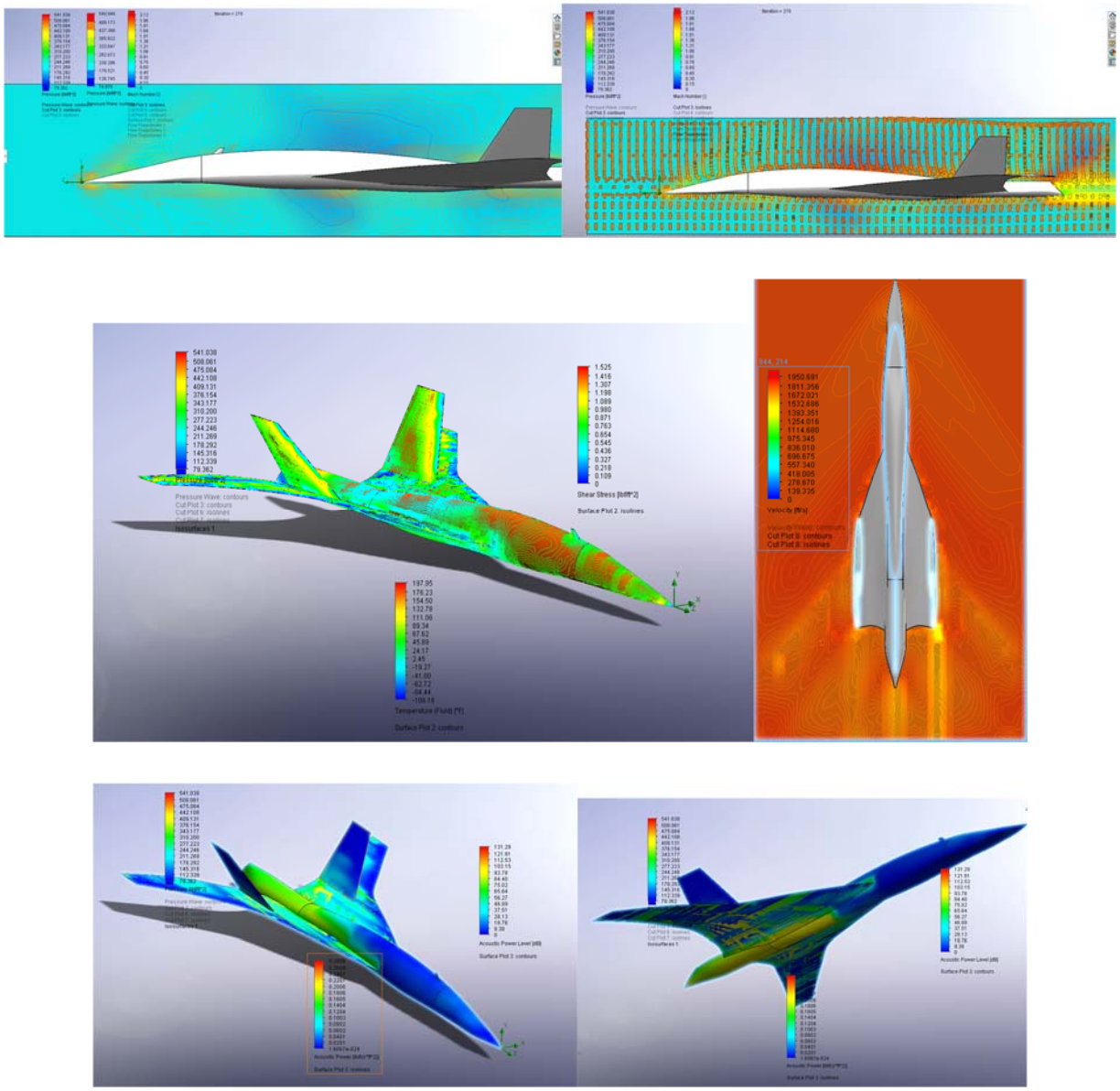

Figure 54: (a) ride side profile of simulated pressure and mach speeds (b) Shear stress and pressure formation (c) Acoustic power level reading at cruise conditions

Appendix B: Inlet Design Analysis Trade Studies

	M_0	h_alt	M_2	P_0 [lbf/ft^2]	D_2 [ft]	T_0 [F]	V_0 [ft/s]
Baseline Conditions	1.8	55000	0.5	194	3.5		1800

Supersonic Inlet Concepts	pt2/pt0	pt0	pt2 [lbf/ft^2]	h_clip [ft]	L [ft]	A_cap [ft^2]	A_fcex [ft^2]	Cd_wave
Design 1 - Ikeda II Similar	1.210700875	12541	151816	1.774	9.645	9.534	2.191	0.0947
Design 2 - Ikeda	1.191878004	90536	107532	1.196	3.626	5.642	5.832	0.3013
Design 3 - Spike	1.161217994	1005.547	116731	1.409	8.24	9.561	4.293	0.2233
Design 4 - Chin	1.027403166	796.62	103483	1.232	12.074	11.641	9.638	0.03654

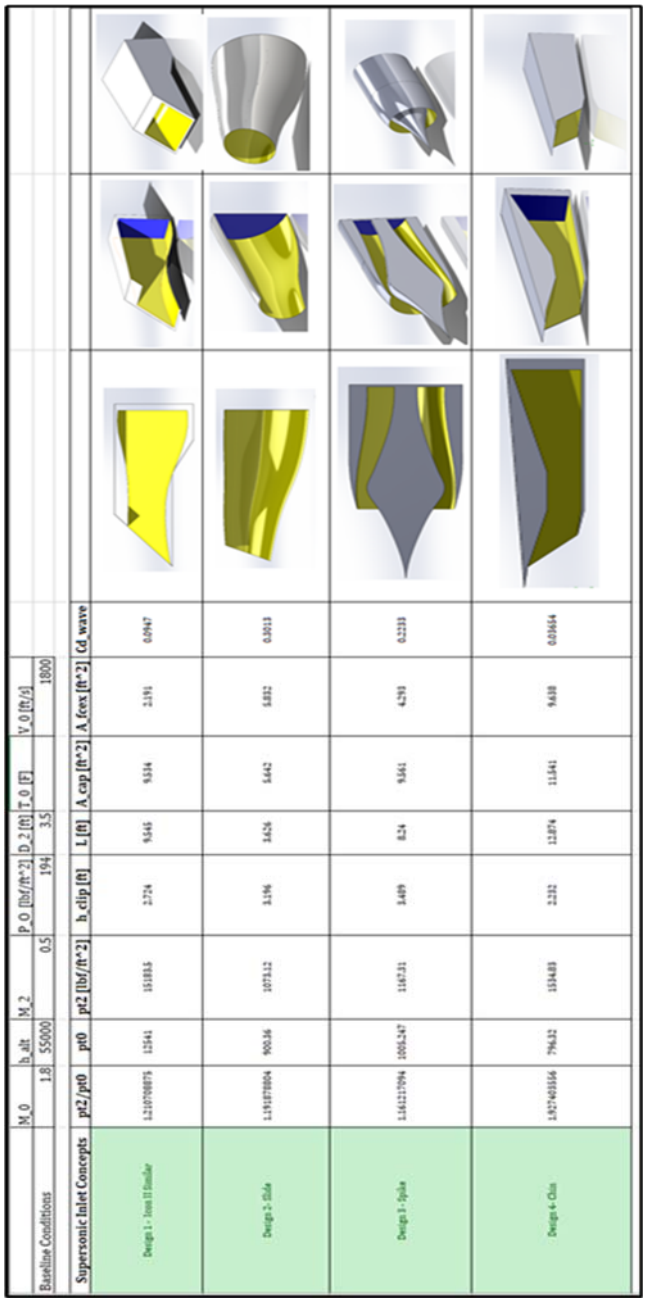

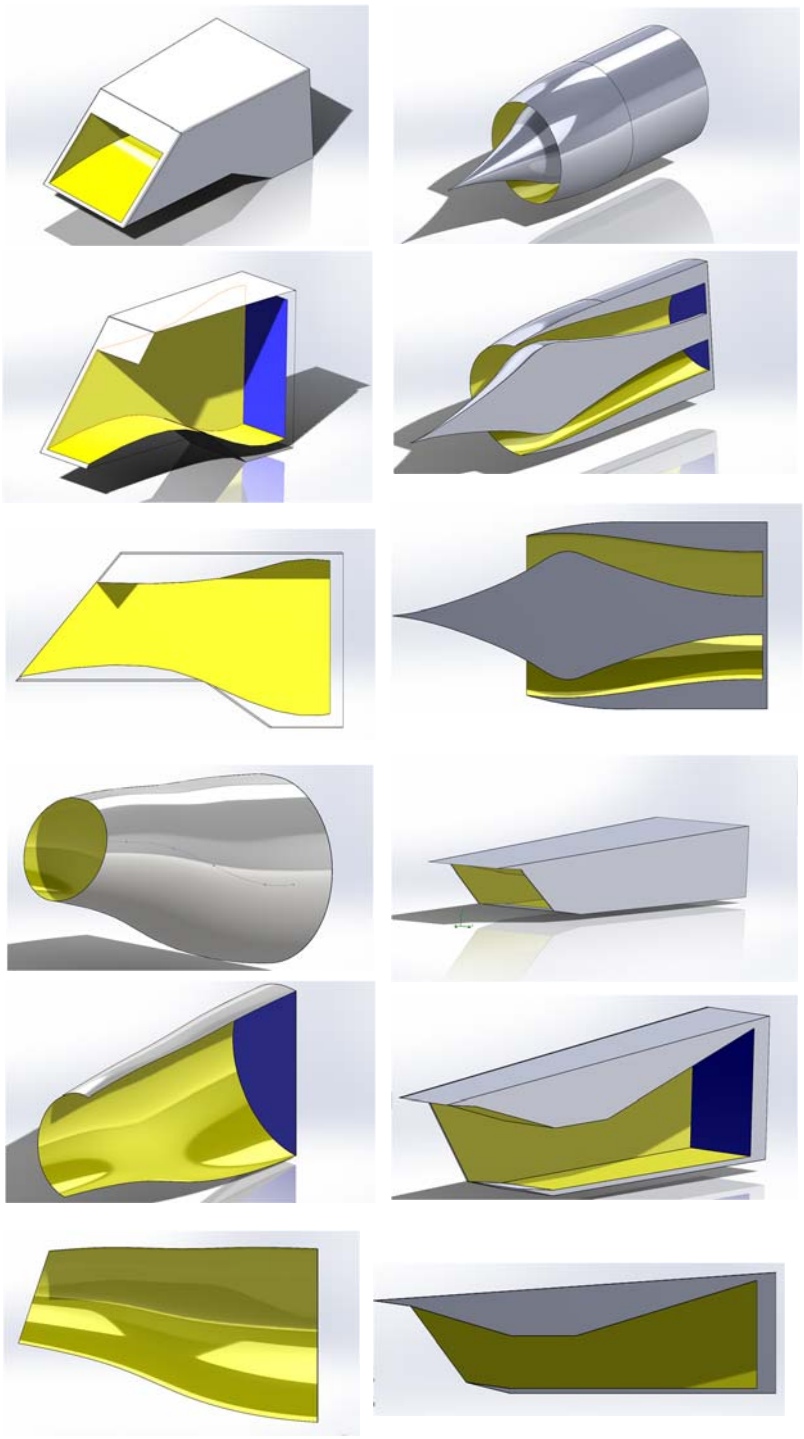

Figure 55: Trade Study and Baseline Inlet Design Choice Selection

Chanel Extended Control Inlet- Design 1

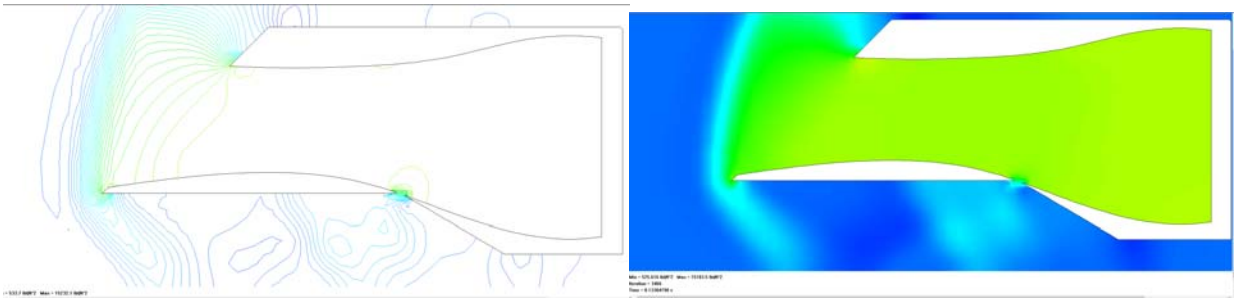

(a)

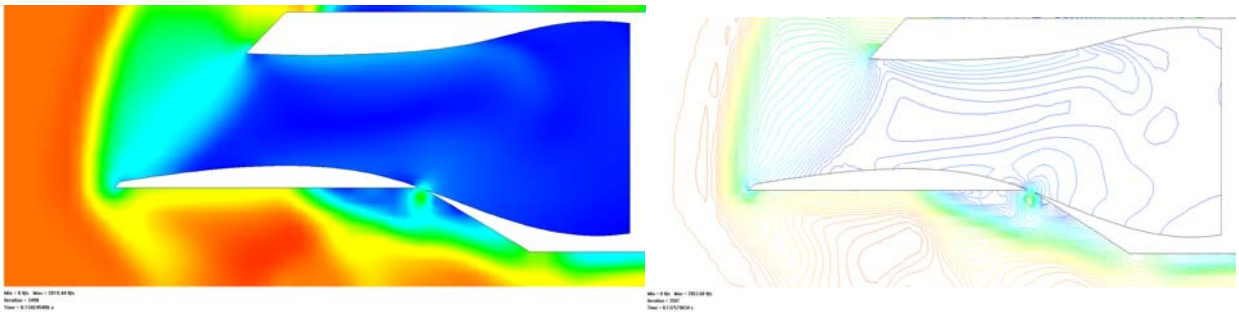

(b)

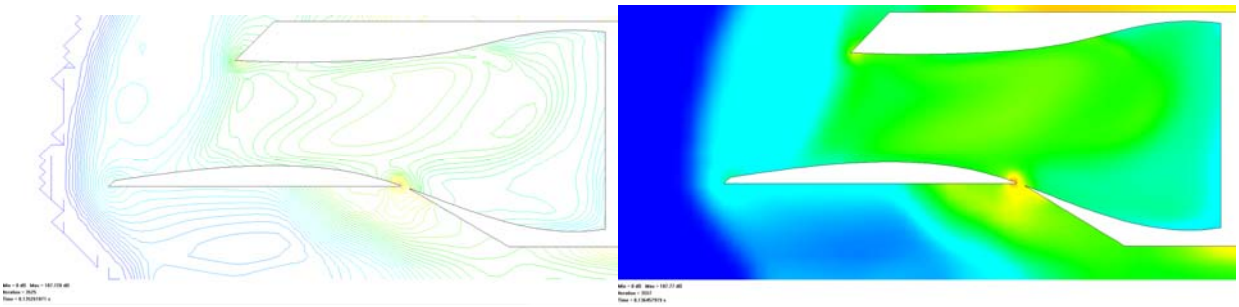

(c)

Figure 56: Design 1 side cut plot profile view for: (a) Pressure (b) Velocity (c) Acoustic Power Level

Supersonic Spike Extended Control Inlet- Design 2

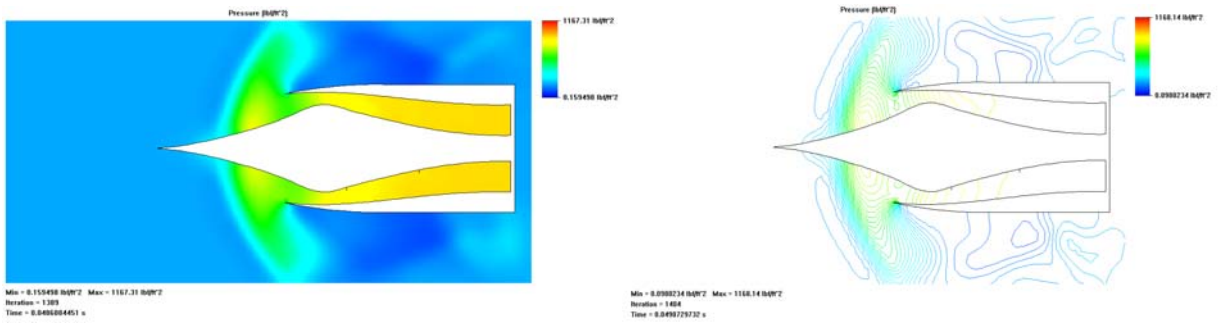

(a)

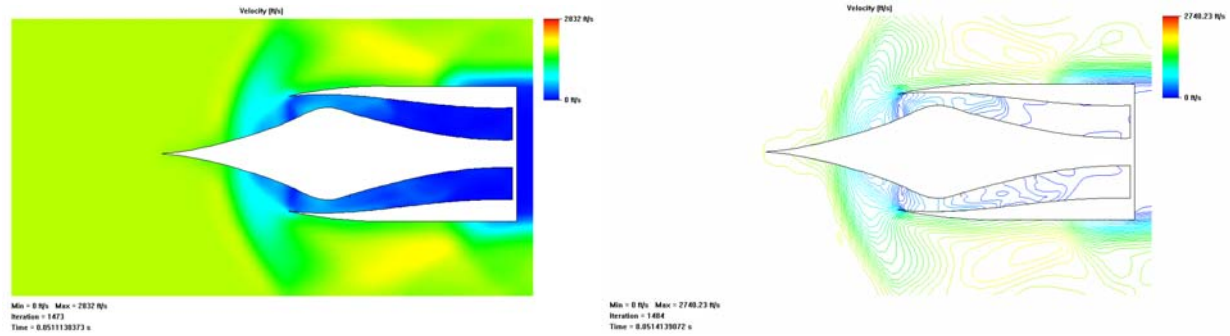

(b)

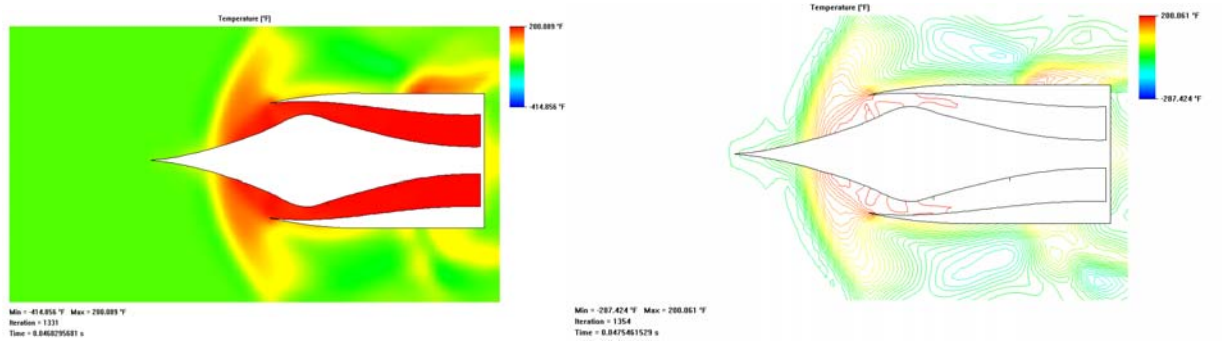

(c)

Figure 57: Design 2 side cut plot profile view for: (a) Pressure (b) Velocity (c) Temperature

Appendix C: Nozzle Design Analysis

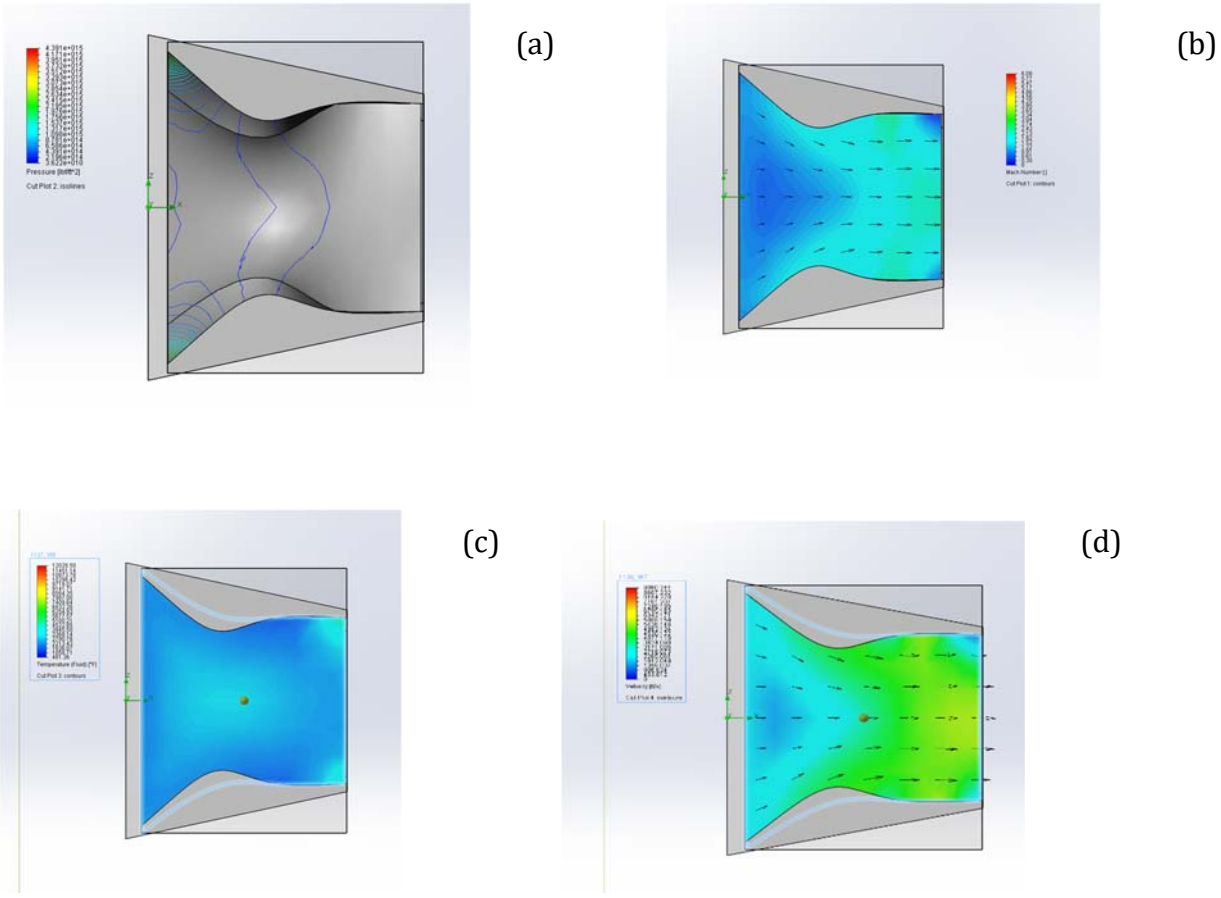

Figure 58: Design 1 side cut plot profile view: (a) Pressure, (b) Mach Number, (c) Temperature, and (d) Velocity.

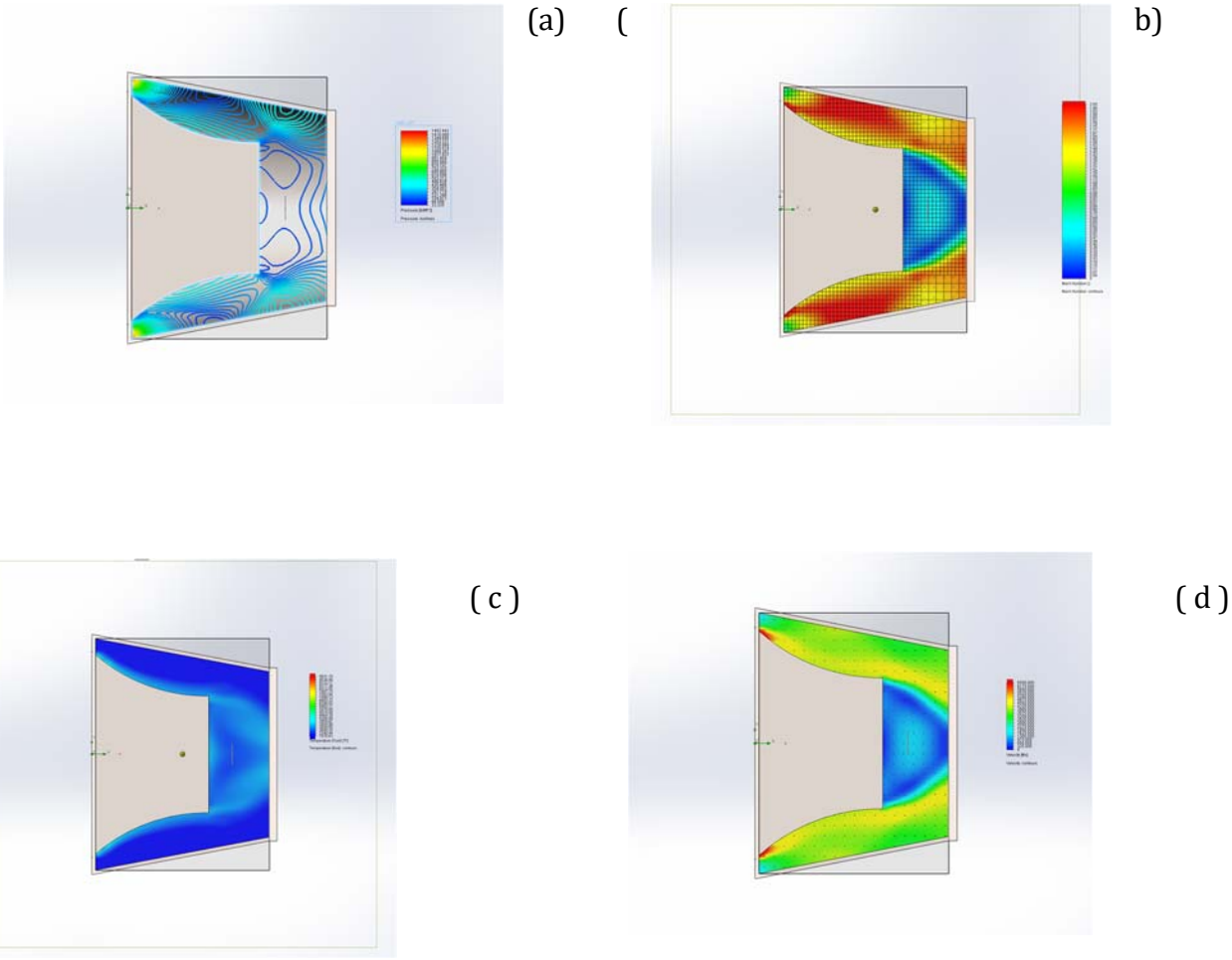

Figure 59: Design 2 side cut plot profile view: (a) Pressure, (b) Mach Number, (c) Temperature, and (d) Velocity.

Appendix D: Carpet Plots

The plots generated in Appendix D provide information on the performance of the baseline as well as the designed engine at the design point. In this case, the design point of the engines is observed at supersonic cruise (Mach 1.6). The PARA program provided by the AIAA software package suite from the Elements of Propulsion Text is used. Input parameters are placed inside the program and the outputs for each of the trade studies are provided in the carpet plots. Each plot is with respect to Specific Thrust and TSFC. The carpet plot features two varying inputs based on a maximum and input value for the number of iterations required for the calculation.

To read the carpet plots the format is as follows:

Cycle - Var M0/ Tt4 /Pic/BPR/Alt

Trade Study 1: T4 vs FPR

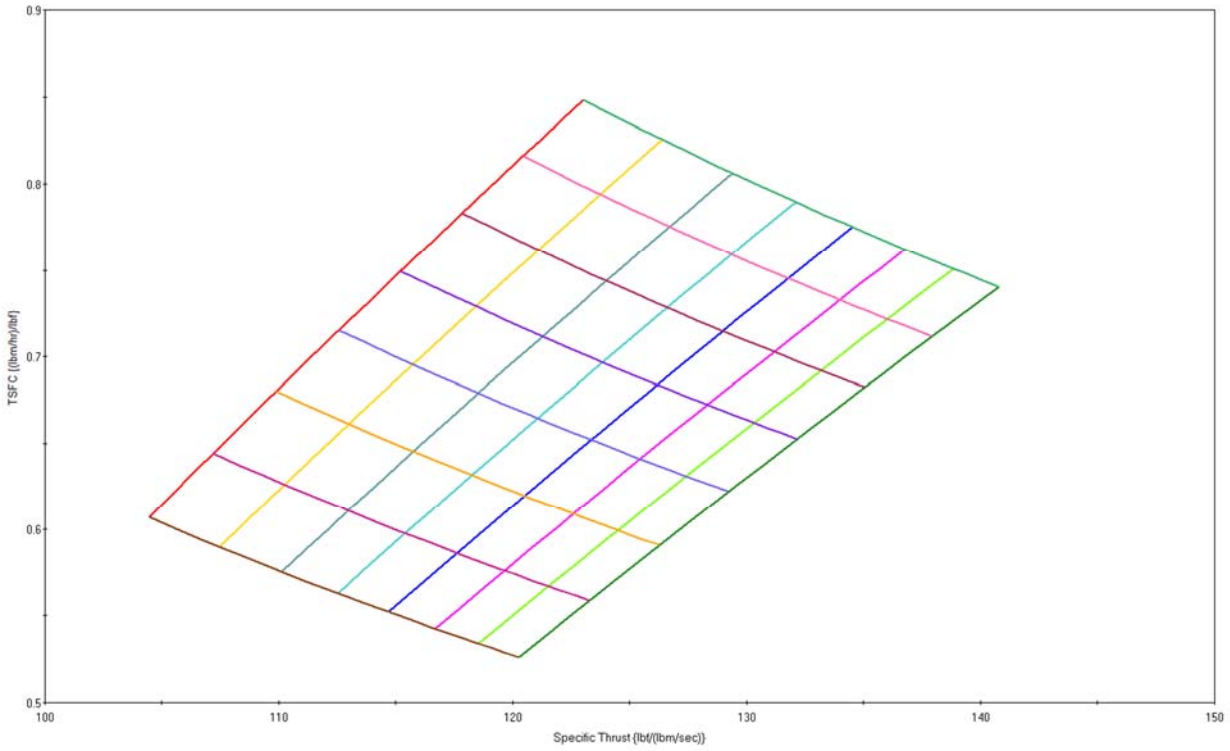

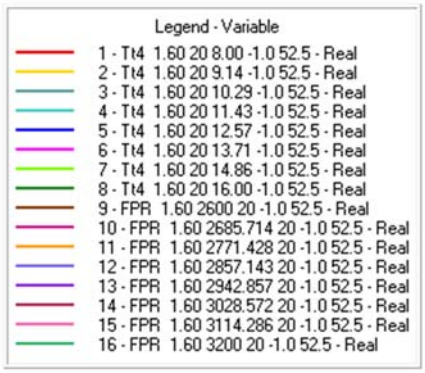

Temperature at T4	Fan Pressure Ratio
Minimum: 2600 R	Minimum: 8
Maximum: 3200 R	Maximum: 16

Trade Study 2: FPR vs CPR

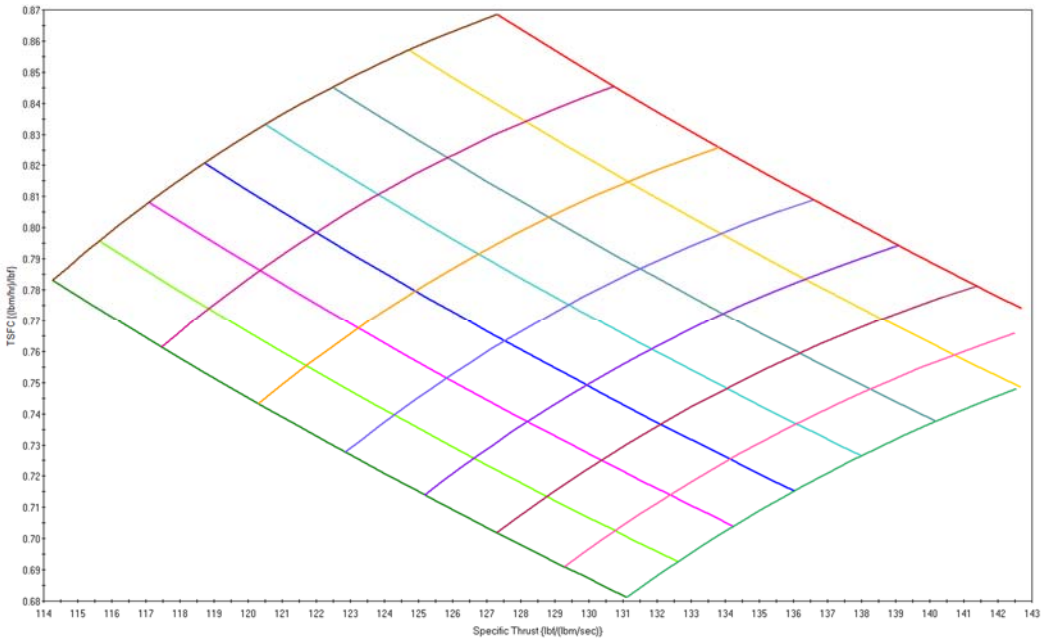

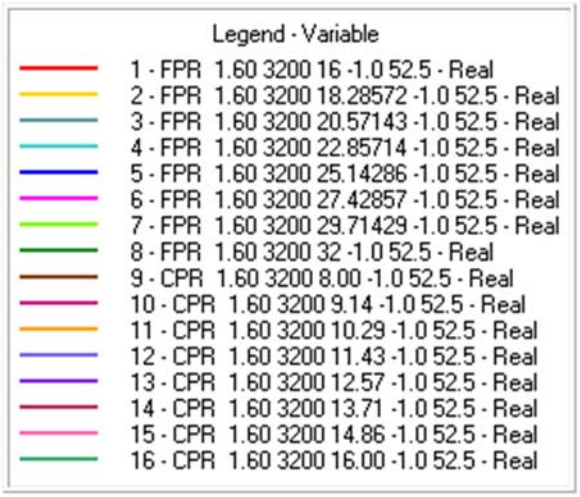

Fan Pressure Ratio	Compressor Pressure Ratio
Minimum: 8	16
Maximum: 16	32

Trade Study 3: T4 vs CPR

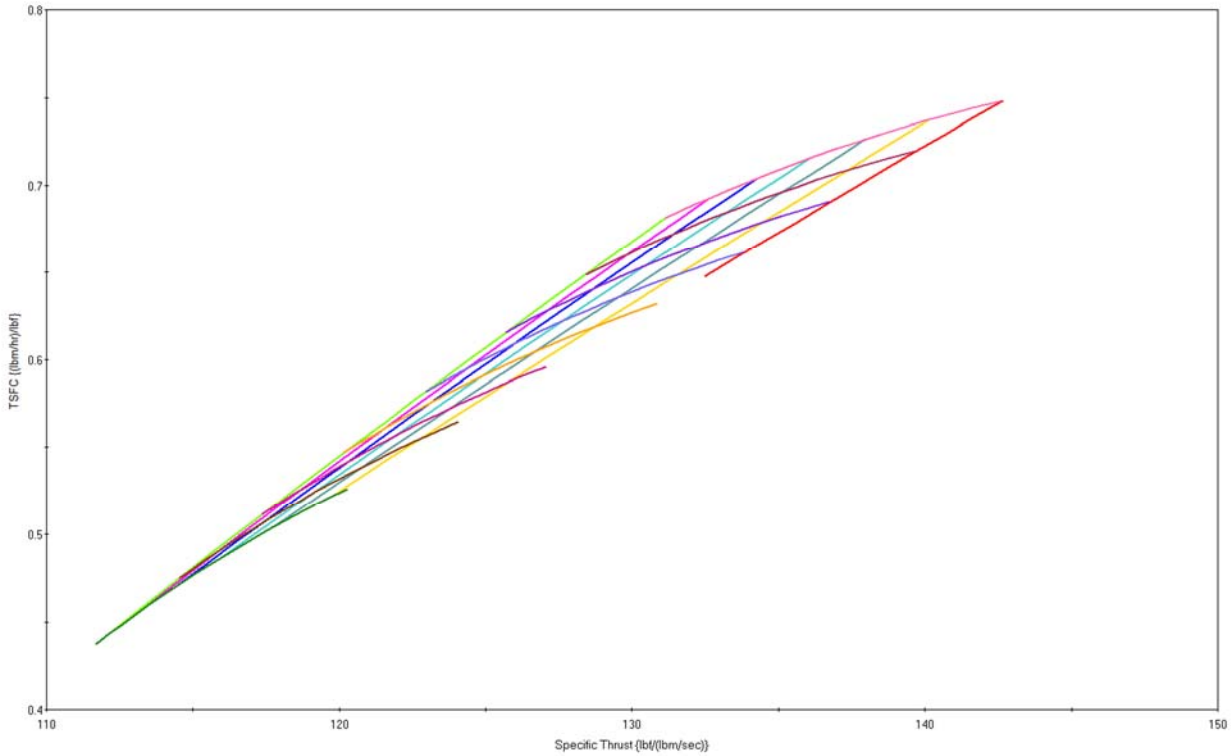

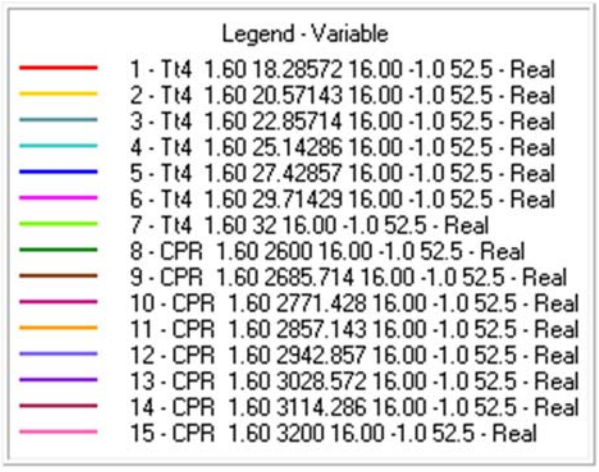

Temperature at Turbine Inlet	Compressor Pressure Ratio
Minimum: 2600 R	16
Maximum: 3200 R	32

Appendix E: Aircraft Design Computer Aid Models

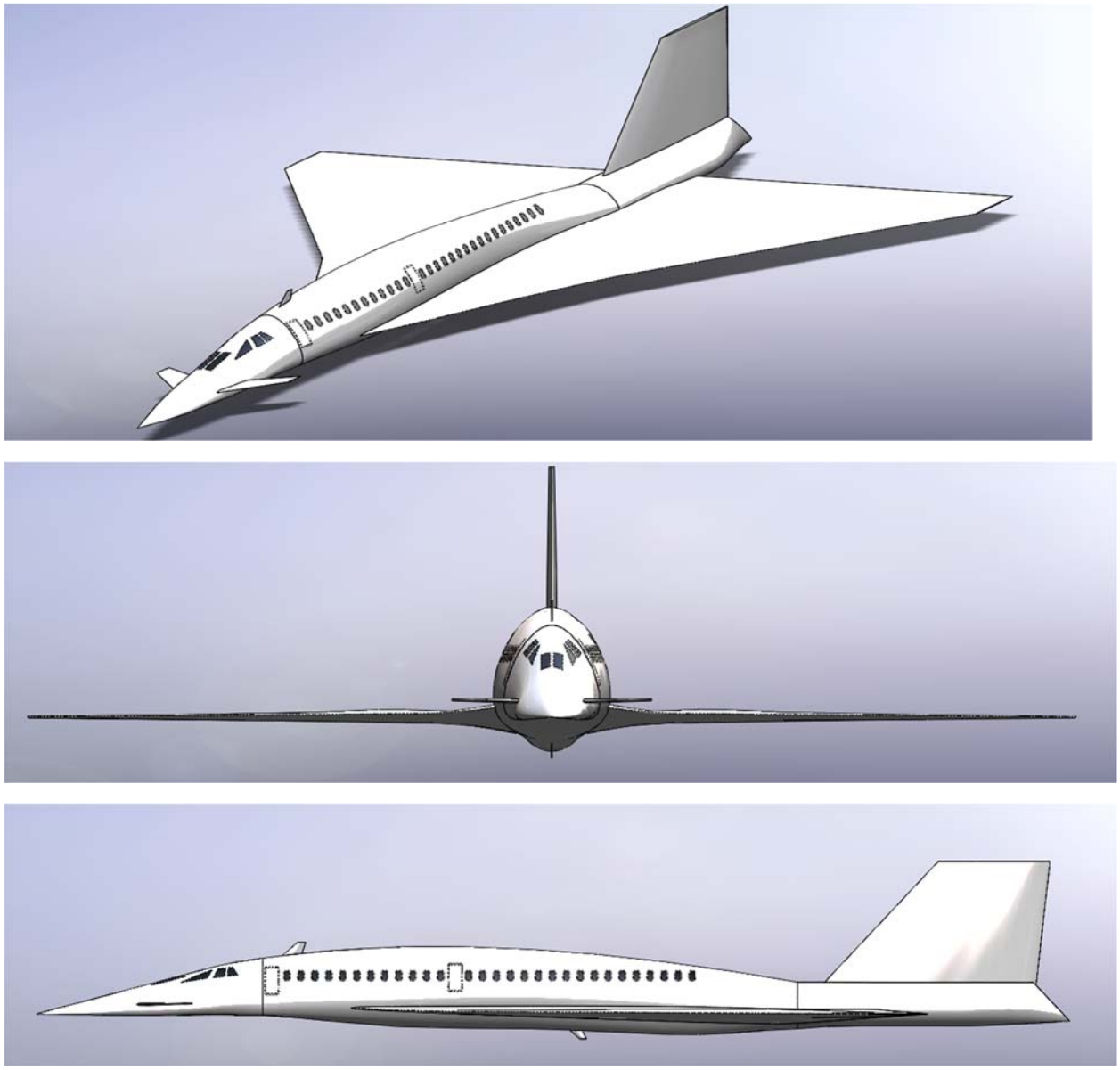

Figure 60: Design 1 concept with straight delta wing geometry (isometric, front, right side respectively profiles)

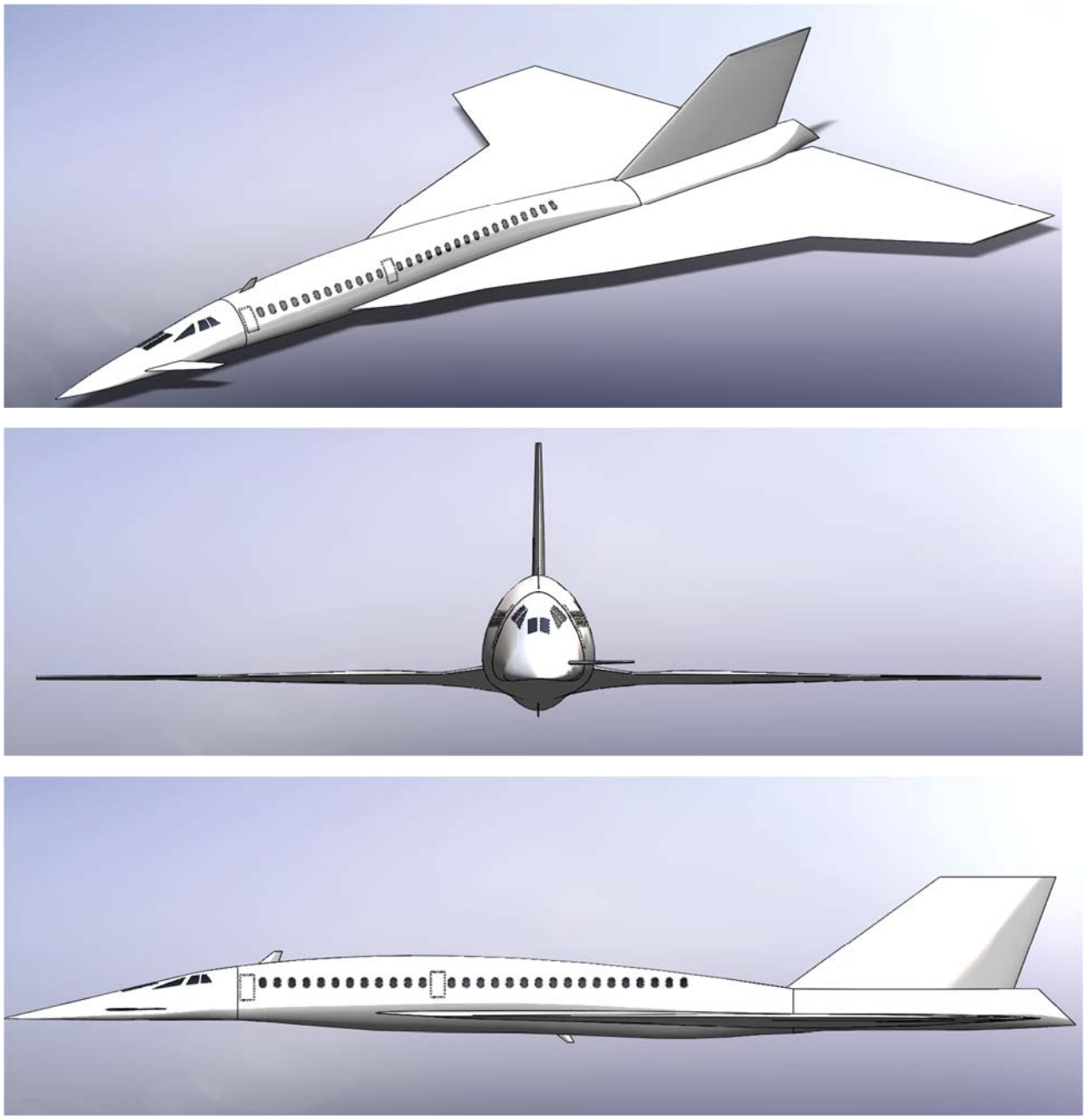

Figure 61: Design 2 concept with double delta straight wing geometry (isometric, front, right side respectively profiles)

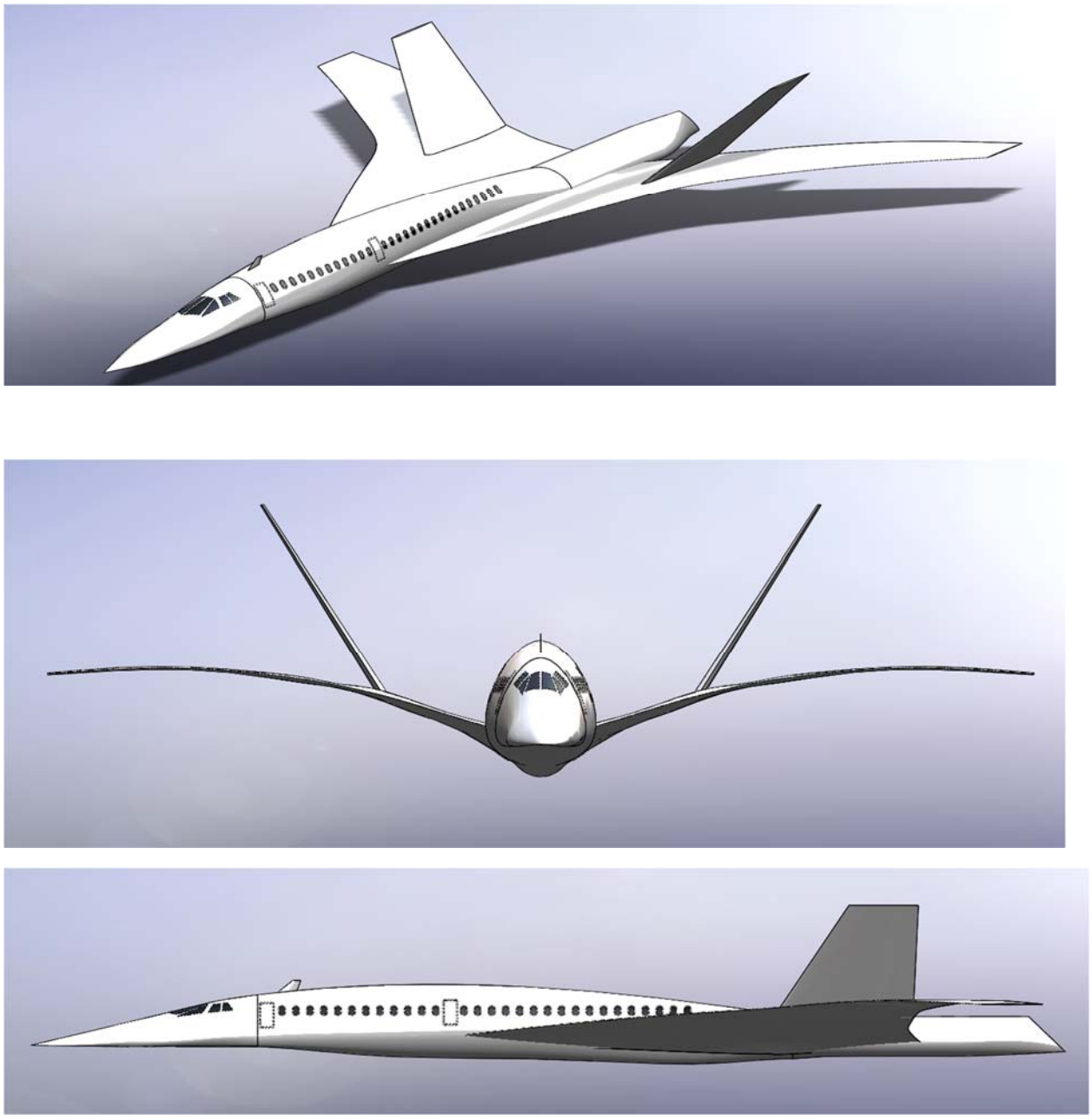

Figure 62: Design 3 concept with arced delta straight wing geometry (isometric, front, right side respectively profiles)

Figure 63: Frontal nose aircraft design baseline: (isometric, right side, front respectively profiles)

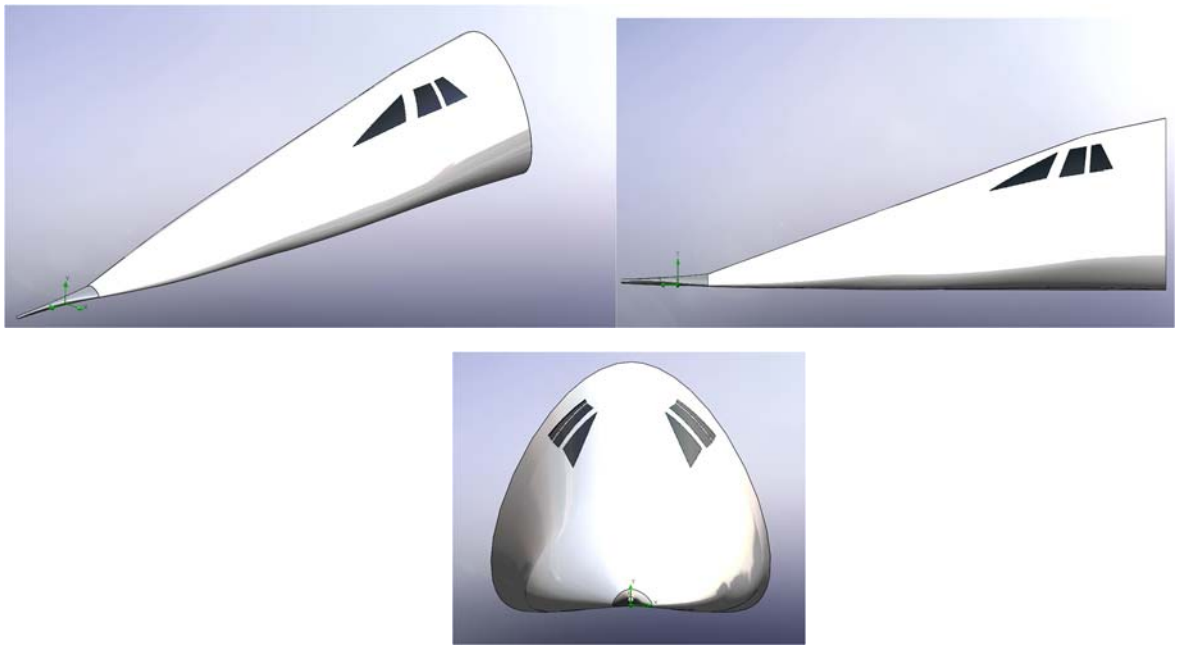

Figure 64: Frontal nose aircraft design extended nose optimization: (isometric, right side, front respectively profiles)

Appendix F: Engine Initial Concepts

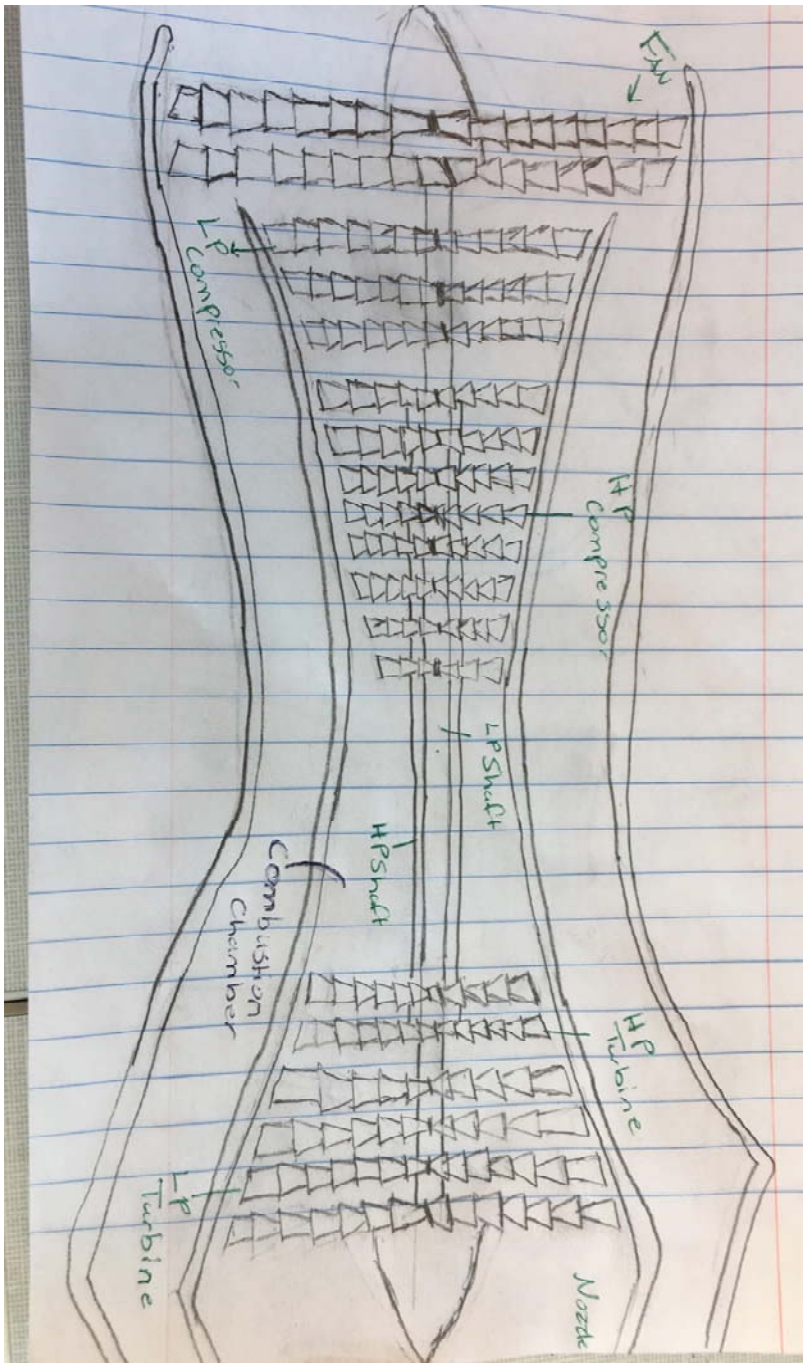

Figure 65: Engine Concept

Shown in Figure 65, the engine concept depicts a dual spool mixed flow turbofan. The engine will be tested with varying number of stages for the compressor and the turbine to

determine the best combination for optimal performance. The engine will be outfitted with a custom inlet and nozzle to exceed design requirements.

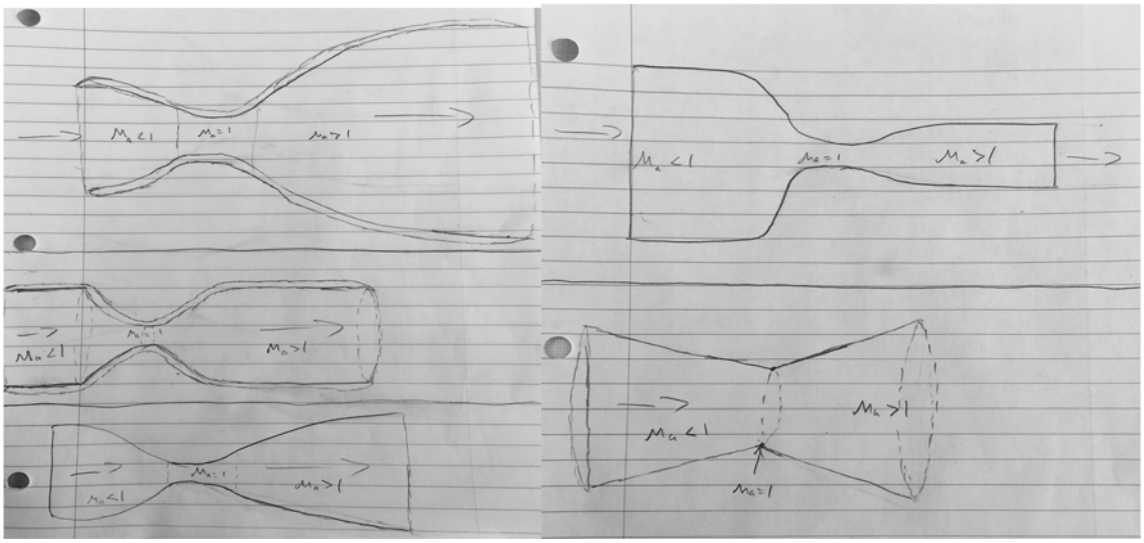

Figure 66: Concept Nozzle Geometries

Figures 66 depicts different convergent-divergent nozzles to achieve supersonic thrust. The two nozzles explored are the bell shaped and cone shaped ones. Further tests to see which nozzle fits the requirements will be conducted after the pressure values are found at the end of the engine's turbine stage. Each nozzle will have a different rate of pressure expansion which will result in different maximum pressure values at the nozzle exit.

Appendix G: Final Engine Design Powerplant

Figure 67: Engine isometric and side profile of internal viewing of supersonic geometry

Appendix H: Historical Data Plots

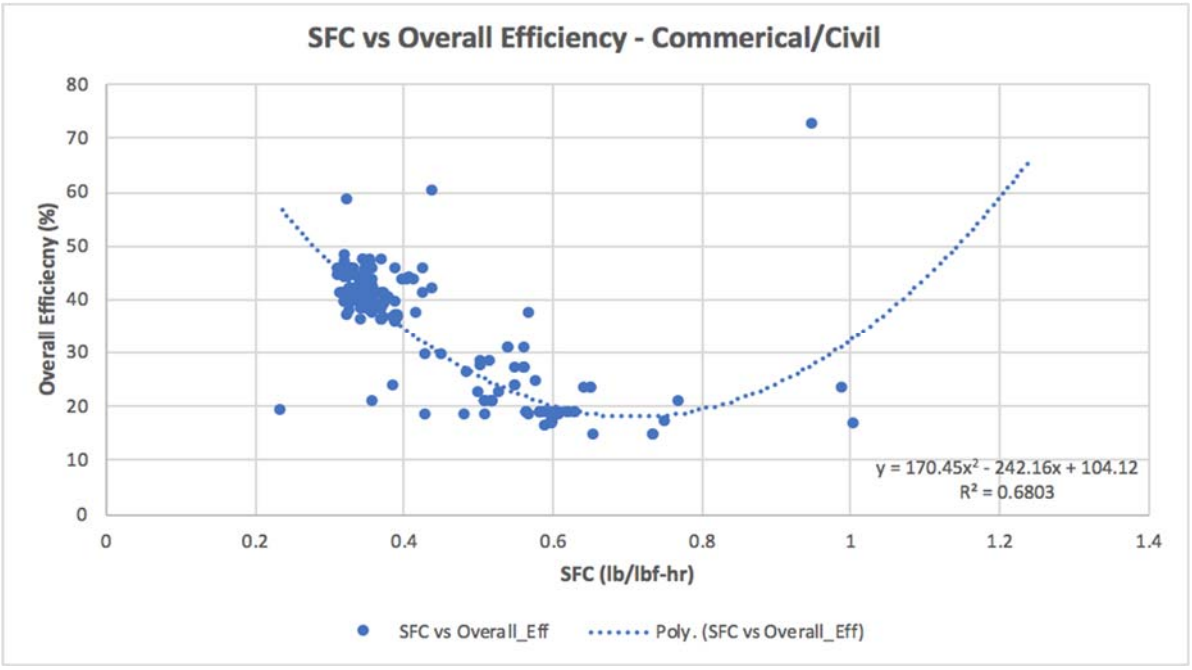

Figure 68: Specific Fuel Consumption vs overall efficiency for commercial/civil aircraft

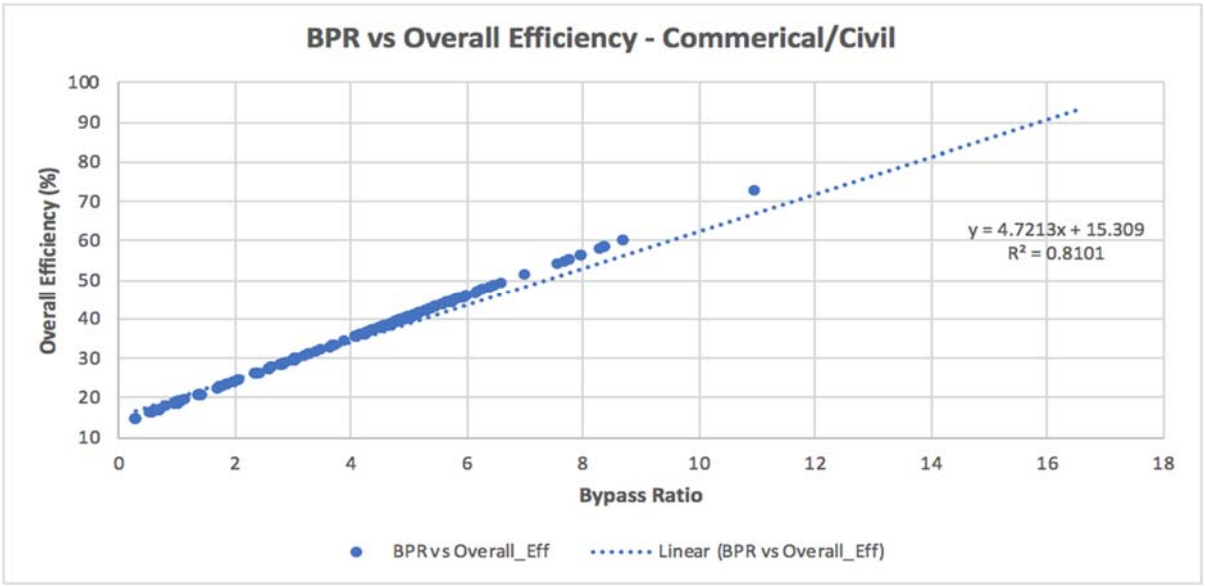

Figure 69: Bypass Ratio vs Overall Efficiency for commercial/civil aircraft

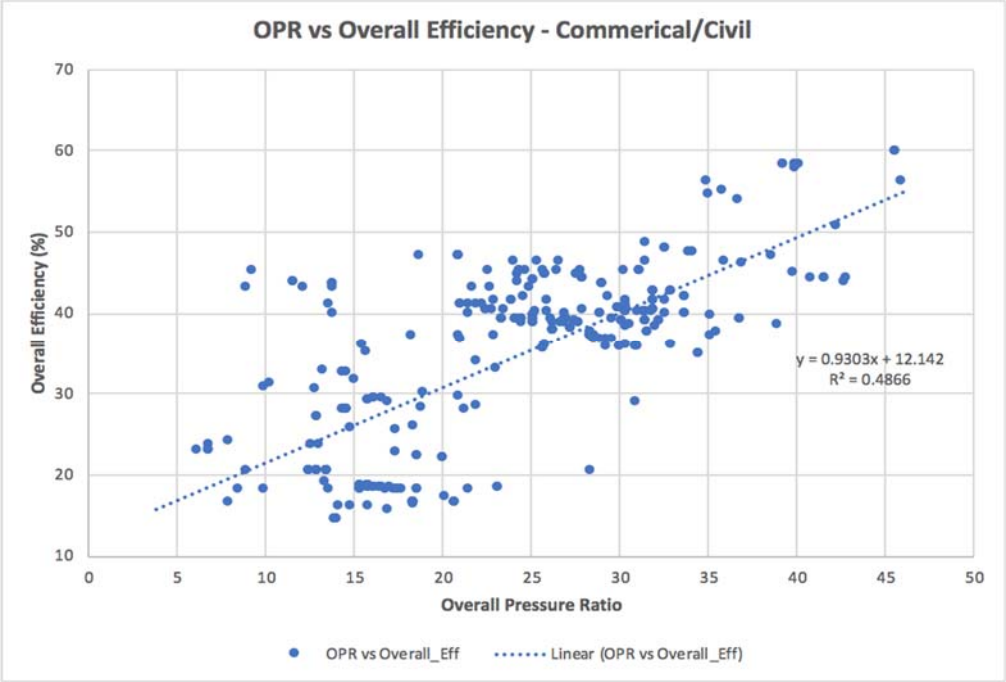

Figure 70: Overall Pressure Ratio vs Overall Efficiency for commercial/civil aircraft

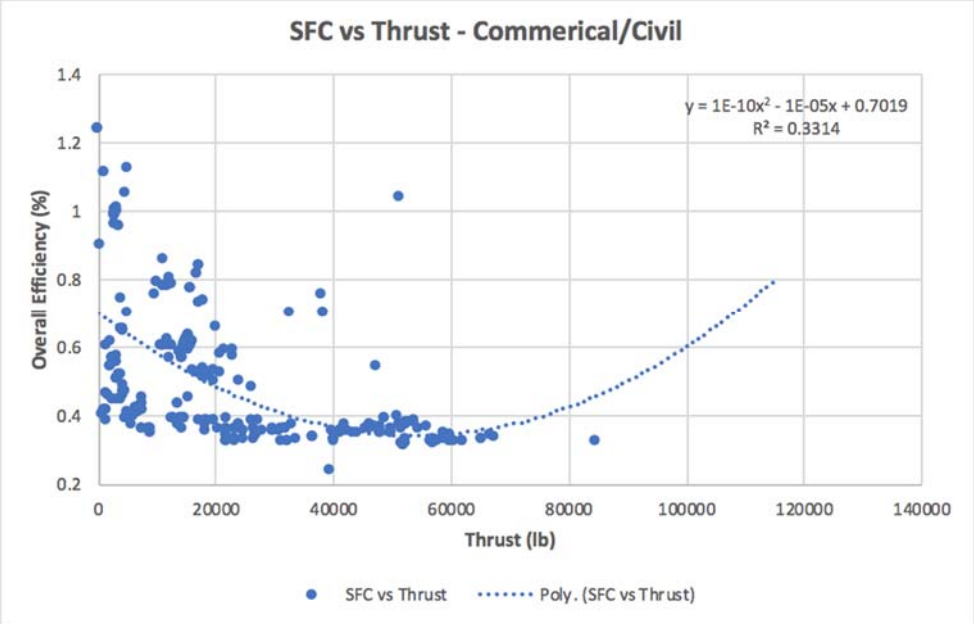

Figure 71: Specific fuel consumption vs thrust for commercial/civil aircraft

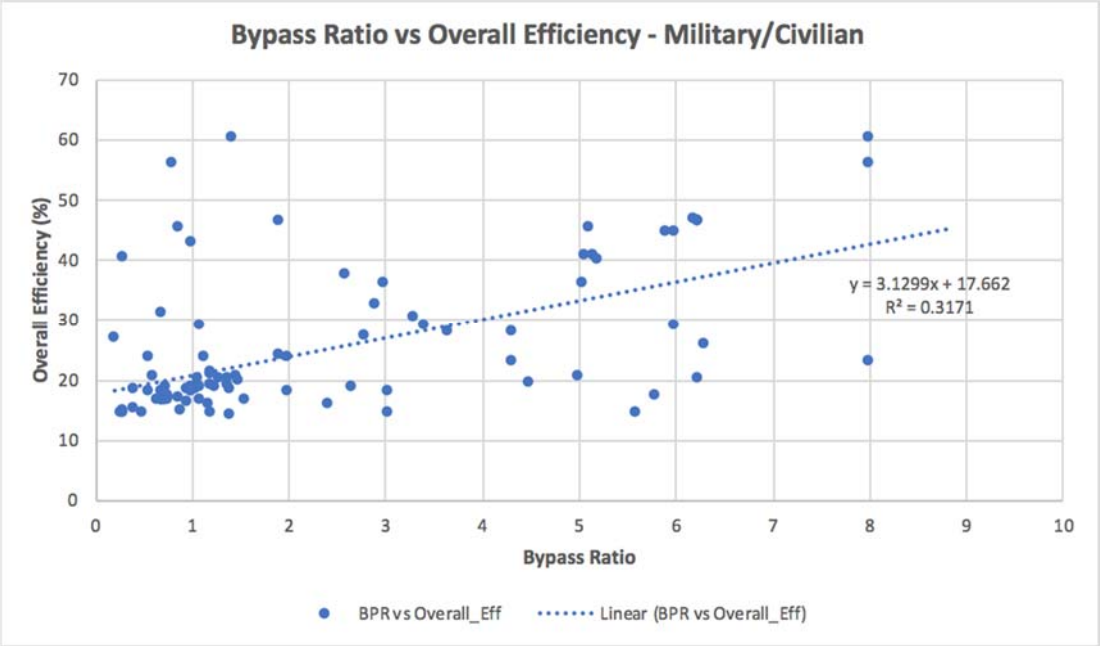

Figure 72: Graph of overall efficiency versus bypass ratio for military aircraft.

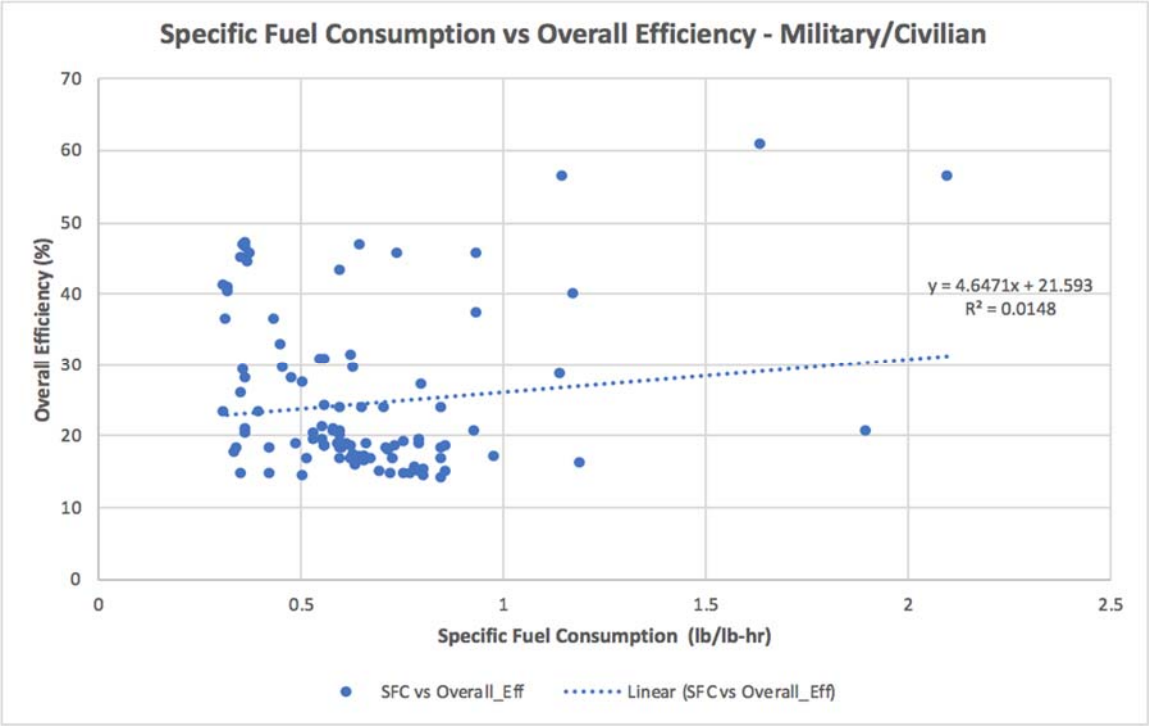

Figure 73: Specific fuel consumption vs Overall efficiency for military vehicles.

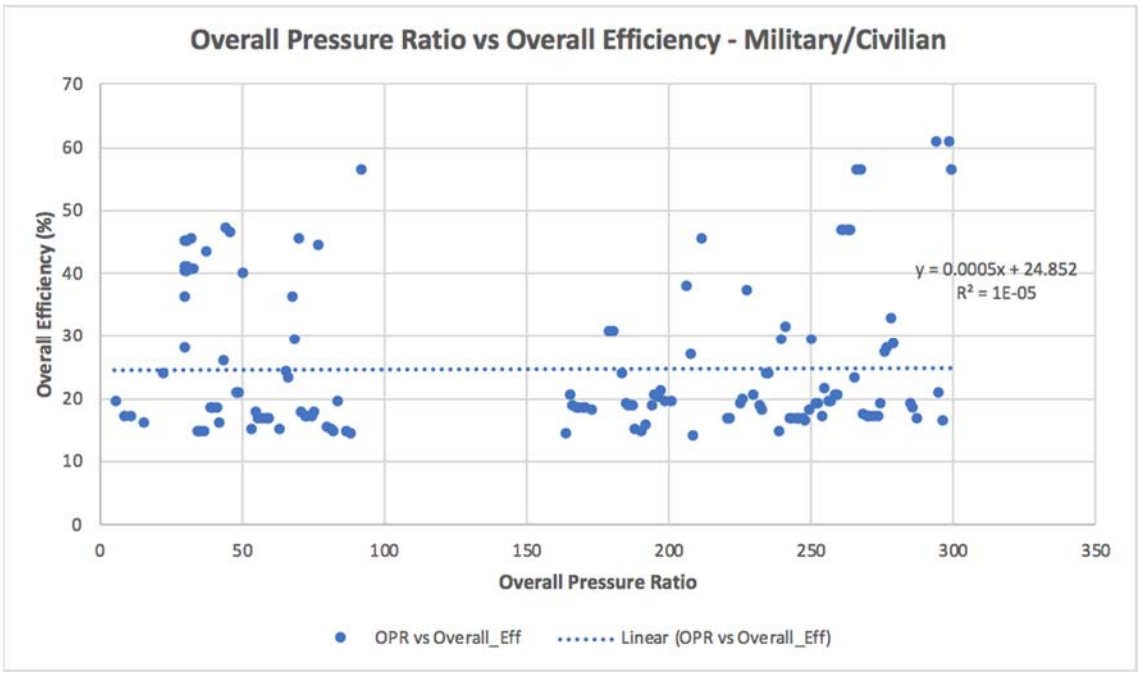

Figure 74: Overall pressure ratio vs overall efficiency for military/civil aircraft

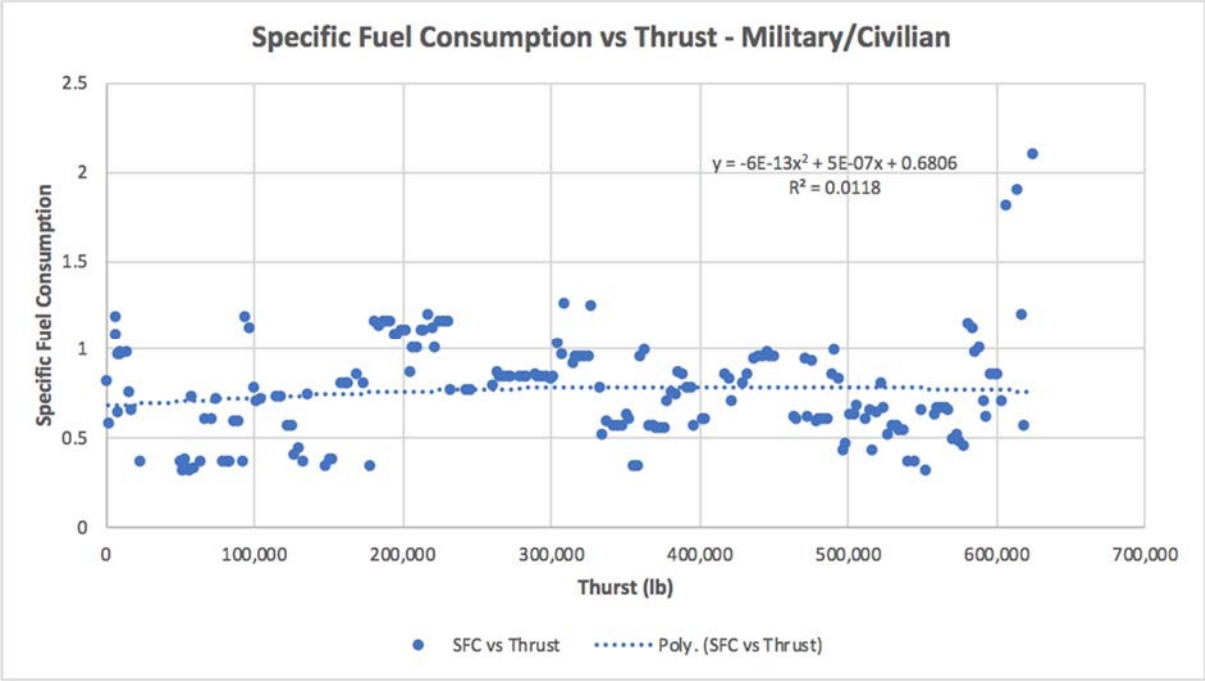

Figure 75: Specific fuel consumption vs thrust for military/civil aircraft

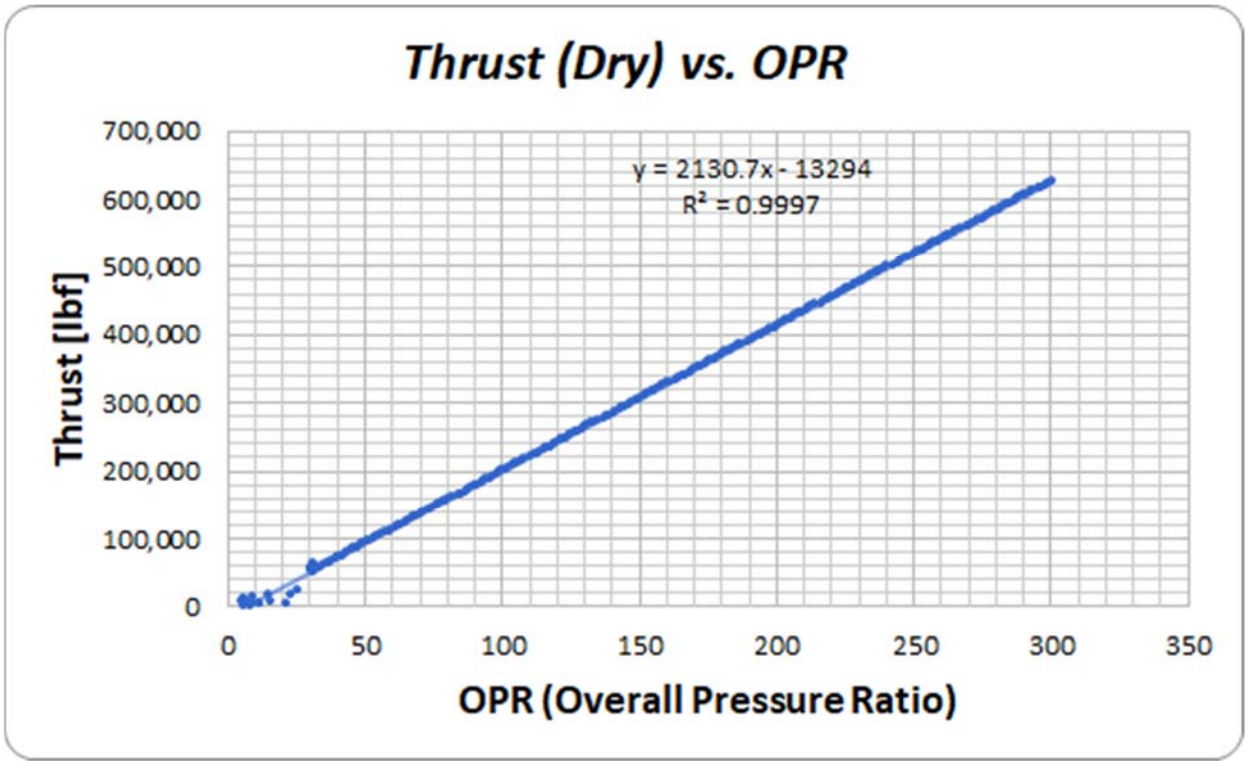

Figure 76: Overall Pressure Ratio vs Thrust for Military Aircraft

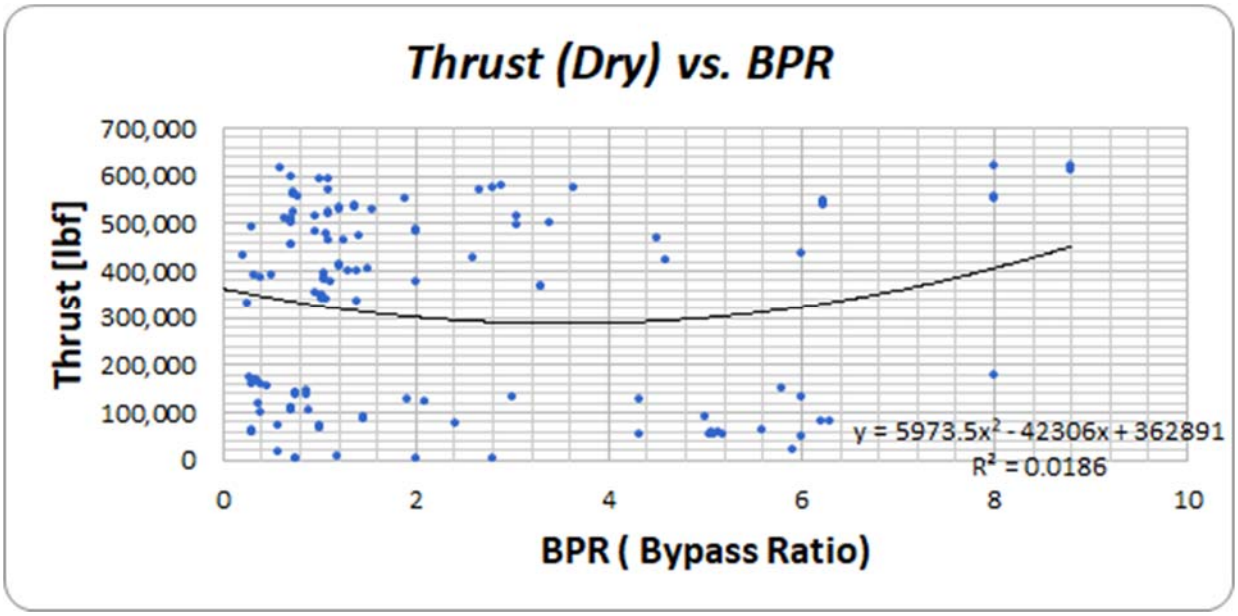

Figure 77: Bypass Ratio vs Thrust for Military Aircraft.

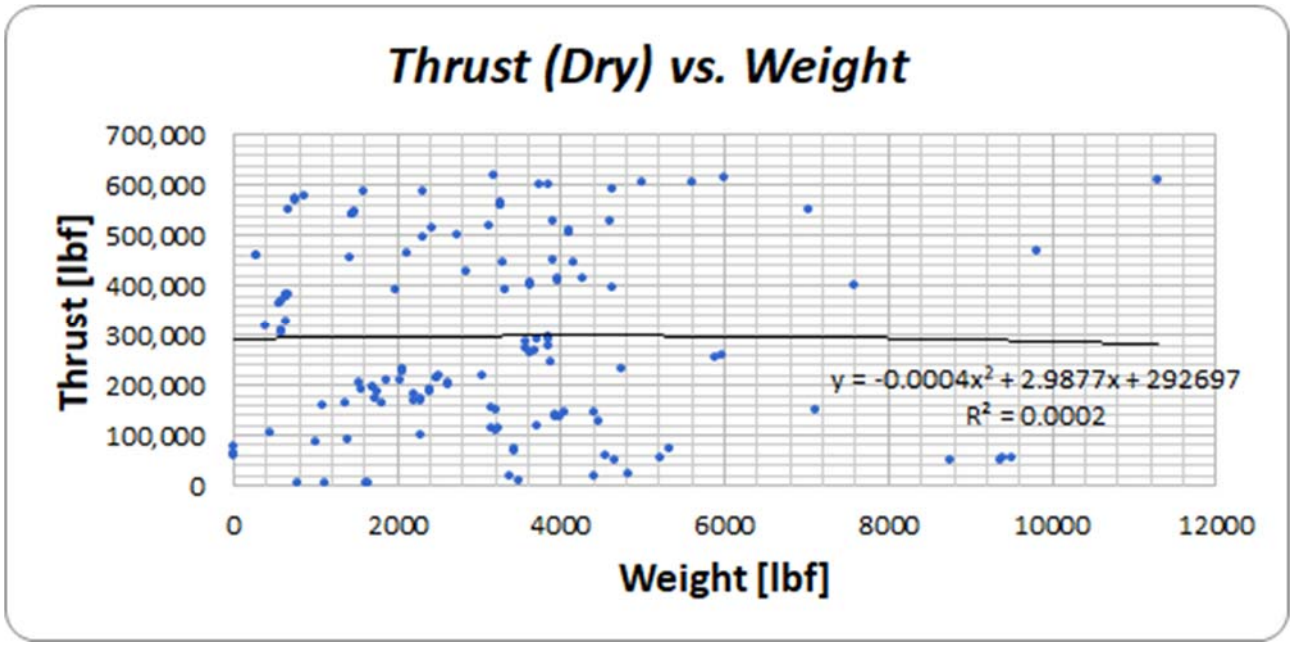

Figure 78: Weight vs Thrust for Military Aircraft

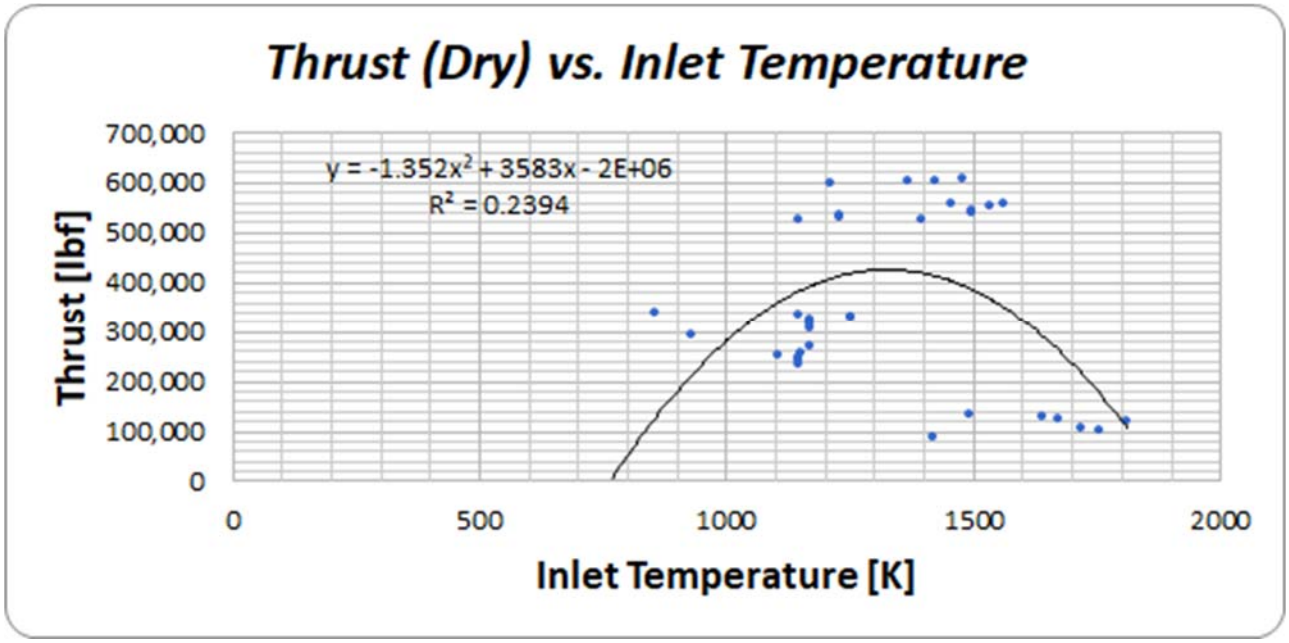

Figure 79: Inlet Temperature vs Thrust for Military Aircraft

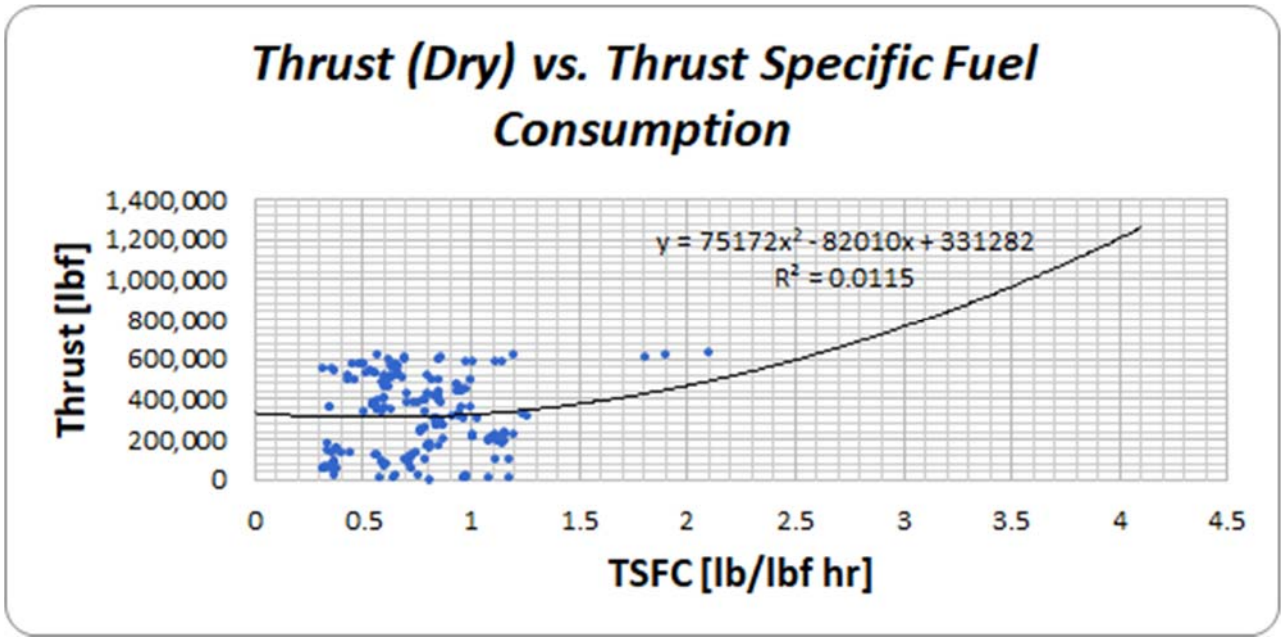

Figure 80: TSFC vs Thrust for Military Aircraft

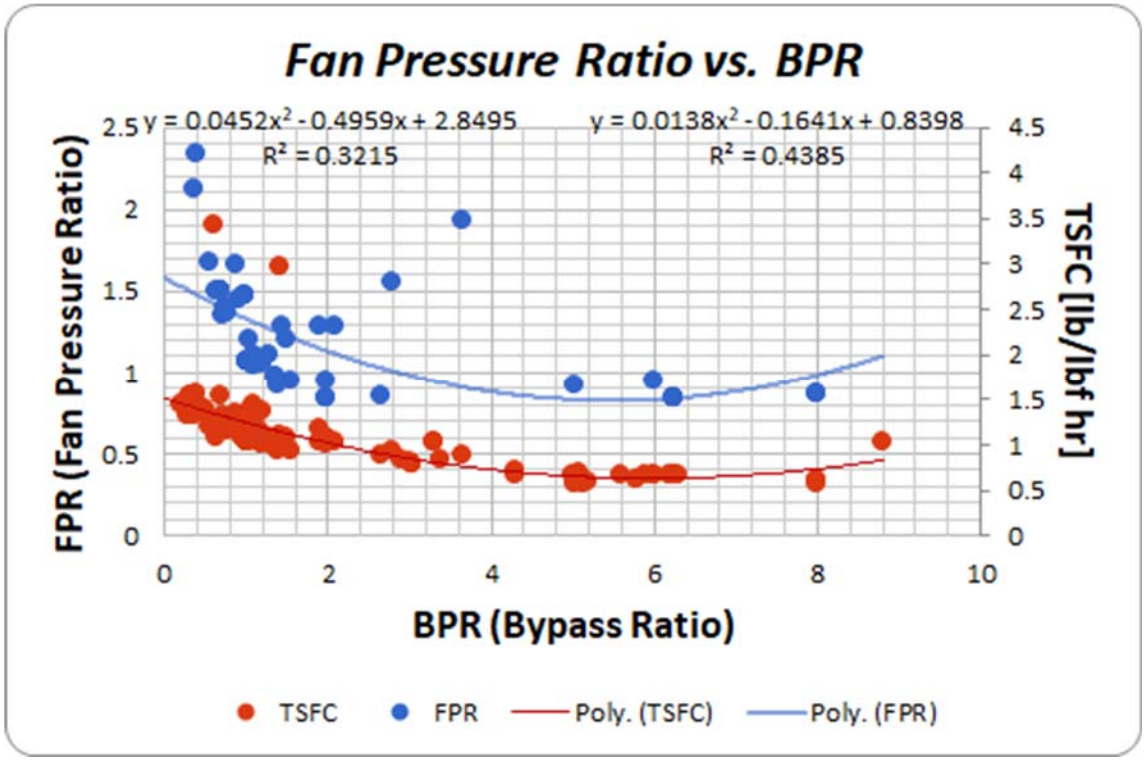

Figure 81: Bypass Ratio vs TSFC and Fan Pressure Ratio for Military Aircraft

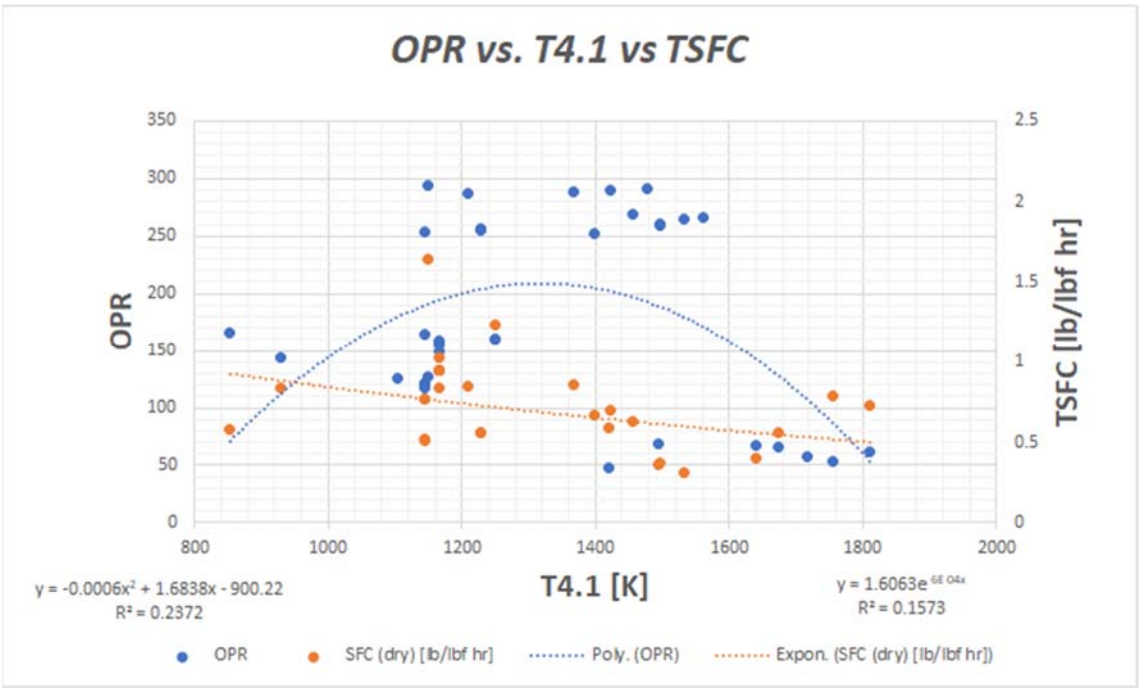

Figure 82: Inlet Temperature vs Overall Pressure Ratio and TSFC for Military Aircraft

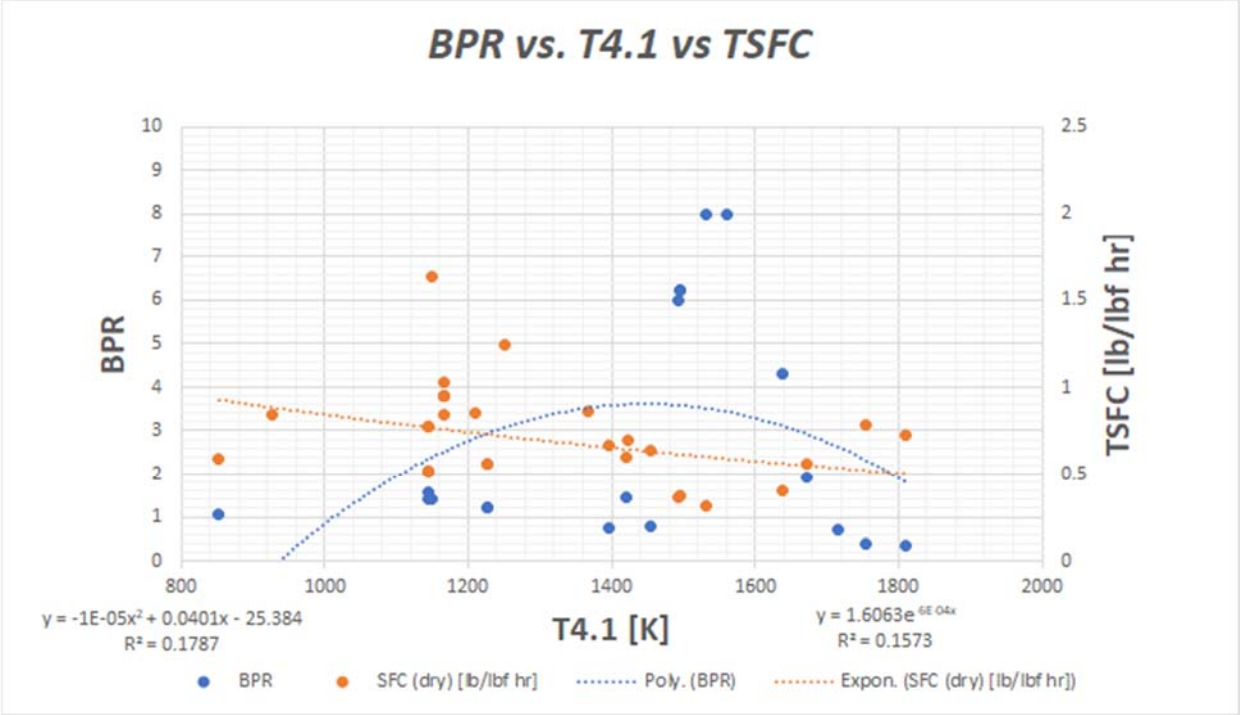

Figure 83: Inlet Temperature vs Bypass Ratio and TSFC for Military Aircraft

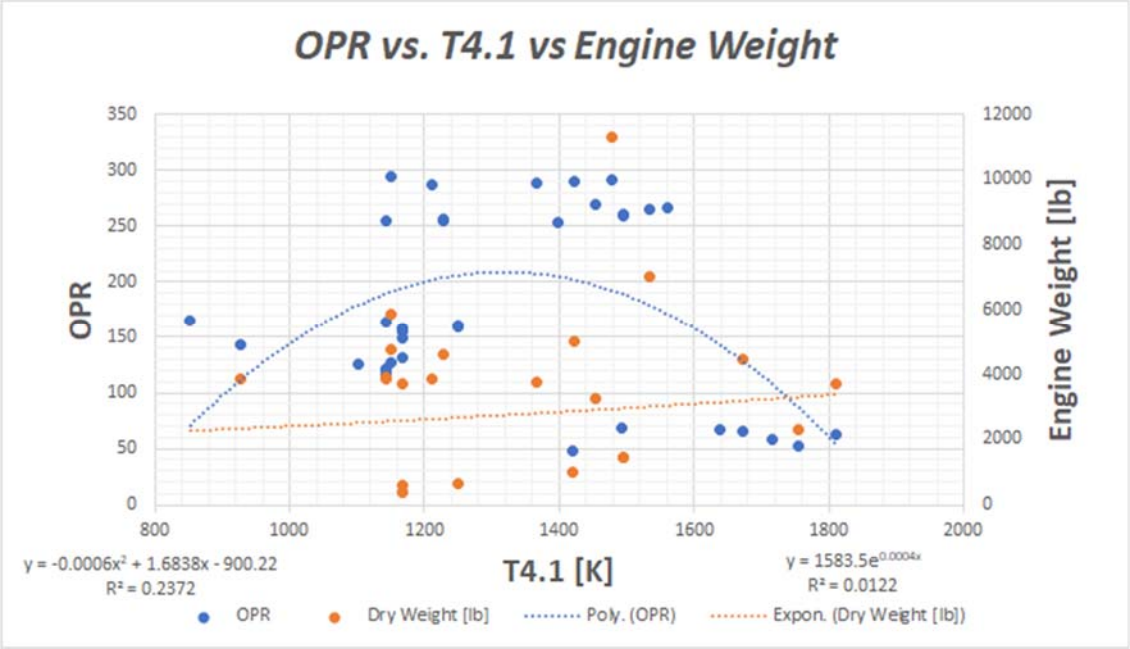

Figure 84: Inlet Temperature vs Overall Pressure Ratio and Engine Weight for Military Aircraft

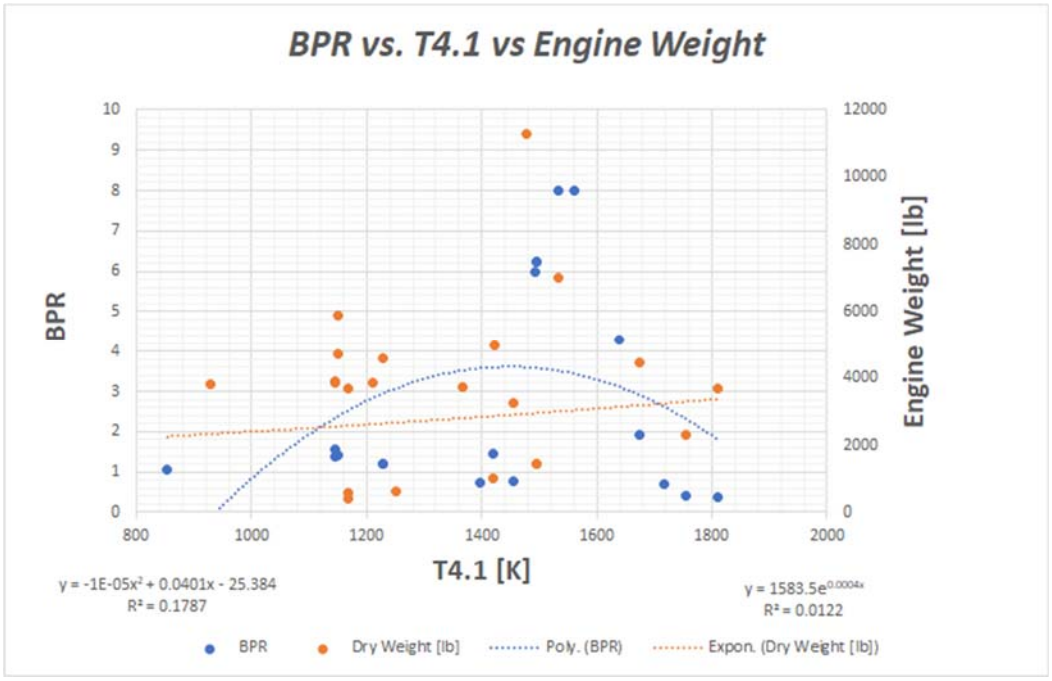

Figure 85: Inlet Temperature vs Bypass Ratio and Engine Weight for Military Aircraft

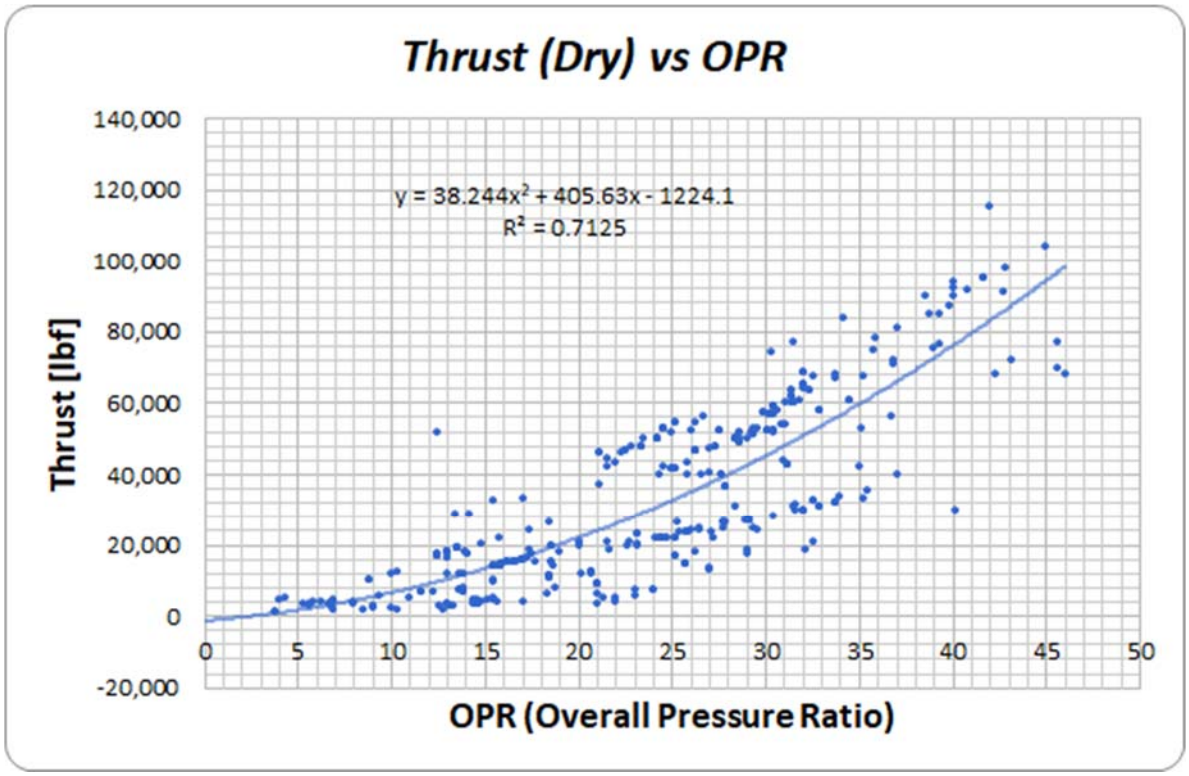

Figure 86: Overall Pressure Ratio vs Thrust for Commercial Aircraft

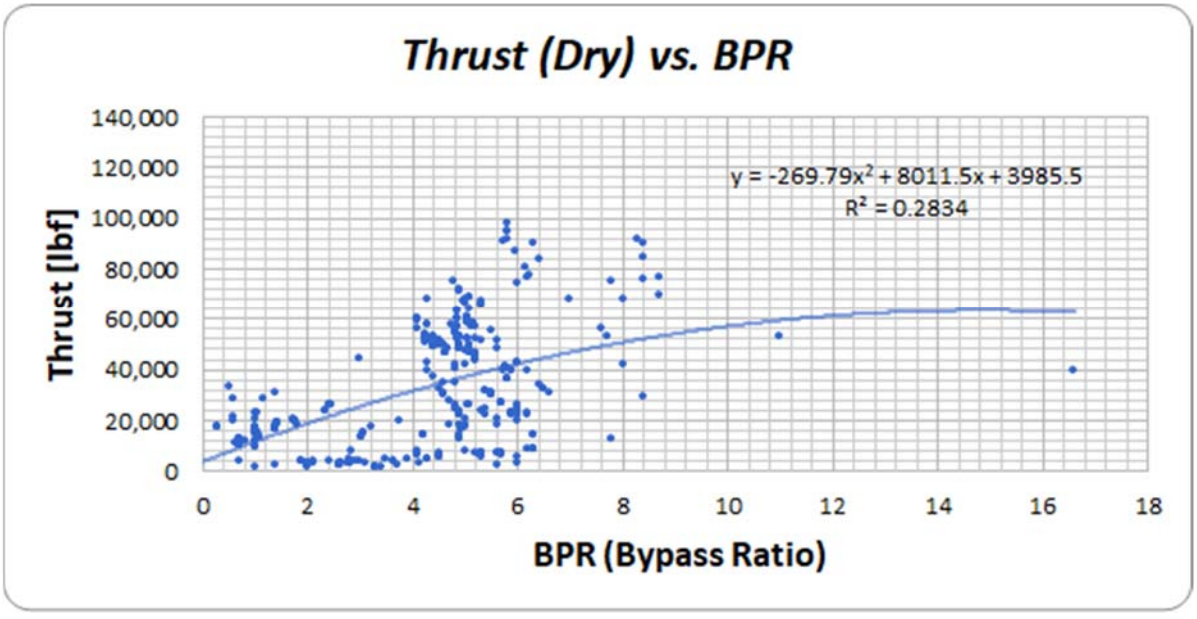

Figure 87: Bypass Ratio vs Thrust for Commercial Aircraft

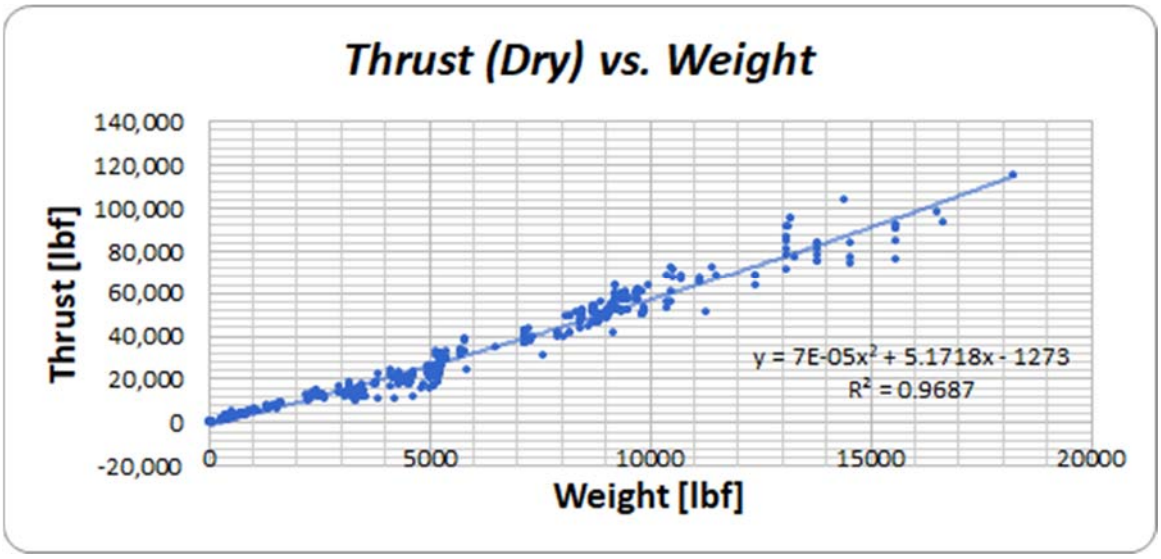

Figure 88: Weight vs Thrust for Commercial Aircraft

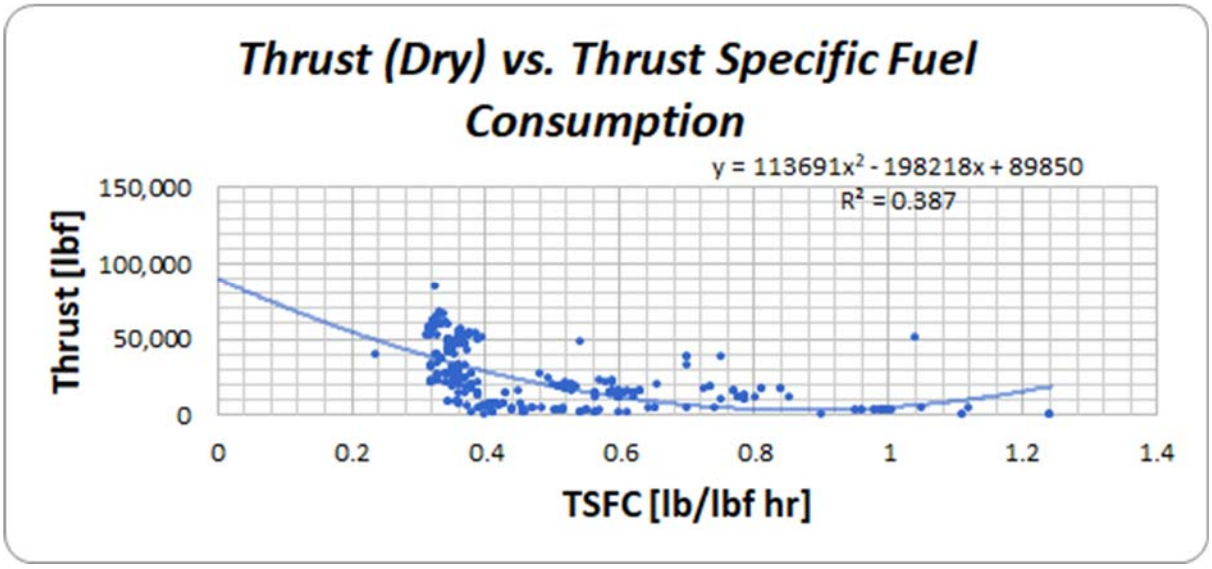

Figure 89: TSFC vs Thrust for Commercial Aircraft

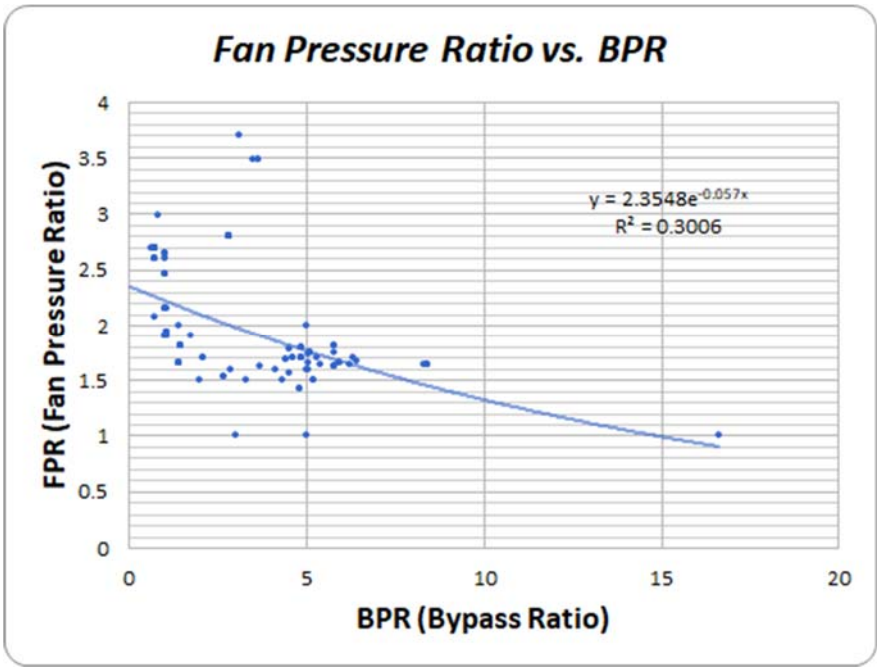

Figure 90: Fan Pressure Ratio vs Bypass Ratio for Commercial Aircraft

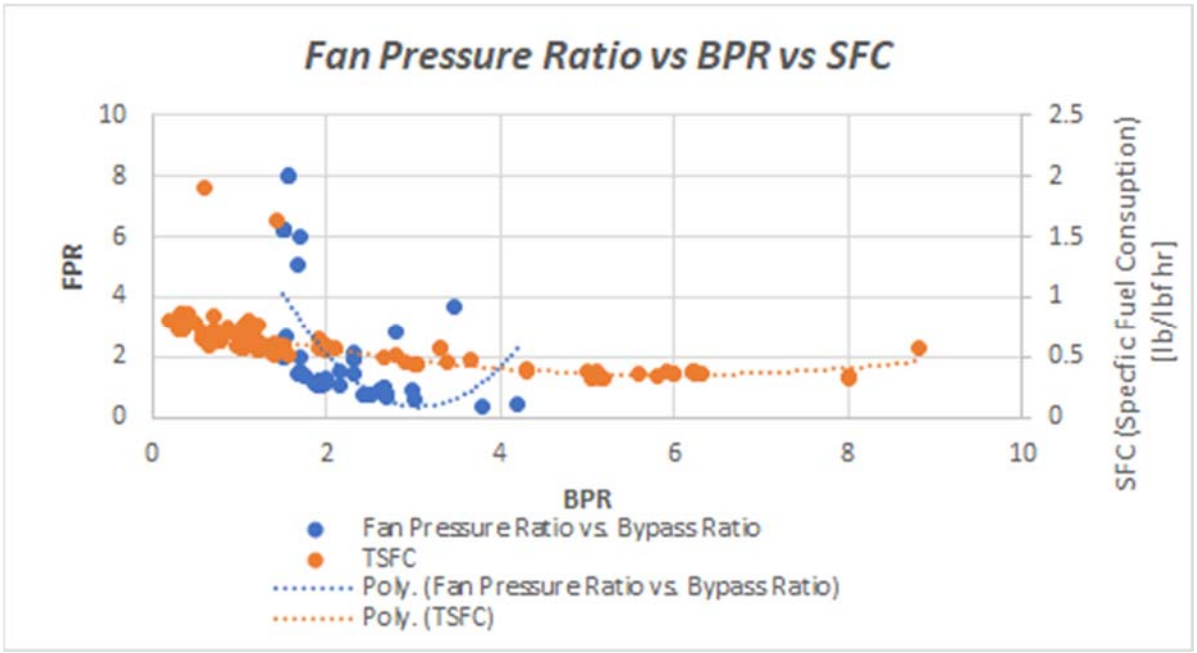

Figure 91: Fan Pressure Ratio vs BPR vs SFC for Supersonic Military Aircrafts

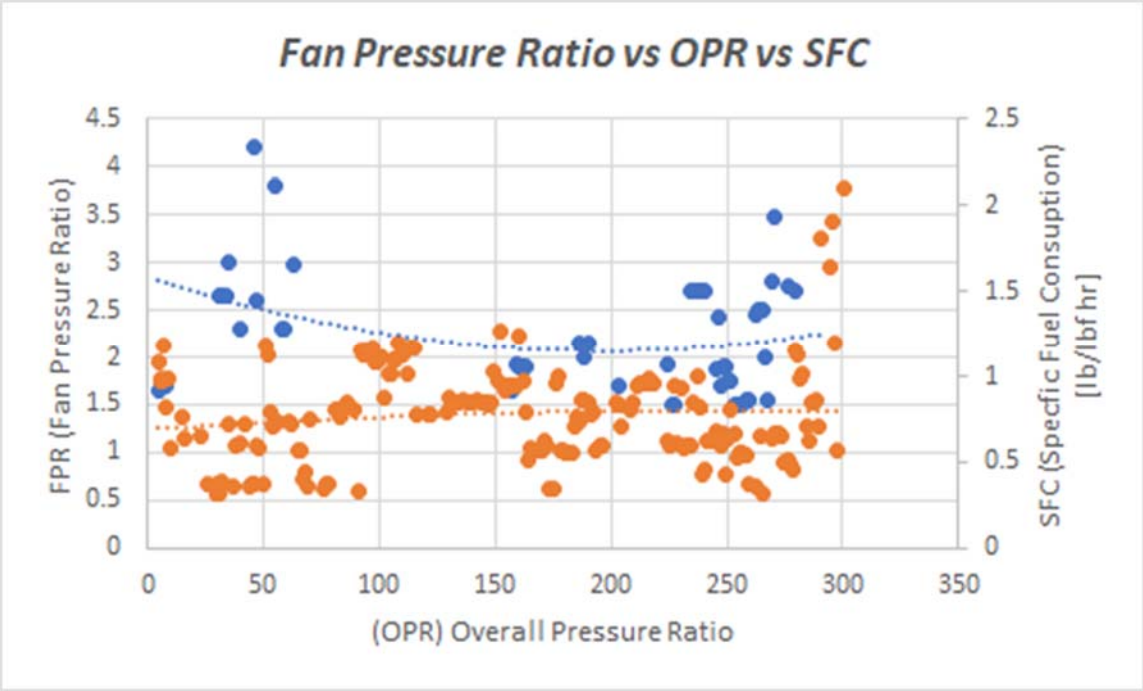

Figure 92: Fan Pressure Ratio vs OPR vs SFC for Supersonic Military Aircrafts

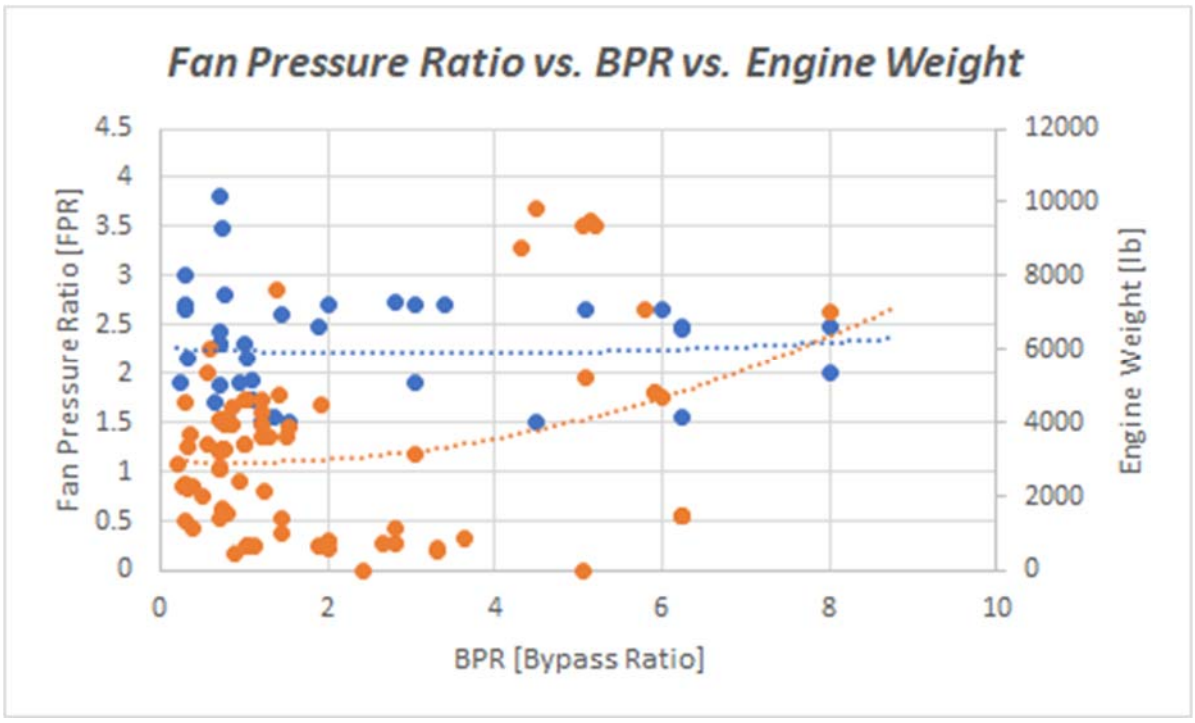

Figure 93: Fan Pressure Ratio vs BPR vs Engine Weight for Supersonic Military Aircrafts

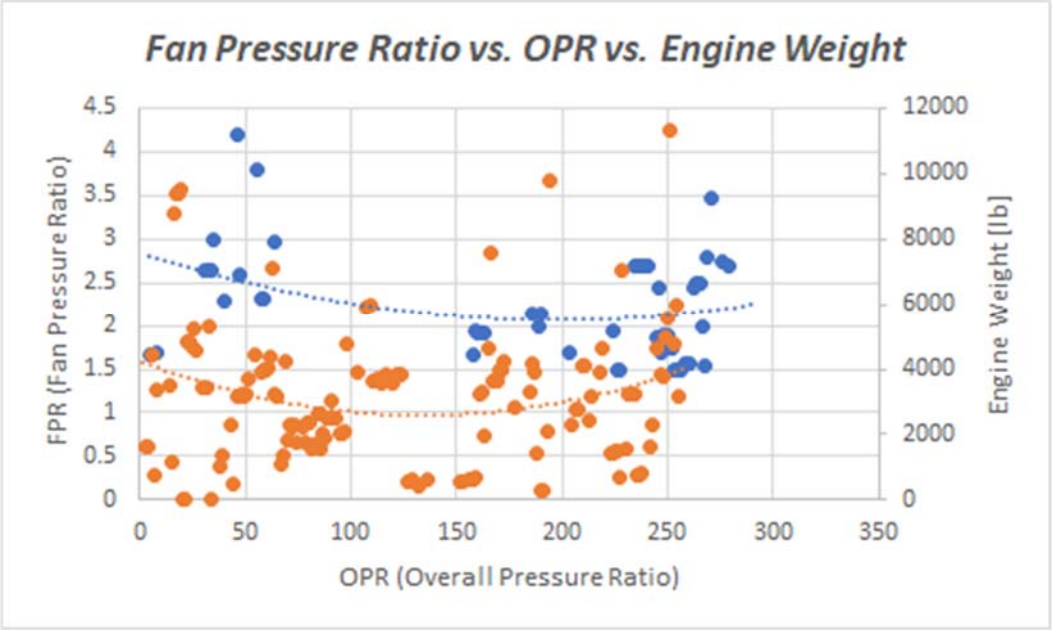

Figure 94: Fan Pressure Ratio vs OPR vs Engine Weight for Supersonic Military Aircrafts

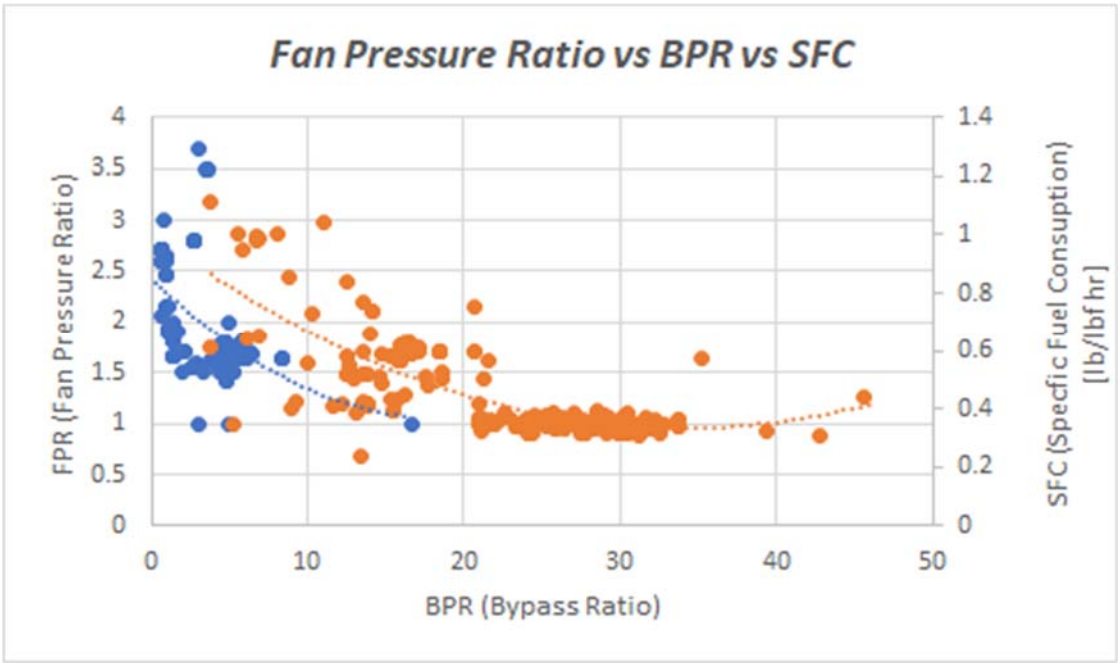

Figure 95: Fan Pressure Ratio vs BPR vs Engine Weight for Commercial Aircrafts

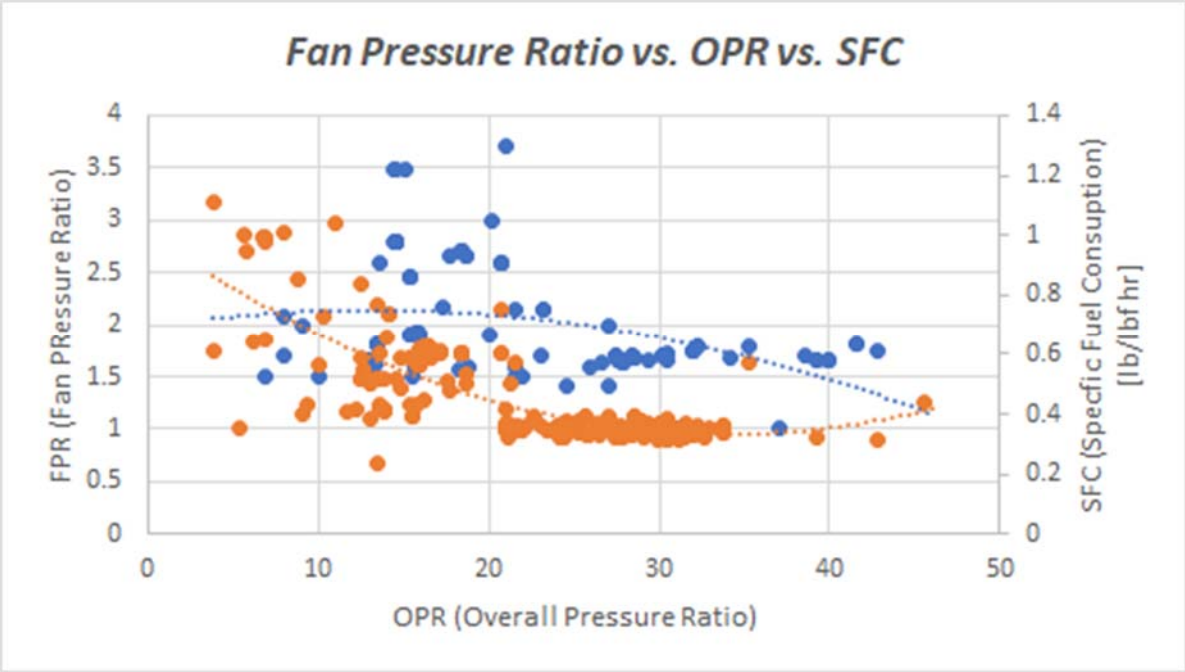

Figure 96: Fan Pressure Ratio vs OPR vs SFC for Commercial Aircrafts

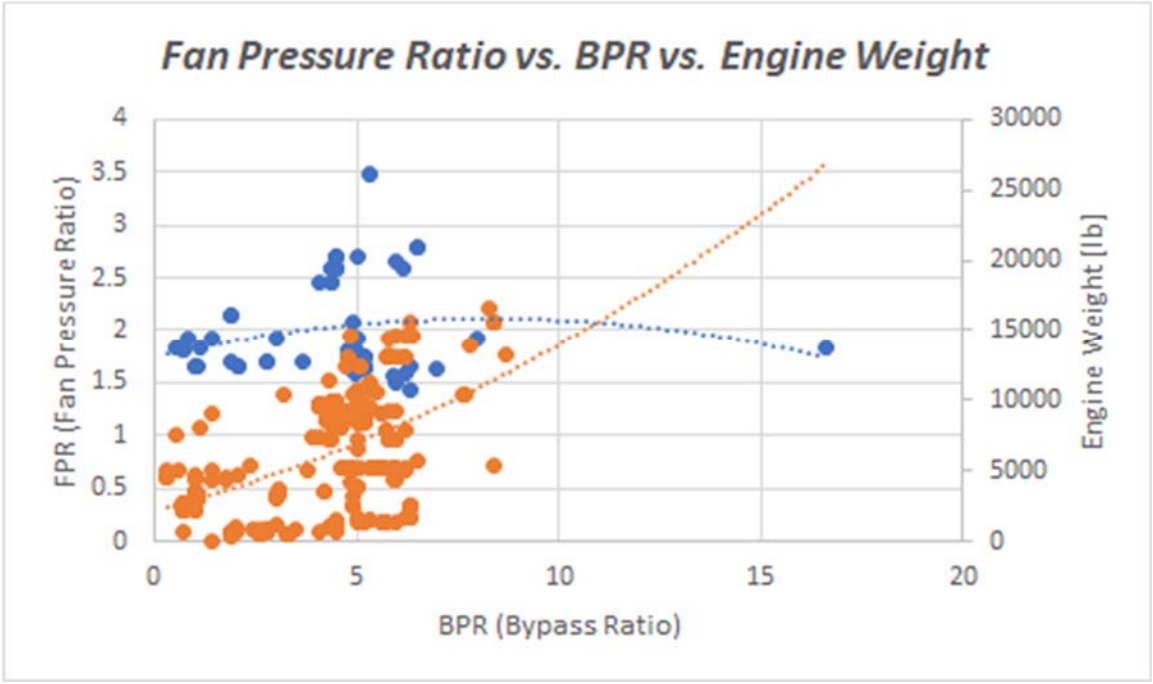

Figure 97: Fan Pressure Ratio vs BPR vs Engine Weight for Commercial Aircrafts

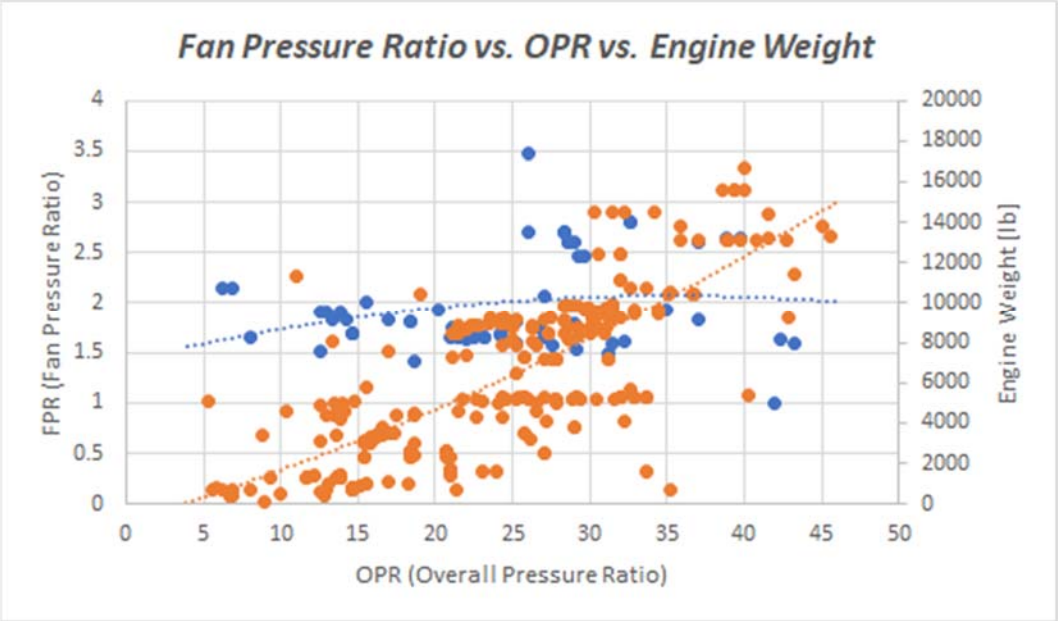

Figure 98: Fan Pressure Ratio vs OPR vs Engine Weight for Commercial Aircrafts

Appendix I: Parametric Cycle Analysis

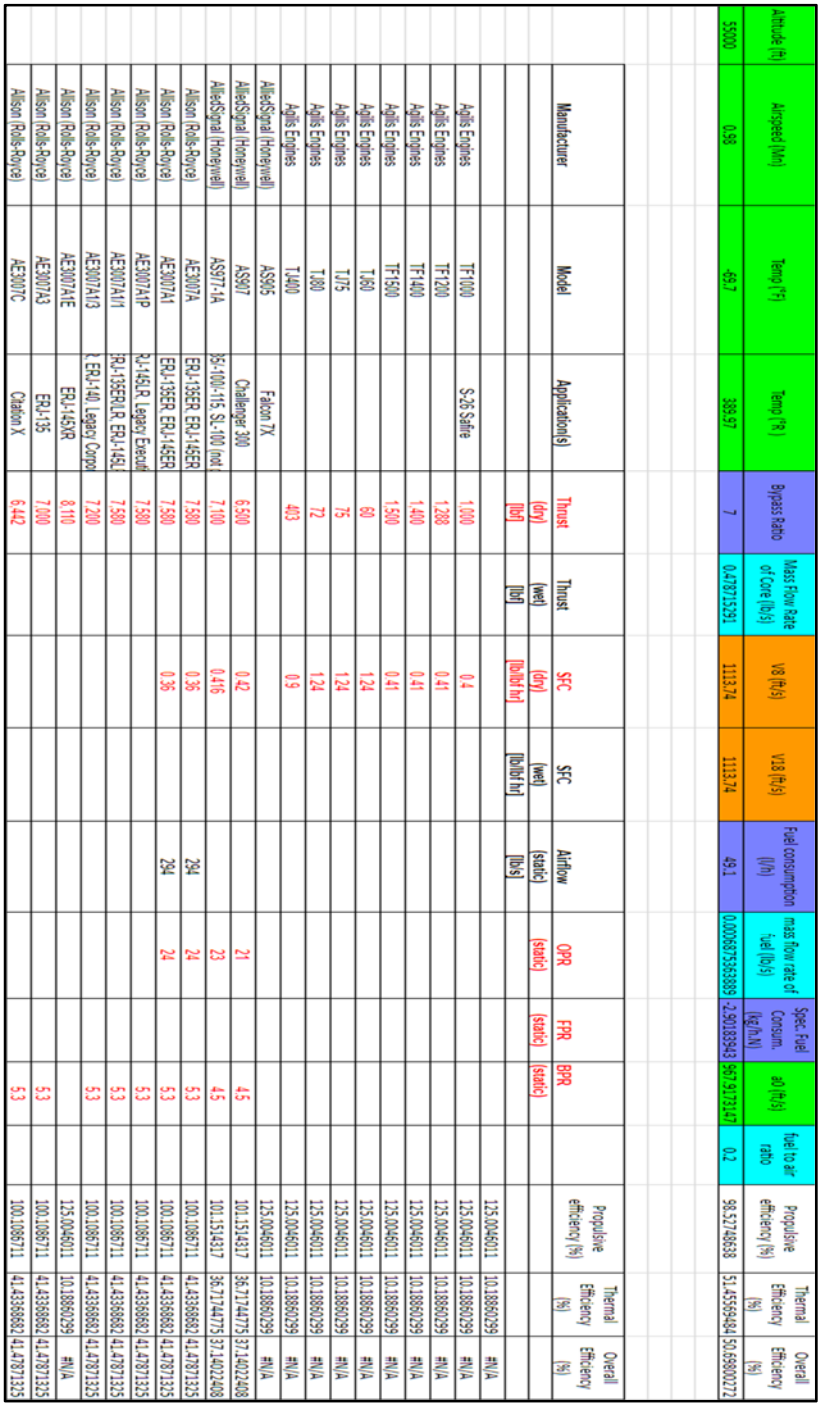

Altitude (ft)	Airspeed (Mn)	Temp (°F)	Temp (°R)	Bypass Ratio	Mass Flow Rate of Core (lb/s)	V8 (ft/s)	V18 (ft/s)	Fuel consumption (l/h)	mass flow rate of fuel (lb/s)	Spec. Fuel Consum. (lbf/h.N)	a0 (ft/s)	fuel to air ratio	Propulsive efficiency (%)	Thermal Efficiency (%)	Overall Efficiency (%)
55000	0.98	-69.7	389.97	7	0.479315291	1113.74	1113.74	49.1	0.003637353889	2.90183943	967.9173147	0.2	98.52746638	51.45559484	50.65800272

Manufacturer	Model	Application(s)	Thrust (dry)	Thrust (wet)	SFC (dry)	SFC (wet)	Airflow	OPR	FPR	BPR	Propulsive efficiency (%)	Thermal Efficiency (%)	Overall Efficiency (%)
			[lbf]	[lbf]	[lbm/lbf hr]	[lbm/lbf hr]	[lbs]	(static)	(static)	(static)			
Agilis Engines	TF1000	S-26 Sefire	1.000		0.4						123.0046011	10.18860299	#N/A
Agilis Engines	TF1200		1.288		0.41						123.0046011	10.18860299	#N/A
Agilis Engines	TF1400		1.400		0.41						123.0046011	10.18860299	#N/A
Agilis Engines	TF1500		1.500		0.41						123.0046011	10.18860299	#N/A
Agilis Engines	TJ60		60		1.24						123.0046011	10.18860299	#N/A
Agilis Engines	TJ75		75		1.24						123.0046011	10.18860299	#N/A
Agilis Engines	TJ80		72		1.24						123.0046011	10.18860299	#N/A
Agilis Engines	TJ400		403		0.9						123.0046011	10.18860299	#N/A
AlliedSignal (Honeywell)	AS905	Falcon 7X									123.0046011	10.18860299	#N/A
AlliedSignal (Honeywell)	AS907	Challenger 300	6.500		0.42			21	4.5	4.5	101.1514317	36.71744775	37.14022408
AlliedSignal (Honeywell)	AS977-1A	35-100-115, SL-100 (not	7.100		0.416			23	4.5	4.5	101.1514317	36.71744775	37.14022408
Allison (Rolls-Royce)	AE3007A	ERJ-135ER, ERJ-145ER	7.580		0.36		294	24	5.3	5.3	100.1086711	41.43366882	41.47871325
Allison (Rolls-Royce)	AE3007A1	ERJ-135ER, ERJ-145ER	7.580		0.36		294	24	5.3	5.3	100.1086711	41.43366882	41.47871325
Allison (Rolls-Royce)	AE3007A1P	RJ-145LR, Legacy Executiv	7.580						5.3	5.3	100.1086711	41.43366882	41.47871325
Allison (Rolls-Royce)	AE3007A1/1	ERJ-135ERLR, ERJ-145LI	7.580						5.3	5.3	100.1086711	41.43366882	41.47871325
Allison (Rolls-Royce)	AE3007A1/3	, ERJ-140, Legacy Corpo	7.200						5.3	5.3	100.1086711	41.43366882	41.47871325
Allison (Rolls-Royce)	AE3007A1E	ERJ-145XR	8.110								125.0046011	10.18860299	#N/A
Allison (Rolls-Royce)	AE3007A3	ERJ-135	7.000						5.3	5.3	100.1086711	41.43366882	41.47871325
Allison (Rolls-Royce)	AE3007C	Citation X	6.442						5.3	5.3	100.1086711	41.43366882	41.47871325

Table 7: Parametric Cycle Analysis Excel Sheet

Table 8: Table of constant values for parametric cycle analysis

Density of Fuel (lb/ft^3)	50.41	R of air (ft-lbf/°R*slug)	1716
Low heating value of Fuel (ft-lbf/lbm)	14445945.86	gc	1
Gamma	1.4	cp	53.67

Table 9: Detailed calculations involving propulsive and thermal efficiency

Check Work						
Propulsive Efficiency						
	1+f	1.2			fuel to air ratio	f
	V9/a0	1.15065613			core exit velocity	v8
	alpha (BPR)	7			bypass ratio	alpha
	v19/a0	1.15065613			Bypass exit velocity	v19
	1+alpha	8			speed of sound	a0
	(v9/a0)^2	1.32400955				
	alpha(v19/a0)^2	9.26806684				
	(1+alpha)M0^2	7.6832				
Numerator			Calculated Propulsive Efficiency			
	3.126945464			98.5274863		
Denomenator						
	3.173678309					
Thermal Efficiency						
	a0^2	936863.928				
	(1+f)	1.2				
	(v9/a0)	1.15065613				
	alpha(V19/a0)^2	9.26806684				
	(1+alpha)(m0^2)	7.6832				
	2*gc*f*h_pr	5778378.34				
Numerator			Calcualted Thermal Efficiency			
	2973304.727			51.4556948		
Denomenator						
	5778378.343					

Figure 99: Parametric Cycle Analysis Program for Candidate Engine (Trial 1)

Appendix J: TOPSIS Analysis and Design Matrix

Design Matrix									
		Concept							
		Icon-II		765-072B		765-076E		Lockheed N+2 Concept	
Selection Criteria	Weight	Rating	Weighted Score	Rating	Weighted Score	Rating	Weighted Score	Rating	Weighted Score
Weight	18%	5	0.9	4	0.72	4	0.72	3	0.54
Material Cost	0%	0	0	0	0	0	0	0	0
Manufacturability	17%	4	0.68	5	0.85	4	0.68	5	0.85
Avoidance of Shock Cone	20%	6	1.2	5	1	6	1.2	5	1
Maintenancability	10%	3	0.3	6	0.6	3	0.3	5	0.5
Aesthetics	5%	7	0.35	4	0.2	4	0.2	5	0.25
Stability	20%	6	1.2	6	1.2	7	1.4	6	1.2
Wing Geometry	10%	6	0.6	4	0.4	5	0.5	5	0.5
	100%								
	Total Weighted Score	5.23		4.97		5		4.34	
	Rank	3		1		5		4	
	Continue?	NO		YES		NO		NO	

Figure 100: Design matrix for preliminary selection

	Weight	Interior Layout	Manufacturability	Avoidance of Shock Cone	Maintenancability	Aesthetics	Stability	Wing Geometry
Weight	1	0.33	2	1	0.5	0.33	3	1
Interior Layout	3	1	0.5	2	2	1	2	2
Manufacturability	2	0.5	1	3	1	1	3	2
Avoidance of Shock Cone	1	0.33	0.5	1	0.5	0.33	1	1
Maintenancability	0.5	0.5	2	2	1	2	2	1
Aesthetics	3	2	3	3	0.5	1	3	3
Stability	1	0.33	1	1	0.33	0.33	1	1
Wing Geometry	2	0.33	0.5	1	0.5	0.33	1	1
Total	13.5	5.32	10.5	14	6.33	6.32	16	12
Weighting	0.161	0.063	0.125	0.167	0.075	0.075	0.191	0.143

Figure 101: Prioritization Matrix for TOPSIS

Qualitative Scale:	
Excellent	9
Above Average	7
Average	5
Below Average	3
Poor	1

FINAL RANKING

	Closeness to Ideal
Icon-II	0.659566
765-072B	0.518155
765-076E	0.618234
Lockheed N+2 Concept	0.443460
	0.000000

Figure 102: Qualitative Scale and Final Ranking for TOPSIS

DATA MATRIX

	Weight	Interior	Manufacturability	Avoidance of Shock Cone	Maintenancability	Aesthetics	Stability	Wing Geometry
Icon-II	7.00	9	3	7	3	9	5	5
765-072B	5.00	3	7	3	5	3	5	3
765-076E	5.00	5	3	5	3	3	7	5
Lockheed N+2 Concept	3.00	7	7	3	5	5	5	5

Figure 103: Finalized TOPSIS Data Matrix

NORMALIZED MATRIX

	Weight	Material Cost	Manufacturability	Avoidance of Shock Cone	Maintenancability	Aesthetics	Stability	Wing Geometry
Icon-II	0.6736	0.7028	0.2785	0.7298	0.3638	0.8082	0.4490	0.5455
765-072B	0.4811	0.2343	0.6499	0.3128	0.6063	0.2694	0.4490	0.3273
765-076E	0.4811	0.3904	0.2785	0.5213	0.3638	0.2694	0.6286	0.5455
Lockheed N+2 Concept	0.2887	0.5466	0.6499	0.3128	0.6063	0.4490	0.4490	0.5455
	0.0000	0.0000	0.0000	0.0000	0.0000	0.0000	0.0000	0.0000

CRITERIA WEIGHTS

	Weight	Material Cost	Manufacturability	Avoidance of Shock Cone	Maintenancability	Aesthetics	Stability	Wing Geometry
Raw Weight	13.5	5.32	10.5	14	6.33	6.32	16	12
Weights	0.161	0.063	0.125	0.167	0.075	0.075	0.191	0.143

WEIGHTED DATA MATRIX

	Weight	Material Cost	Manufacturability	Avoidance of Shock Cone	Maintenancability	Aesthetics	Stability	Wing Geometry
Icon-II	0.1083	0.0445	0.0348	0.1217	0.0274	0.0608	0.0856	0.0780
765-072B	0.0774	0.0148	0.0813	0.0521	0.0457	0.0203	0.0856	0.0468
765-076E	0.0774	0.0247	0.0348	0.0869	0.0274	0.0203	0.1198	0.0780
Lockheed N+2 Concept	0.0464	0.0346	0.0813	0.0521	0.0457	0.0338	0.0856	0.0780
	0.0000	0.0000	0.0000	0.0000	0.0000	0.0000	0.0000	0.0000

IDEAL SOLUTION MATRIX

	Weight	Material Cost	Manufacturability	Avoidance of Shock Cone	Maintenancability	Aesthetics	Stability	Wing Geometry
Positive Ideal	0.1083	0.0000	0.0000	0.1217	0.0457	0.0608	0.1198	0.0000
Negative Ideal	0.0000	0.0445	0.0813	0.0000	0.0000	0.0000	0.0000	0.0780

DIST FROM POSITIVE MATRIX

	Weight	Material Cost	Manufacturability	Avoidance of Shock Cone	Maintenancability	Aesthetics	Stability	Wing Geometry	S*
Icon-II	0.000000	0.001983	0.001213	0.000000	0.000334	0.000000	0.001171	0.006078	0.103824
765-072B	0.000957	0.000220	0.006605	0.004834	0.000000	0.001645	0.001171	0.002188	0.132744
765-076E	0.000957	0.000612	0.001213	0.001209	0.000334	0.001645	0.000000	0.006078	0.109764
Lockheed N+2 Concept	0.003829	0.001199	0.006605	0.004834	0.000000	0.000731	0.001171	0.006078	0.156359
	0.011727	0.000000	0.000000	0.014805	0.002089	0.003700	0.014347	0.000000	0.216031

DIST FROM NEGATIVE MATRIX

	Weight	Material Cost	Manufacturability	Avoidance of Shock Cone	Maintenancability	Aesthetics	Stability	Wing Geometry	S-
Icon-II	0.011727	0.000000	0.002157	0.014805	0.000752	0.003700	0.007320	0.000000	0.201151
765-072B	0.005983	0.000881	0.000000	0.002719	0.002089	0.000411	0.007320	0.000973	0.142747
765-076E	0.005983	0.000392	0.002157	0.007554	0.000752	0.000411	0.014347	0.000000	0.177752
Lockheed N+2 Concept	0.002154	0.000098	0.000000	0.002719	0.002089	0.001142	0.007320	0.000000	0.124589
	0.000000	0.001983	0.006605	0.000000	0.000000	0.000000	0.000000	0.006078	0.121102

Figure 104: Normalized, criteria, weighted data, ideal solution, distance from the positive, and negative matrices for TOPSIS

Appendix K: Initial Weight Calculations

Number	Leg		Mission Segment Weight Fraction (Fuel Ratios)	
1	Warming, Taxi, Take-Off	w1/w0	0.97	Table 3.2
2	Climb	w2/w1	0.985	Table 3.2
3	Cruise	w3/w2	0.5588342237	
4	Landing	w4/w3	0.995	Table 3.2
5				
			Estimated Fuel Fraction	
		w4/w0	0.5312684682	
		wf/w0	0.4968554237	
Iterative Process				
W0 (Guess)	WE/W0	WE	W0	
317500	0.4361639203	138482.0447	317432.7199	

Figure 105: Sizing Calculation

R - Range	Range: 4603.118 mi (4,000 nmi; 3,235 km)
C - SFC (Table 3.4) - Piston-Prop	C = 0.4 {0.068} lb/(hr/bhp) {mg/W-s}
V - Velocity	Maximum speed: 185 mph (298 km/h; 161 kn) (max cruise) Cruise speed: 144 mph (125 kn; 232 km/h) (40% power)
L/D - Lift to Drag Ratio	12.5
E - Endurance	45 mins = 2700 s

Figure 106: Inputs for the Beguet Range equation

w3/w2				
Range	R	4603.118	nmi	
Specific Fuel Consum	C	0.5	/hr	cruise
		0.4	/hour	loiter
Speed	V	1.6	M	
Conversions				
	R	24304463	ft	
	C	0.00027777	/s	
		0.00022222	/s	
	V	1786.29921	ft/s	
Lift to Drag Ratio	L/D_max	7.5		
	L/D_cruise	6.495		
w3/w2		0.5588342237		

Figure 107: Breguet Range Equation calculation

Appendix L: TURBN Turbine Analysis Program

```
TURBN V5.50 - Data File: Default Data
Stage #02    Date - 4/28/2018    Time - 5:55:31 PM
 Corr Flow =   3.98 lbm/s  M1  = 0.7935  Tt1 = 2925.0 R   Pt1 = 194.64 psia
 Mass Flow =  22.20 lbm/s  M2  = 0.6500  AL2 = 35.92      AL1 =  0.00
 u3/u2 = 1.0000 phis= 0.020 et  = 0.900  Um  =  1182 ft/s rm  = 10.00 in
 Stator: Z = 1.0000   c/h = 1.0000   Rotor: Z = 1.0000   c/h = 0.7000
 Gamma = 1.3000 Gas Const = 53.40ft-lbf/lbm-R  w =  1418 rad/s  AL3 =  0.00
 Omega = 0.2532        Cp = 0.2974 Btu/lbm-R

RESULT: Tt3/Tt1 = 0.9487  Pt3/Pt1 = 0.7761  DTt = 150.00 R  AN^2=3.086E+09
  Reaction  Hub = 0.5891  Mean    = 0.6000  Tip = 0.6105    Eff = 90.26%
  Flow   Area 1 =  12.41  Area 2  =  16.84  Area 3 =  19.20  in^2
  Coeff.  Load = 0.8000  Flow = 1.1043  Vel Rat = 0.7906  RPM  = 13,539
  Nozzle - # of Vanes  = 408   c/s = 1.512
  Rotor  - # of Blades = 285   c/s = 0.911  M3Rt = 0.727

   Station    1h    1m    1t    2h    2m    2t   2Rm   3Rm    3h    3m    3t
Prop:     ------------------------------------------------------------------
 Tt     R |  2925  2925  2925  2925  2925  2925  2869  2869  2775  2775  2775
 T      R |  2673  2673  2673  2749  2751  2752  2751  2661  2661  2661  2661
 Pt  psia | 194.6 194.6 194.6 193.7 193.7 193.7 178.1 174.5 151.1 151.1 151.1
 P   psia | 131.6 131.6 131.6 148.1 148.4 148.8 148.4 125.9 125.9 125.9 125.9
 M        | 0.794 0.794 0.794 0.653 0.650 0.647 0.535 0.722 0.535 0.535 0.535
 Vel ft/s |  1939  1939  1939  1619  1611  1604  1326  1760  1305  1305  1305
 u   ft/s |  1939  1939  1939  1305  1305  1305  1305  1305  1305  1305  1305
 v   ft/s |     0     0     0   958   945   933 -0236  1182     0     0     0
 alpha deg| 0.00  0.00  0.00 36.29 35.92 35.56                  0.00  0.00  0.00
 beta  deg|                                      -10.27 42.16
 radius in|  9.90 10.00 10.10  9.87 10.00 10.13 10.00 10.00  9.85 10.00 10.15
```

Figure 108: TURBN Stage 2 Analysis

```
TURBN V5.50 - Data File: Default Data
Stage #03    Date - 4/28/2018    Time - 5:55:42 PM
 Corr Flow =   5.00 lbm/s  M1  = 0.5352  Tt1 = 2775.0 R   Pt1 = 151.06 psia
 Mass Flow =  22.20 lbm/s  M2  = 0.6500  AL2 = 34.21      AL1 =  0.00
 u3/u2 = 1.0000 phis= 0.020 et  = 0.900  Um  =  1182 ft/s rm  = 10.00 in
 Stator: Z = 1.0000   c/h = 0.6000   Rotor: Z = 1.0000   c/h = 0.6000
 Gamma = 1.3000 Gas Const = 53.40ft-lbf/lbm-R  w =  1418 rad/s  AL3 =  0.00
 Omega = 0.2599        Cp = 0.2974 Btu/lbm-R

RESULT: Tt3/Tt1 = 0.9495  Pt3/Pt1 = 0.7794  DTt = 140.00 R  AN^2=3.793E+09
  Reaction  Hub = 0.6141  Mean    = 0.6267  Tip = 0.6387    Eff = 90.26%
  Flow   Area 1 =  19.20  Area 2  =  20.69  Area 3 =  23.66  in^2
  Coeff.  Load = 0.7467  Flow = 1.0985  Vel Rat = 0.8183  RPM  = 13,539
  Nozzle - # of Vanes  = 330   c/s = 1.000
  Rotor  - # of Blades = 255   c/s = 0.859  M3Rt = 0.7458

   Station    1h    1m    1t    2h    2m    2t   2Rm   3Rm    3h    3m    3t
Prop:     ------------------------------------------------------------------
 Tt     R |  2775  2775  2775  2775  2775  2775  2729  2729  2635  2635  2635
 T      R |  2661  2661  2661  2608  2610  2611  2610  2522  2522  2522  2522
 Pt  psia | 151.1 151.1 151.1 150.4 150.4 150.4 139.8 137.0 117.7 117.7 117.7
 P   psia | 125.9 125.9 125.9 114.9 115.2 115.5 115.2  97.3  97.3  97.3  97.3
 M        | 0.535 0.535 0.535 0.654 0.650 0.646 0.552 0.739 0.547 0.547 0.547
 Vel ft/s |  1305  1305  1305  1578  1569  1561  1332  1755  1298  1298  1298
 u   ft/s |  1305  1305  1305  1298  1298  1298  1298  1298  1298  1298  1298
 v   ft/s |     0     0     0   897   882   868 -0299  1182     0     0     0
 alpha deg| 0.00  0.00  0.00 34.65 34.21 33.77                  0.00  0.00  0.00
 beta  deg|                                     -12.99 42.31
 radius in| 9.85 10.00 10.15  9.84 10.00 10.16 10.00 10.00  9.81 10.00 10.19
```

Figure 109: TURBN Stage 3 Analysis

Figure 110: TURBN Stage 4 Analysis

```
TURBN V5.50 - Data File: Default Data
Stage #04    Date - 4/28/2018    Time - 5:55:53 PM
 Corr Flow =   6.25 lbm/s  M1  = 0.5468  Tt1 = 2635.0 R   Pt1 = 117.73 psia
 Mass Flow =  22.20 lbm/s  M2  = 0.6500  AL2 = 33.80      AL1 =  0.00
 u3/u2 = 1.0000 phis= 0.020 et  = 0.900  Um  =  1182 ft/s rm  = 10.00 in
 Stator: Z = 1.0000   c/h = 0.5000   Rotor: Z = 1.0000   c/h = 0.5000
 Gamma = 1.3000 Gas Const = 53.40ft-lbf/lbm-R  w =  1418 rad/s  AL3 =  0.00
 Omega = 0.2668        Cp = 0.2974 Btu/lbm-R

RESULT: Tt3/Tt1 = 0.9488  Pt3/Pt1 = 0.7763  DTt = 135.00 R  AN^2=4.719E+09
  Reaction  Hub = 0.6248  Mean    = 0.6400  Tip = 0.6543    Eff = 90.26%
  Flow   Area 1 =  23.66  Area 2  =  25.75  Area 3 =  29.58  in^2
  Coeff.  Load = 0.7200  Flow = 1.0755  Vel Rat = 0.8333  RPM  = 13,539
  Nozzle - # of Vanes  = 323   c/s = 1.011
  Rotor  - # of Blades = 240   c/s = 0.841  M3Rt = 0.759

   Station    1h    1m    1t    2h    2m    2t   2Rm   3Rm    3h    3m    3t
Prop:     ------------------------------------------------------------------
 Tt     R |  2635  2635  2635  2635  2635  2635  2594  2594  2500  2500  2500
 T      R |  2522  2522  2522  2476  2478  2480  2478  2392  2392  2392  2392
 Pt  psia | 117.7 117.7 117.7 117.2 117.2 117.2 109.4 107.2  91.4  91.4  91.4
 P   psia | 97.35 97.35 97.35 89.47 89.79 90.09 89.79 75.42 75.42 75.42 75.42
 M        | 0.547 0.547 0.547 0.655 0.650 0.646 0.558 0.751 0.550 0.550 0.550
 Vel ft/s |  1298  1298  1298  1539  1529  1520  1313  1735  1271  1271  1271
 u   ft/s |  1298  1298  1298  1271  1271  1271  1271  1271  1271  1271  1271
 v   ft/s |     0     0     0   868   851   834 -0331  1182     0     0     0
 alpha deg| 0.00  0.00  0.00 34.35 33.80 33.27                  0.00  0.00  0.00
 beta  deg|                                     -14.59 42.92
 radius in| 9.81 10.00 10.19  9.80 10.00 10.20 10.00 10.00  9.76 10.00 10.24
```

```
TURBN V5.50 - Data File: Default Data
Stage #05    Date - 4/28/2018    Time - 5:56:04 PM
 Corr Flow =   7.84 lbm/s  M1  = 0.5498  Tt1 = 2500.0 R   Pt1 =  91.40 psia
 Mass Flow =  22.20 lbm/s  M2  = 0.6500  AL2 = 30.51      AL1 =  0.00
 u3/u2 = 1.0000 phis= 0.020 et  = 0.900  Um  =  1182 ft/s rm  = 10.00 in
 Stator: Z = 1.0000   c/h = 0.4000   Rotor: Z = 1.0000   c/h = 0.4000
 Gamma = 1.3000 Gas Const = 53.40ft-lbf/lbm-R  w =  1418 rad/s  AL3 =  0.00
 Omega = 0.2739        Cp = 0.2974 Btu/lbm-R

RESULT: Tt3/Tt1 = 0.9520  Pt3/Pt1 = 0.7891  DTt = 120.00 R  AN^2=5.711E+09
  Reaction  Hub = 0.6635  Mean    = 0.6800  Tip = 0.6953    Eff = 90.24%
  Flow   Area 1 =  29.58  Area 2  =  31.16  Area 3 =  35.72  in^2
  Coeff.  Load = 0.6400  Flow = 1.0861  Vel Rat = 0.8839  RPM  = 13,539
  Nozzle - # of Vanes  = 298   c/s = 0.917
  Rotor  - # of Blades = 224   c/s = 0.759  M3Rt = 0.785

   Station     1h     1m     1t     2h     2m     2t    2Rm    3Rm     3h     3m     3t
Prop:      ------------------------------------------------------------------------
 Tt      R |  2500   2500   2500   2500   2500   2500   2474   2474   2380   2380   2380
 T       R |  2392   2392   2392   2349   2351   2353   2351   2269   2269   2269   2269
 Pt   psia | 91.40  91.40  91.40  90.97  90.97  90.97  86.90  85.27  72.12  72.12  72.12
 P    psia | 75.42  75.42  75.42  69.45  69.70  69.94  69.70  58.68  58.68  58.68  58.68
 M         | 0.550  0.550  0.550  0.655  0.650  0.646  0.590  0.775  0.570  0.570  0.570
 Vel ft/s  |  1271   1271   1271   1499   1489   1480   1352   1744   1283   1283   1283
 u   ft/s  |  1271   1271   1271   1283   1283   1283   1283   1283   1283   1283   1283
 v   ft/s  |     0      0      0    775    756    738 -0425   1182      0      0      0
 alpha deg |  0.00   0.00   0.00 31.14  30.51  29.90                   0.00   0.00   0.00
 beta  deg |                                          -18.34 42.64
 radius in |  9.76  10.00  10.24   9.75  10.00  10.25  10.00  10.00   9.72  10.00  10.28
```

Figure 111: TURBN Stage 5 Analysis

```
TURBN V5.50 - Data File: Default Data
Stage #06    Date - 4/28/2018    Time - 5:56:14 PM
 Corr Flow =   9.69 lbm/s  M1  = 0.5700  Tt1 = 2380.0 R   Pt1 =  72.12 psia
 Mass Flow =  22.20 lbm/s  M2  = 0.6500  AL2 = 28.49      AL1 =  0.00
 u3/u2 = 1.0000 phis= 0.020 et  = 0.900  Um  =  1182 ft/s rm  = 10.00 in
 Stator: Z = 1.0000   c/h = 0.3500   Rotor: Z = 1.0000   c/h = 0.3500
 Gamma = 1.3000 Gas Const = 53.40ft-lbf/lbm-R  w =  1418 rad/s  AL3 =  0.00
 Omega = 0.2807        Cp = 0.2974 Btu/lbm-R

RESULT: Tt3/Tt1 = 0.9538  Pt3/Pt1 = 0.7963  DTt = 110.00 R  AN^2=6.922E+09
  Reaction  Hub = 0.6882  Mean    = 0.7067  Tip = 0.7235    Eff = 90.23%
  Flow   Area 1 =  35.72  Area 2  =  37.76  Area 3 =  43.26  in^2
  Coeff.  Load = 0.5867  Flow = 1.0811  Vel Rat = 0.9232  RPM  = 13,539
  Nozzle - # of Vanes  = 272   c/s = 0.886
  Rotor  - # of Blades = 197   c/s = 0.708  M3Rt = 0.8048

   Station     1h     1m     1t     2h     2m     2t    2Rm    3Rm     3h     3m     3t
Prop:      ------------------------------------------------------------------------
 Tt      R |  2380   2380   2380   2380   2380   2380   2364   2364   2270   2270   2270
 T       R |  2269   2269   2269   2236   2238   2240   2238   2160   2160   2160   2160
 Pt   psia | 72.12  72.12  72.12  71.79  71.79  71.79  69.69  68.43  57.43  57.43  57.43
 P    psia | 58.68  58.68  58.68  54.79  55.00  55.20  55.00  46.35  46.35  46.35  46.35
 M         | 0.570  0.570  0.570  0.655  0.650  0.645  0.612  0.792  0.581  0.581  0.581
 Vel ft/s  |  1283   1283   1283   1464   1453   1444   1368   1740   1277   1277   1277
 u   ft/s  |  1283   1283   1283   1277   1277   1277   1277   1277   1277   1277   1277
 v   ft/s  |     0      0      0    715    693    673 -0488   1182      0      0      0
 alpha deg |  0.00   0.00   0.00 29.23  28.49  27.78                   0.00   0.00   0.00
 beta  deg |                                          -20.92 42.77
 radius in |  9.72  10.00  10.28   9.70  10.00  10.30  10.00  10.00   9.66  10.00  10.34
```

Figure 112: TURBN Stage 6 Analysis

Appendix M: Reflections

Challenges have been faced from the beginning of the project. Initially, to gain an understanding on what direction the group was to take, research was explored on any current supersonic transport aircraft. Later research was conducted on those incorporating the use of turbofan engines. Both situations were initially retarded by lack of public information and a seemingly never-ending encounter with proprietary information. Eventually, through persistent and collaborative research, enough data was found to create a starting design point. After a design point and correlating engine choices were found, the focus shifted towards gathering historical data. This again became challenging due to limited information and halts in retrieving outside sources (e.g. Jane's Aero Engines). However, the team was able to find a list of hundreds of engines to use for trade studies. This was completed simultaneous with individual research and data collection from various sources.

Once enough historical data was found, the parametric cycle analysis began. This process proved more challenging the more it was worked on. Having to analyze the many parameters, equations, and variables that go into PCA was challenging. After all of the constants, assumptions, and standard values were collected and documented on an Excel sheet, the necessary thought process began to unravel. This was aided by the use of aerospace textbooks and websites to help break down the many equations and variables. Eventually, enough research was done and the equations were translated onto the Excel document; however, the values that the numerical analysis yielded did not make sense based on the references used. To check if the problem came from the formulas, hand calculations were done. The problem was not with the equations, but it was later found that the units used in some of the variables had to be converted to match the rest of the document. After several iterations, the team was able to successfully generate a PCA for the baseline engine with the intentions of running the program again with the values from the different computational methods.

Proceeding the PCA was the generation of a chart that displayed the thrust and TSFC (thrust specific fuel consumption) design margins. To do this, the total drag had to be

calculated. This had to be strategically tackled by separating the calculations for the wave drag from the other drag forces the aircraft and engine will face. Using design parameters from NASA/CR-2010-216842, the Excel documents created for the project, and the baseline model described by AIAA, the total wave drag was calculated on Excel and then used to determine which powerplant the team would choose. This thrust value will help show where the design falls in respect to a thrust versus TSFC graph and if the design criteria were met. Creating the design curve has been halted due to insufficient information on the actual design. This will be later corrected after enough simulations and calculations are performed.

Another challenge comes through attempting to create budget for the project. Most of the project will be done through computer software that is free or has a minimal cost. The team did set up a prescribed budget to complete the project covering any fees deemed necessary for completion. Concerning a theoretical budget for manufacturing the design, this has proved difficult since a market for supersonic transport vehicles do not exist outside of the military (whom do not tend to have budgets). Further research into this will be done in future work.

Appendix O: Contributions

Task	
CAD Modeling	AJC
Presentation	AJC
Wave Drag Calculations	C
Sizing	C
Interior Design	A
Poster	AC
Component Design	JC
Parametric Cycle Analysis	AJ
PARA	A
TURBN	J
3D Printing	C
Historical Data	AJC
Gantt Chart	AJC
Presentation	AJC
Trade Studies	AJC
TOPSIS	AJC
CFD Simulations	AJC
Carpet Plots	A
Literature Review	AJC
Video	AJC

A - Alain J - Jordan C - Chris

Chapter 1: Introduction		Chapter 4: Engineering Analysis	
1.1	A	4.1	J,A
1.2	A	4.2	C
1.3	A	4.3	C
1.4	ALL	4.4	A
1.5	A	4.5	J
1.6	A	4.6	A
1.7	C	4.7	J
1.8	C	Chapter 5: Results and Discussion	
1.9	A	5.1	A
Chapter 2: Literature Review		5.2	A
2.1	A	5.3	A,J
2.2	J	Chapter 6: Prototype	
2.3	C,A	6.1	J,A
2.4	C,A	6.2	C
2.5	J	6.3	C
2.6	C	6.4	A
2.7	J	Chapter 7: Conclusion	A,J
2.8	J	Chapter 8: Future Work	A,J
Chapter 3: Design Approach		Chapter 9: Acknowledgements	ALL
3.1	A	References	ALL
3.2	A	Appendicies	ALL
3.3	A		
3.4	A		

A - Alain, J -Jordan, C - Chris